Modeling the woody biomass supply chain for energy production in northwestern Ontario

by

Md. Bedarul Alam

A doctoral thesis submitted

in partial fulfillment of the requirements for the

degree of Doctor of Philosophy (Forest Sciences)

Faculty of Natural Resources Management

Lakehead University

February 2012

LIBRARY RIGHTS STATEMENT

Signature:

Date:

A CAUTION TO THE READER

This Ph.D. (Forest Sciences) thesis has been through a formal process of review and comment by four faculty members and an external examiner. It is made available for loan by the Faculty of Natural Resources Management for the purpose of advancing the practice of professional and scientific forestry.

The reader should be aware that opinions and conclusions expressed in this document are those of the student and do not necessarily reflect the opinions of the thesis supervisor, the faculty or Lakehead University.

Abstract

Alam, M.B. 2011. Modeling the woody biomass supply chain for energy production in northwestern Ontario. Ph.D. Thesis, Lakehead University, Thunder Bay. 191 pp.

Keywords: bioenergy, forest cells, forest harvest residue, forest management units, optimization, power plants, procurement cost, gross margins, road network, underutilized wood.

Efficient procurement and optimal utilization of woody biomass for bioenergy production requires a good understanding of biomass supply-chain management. The general objective of this research is to develop decision support models for analyzing and aiding decision-making for optimal woody biomass supply chain management for energy production in northwestern Ontario (NWO). The specific objectives are: exploration of data sources and methods for assessing woody biomass availability, assessment of availability of woody biomass feedstock for energy production in the forest management units (FMUs) of NWO; development of a road network optimization model to optimize woody biomass feedstock transportation from forest cells (1 km x 1 km grid) to power plants; and development of optimization models for analyzing the optimal woody biomass supply from forest cells to one power plant with monthly production schedules (dynamic mathematical programming model) and to four competing power plants (modeling the woody biomass competition issues) in NWO.

The spatial assessment study found that in the 19,315 depletion cells (the forest areas where some level of timber harvest took place during 2002-2009) within the study area about 2.1 million green tonnes (gt) of forest harvest residue and 7.6 million gt of underutilized wood are technically available, which is enough to supply the annual biomass demand (2.21 million gt) of the four power plants were they to convert to using only renewable energy sources.

The road network optimization model incorporates speed and load constraints on different types of roads and seeks the minimum time and cost (or shortest distance) from any forest cell to any road containing cell in the study area. From this model variable cost zones of woody biomass feedstock transportation surrounding each of the four power plants are established. The results of the spatial woody biomass assessment and road network model are used as an input dataset for optimization models later.

An optimization model, based on dynamic mathematical programming, was developed and applied to estimate the monthly supply of optimal quantity and type of woody biomass required for the Atikokan Generating Station (AGS) based on its monthly electricity production schedules. The model selects optimal woody biomass harvest levels from 19,315 depletion cells in order to meet the monthly feedstock requirement, and calculates woody biomass procurement costs. Sixteen alternative scenarios are tested to analyze the sensitivities of changing economic and technological parameters on procurement costs. Changes in moisture contents and conversion efficiency show relatively higher changes in monthly and total costs of the woody biomass feedstock for the AGS.

Finally, two optimization models (cost minimization and profit maximization) were developed to test the sensitivities of changing various economic and technological parameters to the optimality of woody biomass competition issues among the four power plants in the region, thereby generating policy relevant costs and gross margin structures of woody biomass supply chains. The results of the cost minimization model in different scenarios, which are relevant for demand side management (power plants), determine that per unit procurement costs are directly proportional to the size of the power plants. The highest increase in unit woody biomass procurement cost is found in the increased truck charge rate scenario followed by the harvesting only forest harvest residue scenario. The profit maximization model, which is relevant from the woody biomass supplier's (contractors) perspective, explores the gross margin structures of woody biomass supplying FMUs. The FMUs that are closer to the power plants potentially offering higher prices make relatively higher gross margins at different levels of price increase on the part of bigger power plant scenarios.

The findings of this study are useful in understanding the cost structures of woody biomass procurement, given the spatial distribution of woody biomass feedstocks, for single and multiple competing power plants as well as the gross margin structures of each woody biomass supplying FMU in NWO. Moreover, the optimization models could be an important tool in decision support systems of woody biomass supply chains for bioenergy production in general.

Contents

Tables

Figures

Acronyms

AAC	Annual Allowable Cut
ABFF	Abitibi-Bowater Fort Frances
ABTB	Abitibi-Bowater Thunder Bay
AGS	Atikokan Generating Station
ASCII	American Standard Code for Information Interchange
BAF	Basal Area Factor
CE	Conversion Efficiency
CHP	Combined Heat and Power
CONFOR	Conference on Forestry and Environmental Sciences
CTL	Cut-to-Length
CWM	Coarse Woody Material
DBH	Diameter at Breast Height
DDPP	Domtar Dryden Power Plant
DOB	Diameter Outside Bark
DSS	Decision Sopport System
ESRI	Environmental Systems Research Institute
FHR	Forest Harvest Residue
FMP	Forest Management Planning
FMU	Forest Management Unit
FRI	Forest Resource Inventory
FT-CH	Full-tree to Roadside Chip-to-Mill

FT-SW	Full-Tree to Roadside Shortwood-to-Mill
FT-TL	Full-Tree to Roadside Tree-Length-to-Mill
FWM	Fine Woody Material
GAMS	General Algebraic Modeling System
GIS	Geographic Information System
GHG	Green House Gas
GJ	Gigajoule
GPS	Global Positioning System
gt	green tonne
ha	hectare
HF	Harvesting Factor
HHV	Higher Heating Value
LHV	Lower Heating Value
LIO	Land Information Ontario
MNDMF	Ministry of Northern Development, Mines and Forestry
MTO	Ministry of Transportation
MW	Megawatt
MW_e	Megawatt (electricity)
MW_{th}	Megawatt (thermal)
MWh	Megawatt hour
NSERC	Natural Sciences and Engineering Research Council of Canada
NWOPA	Northwestern Ontario Prospectors Association
ODt	Oven dry tonne

OME	Ontario Ministry of Energy
OMNR	Ontario Ministry of Natural Resources
SCM	Supply Chain Management
SFISL	Sumac Forest Information Services Ltd
SFL	Sustainable Forest Licence
SPSS	Statistical Package for the Social Sciences
UW	Underutilized Wood
VCO	Value Chain Optimization

Acknowledgements

I would like to acknowledge people who helped me with this PhD study. First and foremost, I would like to thank my supervisor Dr. Reino Pulkki as well as the rest of my committee Drs. Ulf Runesson, Mathew Leitch and Chander Shahi. They have all been very kind, helpful and painstaking advisors, guides and mentors, leading me to a better understanding than I would have accomplished on my own. I appreciate fruitful help of following officers of Faculty of Natural Resources Management, Lakehead University: Mr. Tomislav Sapic, Technologist provided me Geographic Information System (GIS) help, Mr. Frank Luckai, Technologist gave me guidance how to conduct field inventory, Mr. Pat Cybulski, Technologist helped me in collecting up to date information about logging in northwestern Ontario and Dr. Thakur Upadhyay, Post Doctoral Fellow helped me in modeling. I am thankful to my colleagues Brian Brassard, Scott Wiebe and Vijayan Sundararaj who gave me valuable suggestions during my PhD study.

I am grateful that the Ontario Ministry of Energy and Infrastructure through the Ontario Centres of Excellence, NSERC Strategic Network on Value Chain Optimization, Abitibi-Bowater Inc., and Thunder Bay Community Economic Development Commission funded this research. I also acknowledge that Lakehead University, Confederation College, FPInnovations FERIC Division, Lac Des Mille Lac First Nation, Buchanan Group and Ontario Ministry of Natural Resources gave further support to pursue this research.

I am very much thankful to Land Information Ontario, Ontario Ministry of Natural Resources, Abitibi-Bowater Inc. Thunder Bay, Abitibi-Bowater Inc. Fort Frances, GreenForest Management Inc., Thunder Bay and Greenmantle Forest Inc. Thunder Bay for providing me with GIS data to pursue my PhD research.

I would like to thank my family for the support they provided on a very regular basis, without you none of this would have been possible, particularly my wife Cassia Sanzida Baten who has been extremely understanding of the time commitment necessary for me to complete this thesis. I am grateful to my mother Anwara Begum who always gave me courage to pursue my PhD research. I appreciate all other people who gave me support to complete my thesis.

Chapter 1

Introduction

1.1 Background

Woody biomass is a low greenhouse gas (GHG) emitting and renewable fuel that is replacing non-renewable fossil fuels for energy production to some extent (Yoshioka *et al.* 2002; Gan and Smith 2006). The ever-increasing prices of fossil fuels coupled with their high GHG emissions have led many countries to supplement energy production through biomass resources (Allen *et al.* 1998; Layzell *et al*. 2006; Meehan *et al.* 2010). It is estimated that the energy content of one oven dry tonne (ODt) of woody biomass is about 19.6 GJ (Etcheverry *et al.* 2004; Hosegood 2010), which indicates that it can be used as an energy source for different purposes. A good understanding of both the technological processes of biomass to bioenergy conversion and competency in biomass supply-chain management are essential for efficient procurement and optimal utilization of woody biomass for bioenergy production. In general, the entire supply chain is the decision focus in supply chain management (SCM), which stretches from the raw materials to ultimate consumption (Pulkki 2001). SCM develops better knowledge of the overall process chain by the cooperation within and between organizations. SCM helps achieve many important breakthroughs of the process, such as improving yield, improving productivity, reducing cost, improving product quality and introducing new products (Mattsson 1999; Pulkki 2001; Haartveit *et al.* 2004; Alam and Pulkki 2009a;

Alam and Pulkki 2009b). However, a detailed study on SCM of woody biomass procurement for energy production in northwestern Ontario (NWO) does not exist.

At present, bioenergy is fulfilling around 6% of the energy demand of Canada (CanmetENERGY 2011). Canada has 402 million hectares (ha) of forest land (44% of Canada's land area; and 10% of the world's forest land), which can fulfill 60% of the domestic renewable energy requirements (Bradley 2006a; Alam *et al.* 2008). The forest area of Ontario is 58 million ha. Currently Ontario is an energy-importing province depending on western and eastern Canadian provinces and the USA to fulfill its energy requirements. Woody biomass can be used to fulfill at least 27% of the energy requirements of the province, which could offset energy imports significantly (Etcheverry *et al.* 2004; Forest BioProducts Inc. 2006).

There are three major biomass-based combined heat and power (CHP) plant developments and one proposed biomass-based power generating station west of Lake Nipigon in NWO. The three CHP plants are: Abitibi-Bowater (recently renamed Resolute Forest Products) Thunder Bay, Abitibi-Bowater Fort Frances and Domtar Dryden CHP plants (Abitibi-Bowater Inc. 2011; McKinnon 2011). The proposed power plant is the Atikokan Generating Station (AGS) which is currently being converted from a coal-based to a biomass-based power plant. The total annual woody biomass feedstock requirement is estimated at 2.2 million gt to run these four power plants.

A study conducted by the Ontario Ministry of Energy (Forest BioProducts Inc. 2006; OME 2007) found that within a 500 km radius of the AGS, approximately 2.7 million ODt of woody biomass feedstock is available annually from forest harvest residues, underutilized wood supply and mill wood waste. However, the OME study is based on estimates of woody biomass availability using personal surveys and approximate methods. Moreover, as most sawmills are not operating at present, there is not much wood waste being generated. Reynolds *et al*. (2008) conducted research on the feasibility of woody biomass feedstock for bioenergy production from one forest management unit (FMU) in NWO. No other study has ever attempted to quantify in detail the woody biomass availability for bioenergy production in NWO. Further, an exploratory study on data sources and methods to assess the biomass availability is also an important first step for modeling biomass supply chain management issues.

Woody biomass is available in the FMUs mainly in two forms, forest harvest residues (FHR), and underutilized wood (UW). FHR are in the form of tree tops, branches and broken pieces left in the forest after harvesting for traditional forest wood assortments. The harvesting operations result in forest depletion of productive forest areas. UW are the tree species and unmerchantable wood, which are not commercially important to harvest for lumber and pulpwood production, and trees damaged by wildfire, windthrow and insects that are currently not salvaged (Hosegood 2010; Hosegood *et al.* 2011). The extent of forest depletion of productive forest area can be used for accurately assessing the availability of woody biomass per unit area from the FMUs (Alam *et al.* 2008). A detailed assessment of biomass availability in terms of FHR and UW around each of the four power plants is the first step to model a woody biomass supply chain.

Optimized transport over the road network plays a vital role in bioenergy production, as the road network can provide a cost-effective path to transport bulky and low value woody biomass, thereby helping save on hauling costs (Searcy *et al.* 2007;

Gold and Seuring 2011). The mathematical models and algorithms for biomass transportation can focus either on cost calculation or optimal location of bioenergy power plants (Singh *et al.* 2010). A mathematical algorithm can optimally locate biomass-based power plants based on minimum transportation cost (Velazquez-Marti and Fernandez-Gonzalez 2010). A crucial decision of the road network optimization problem is the full capacity utilization of existing roads and/or the addition of new links. Such a decision is referred to as the network design problem, which determines the optimal decision variables (e.g., full capacity utilization and/or new link additions) to minimize a specific network performance index (e.g., total travel time or generalized cost), while accounting for different route characteristics in the network (Zhu *et al.* 2011). The generalized cost of energy recovery from woody biomass mainly depends on the logistics cost of supplying biomass feedstock to the power plants (Yoshioka *et al.* 2002; Edward *et al.* 2007; Searcy *et al.* 2007). Biomass logistics costs constitute a significant part of the total cost of the biomass supply chain (Allen *et al.* 1998). Road type and conditions also have a substantial effect on transportation costs (Nichols *et al.* 2006).

Spatial data analysis techniques are often used to find the shortest distance in road network problems. Geographic Information Systems (GIS) have been used to compile, clean and analyze all types of spatial data and to build raster spatial databases of road networks for supplying woody biomass for energy production (Burrough 1986; ESRI 2010; Tittmann *et al.* 2010; ESRI 2011). The technique of data storage in raster format makes the data analysis much easier in network optimization models and has allowed the development of efficient solution techniques for solving very large cyclic network problems (Pulkki 1994 and 1996). The raster format is also better than the vector format, as it works even in areas where predefined paths do not exist and many attribute layers are not available (Husdal 1999).

The sources and destinations of the network can be identified in a GIS based system for biomass logistics and transport optimization (Perpiña *et al.* 2009; Velazquez-Marti and Fernandez-Gonzalez 2010). The nodes of network structure as biomass sources, storage locations or biomass-based power plants are connected through arcs in the network (Jensen *et al.* 2005; MSDN 2009; ESRI 2010; Microsoft 2010; ESRI 2011). By the combination of GIS and linear programming (LP) woody biomass feedstock supply logistics can be optimized (Kanzian *et al.* 2009). However, there has been no such study in NWO to optimize the woody biomass feedstock supply to power plants with minimum cost or minimum time (or shortest distance) using road network optimization models.

Efficient optimization models to minimize costs and make the biomass procurement business more profitable need to be developed for supplying woody biomass feedstock for bioenergy production (Alam and Pulkki 2009a; Alam and Pulkki 2009b). Some LP models have been developed using GIS-based woody biomass data both for estimating the feedstock availability and for reducing transportation distances and costs (Ranta 2002; Panichelli and Edgard 2008; Perpiña *et al.* 2009). All these studies have been conducted either in Nordic or central European countries. In Canada, most of the studies focus on optimizing harvesting and transportation of raw material for forest products industries from FMUs (Pulkki 2001; Alam *et al.* 2009a; Alam *et al.* 2009b; Chauhan *et al.* 2009; Sowlati 2009). Kumar *et al.* (2008) conducted a techno-economic analysis of producing power from mountain pine beetle killed wood in British Columbia. They found that transportation distances can be minimized by locating the power plant in an area of high infestation. In NWO, if the four major biomass-based power plants become fully operational, the power plant managers (buyers of biomass) would like to have a sustainable supply of the biomass at the least cost and the contractors (suppliers of biomass) would like to increase their profits from biomass supplying. Therefore, the optimization of woody biomass feedstock supply needs to be addressed from both cost minimization and profit maximization points of view. We found no optimization models dealing with biomass supply competition among various power plants in the Canadian context with large contiguous wood supply areas.

1.2 Objectives

The general objective of this research is to develop optimization models for aiding and supporting decision-makers to make decisions on the optimum supply chain management of woody biomass feedstock for energy production in NWO. The specific objectives of this study are:

(1) To explore the data sources and methods to be used for assessment of woody biomass availability for bioenergy purpose;

(2) To assess and quantify the amount of woody biomass available for bioenergy production in NWO;

(3) To build a road network optimization model to assist in planning woody biomass transportation and logistics for bioenergy production at minimum cost in a sustainable way;

(4) To develop an integrated NLDP model for procuring woody biomass from the FMUs surrounding the AGS in the most economical and sustainable way; and

(5) To develop and apply optimization models to analyze the impact of inter-power plant competition for the available biomass feedstock on cost structures and gross margins of each power plant in NWO.

Each specific objective is achieved with an individual research paper (Chapter 2, Chapter 3, Chapter 4, Chapter 5 and Chapter 6). The research area extends 167,184 km^2 (324 km (N-S) x 516 km (E-W)) consisting of 18 FMUs (Armstrong Forest, Black Sturgeon Forest, Caribou Forest, Crossroute Forest, Dog-River Matawin Forest, Dryden Forest, English River Forest, Kenora Forest, Lac Seul Forest, Lake Nipigon Forest, Lakehead Forest, Ogoki Forest, Red Lake Forest, Sapawe Forest, Spruce River Forest, Trout Lake Forest, Wabigoon Forest and Whiskey Jack Forest), which fall in seven Ontario Ministry of Natural Resources (OMNR) districts (Dryden, Fort Frances, Kenora, Nipigon, Red Lake, Sioux Lookout and Thunder Bay) west of Lake Nipigon in NWO (NWOPA 2007).

1.3 Thesis Outline

Chapter 1 gives the general introduction. In this chapter the background of the study, the research objectives and the thesis outline are discussed. In Chapter 2, exploration of data sources and methods for assessing biomass availability are elaborated on. The importance of accurate and appropriate types of data is described in this chapter. In Chapter 3, the assessment of woody biomass availability for bioenergy production using forest depletion spatial data in the study area for the four bioenergy generating plants is described. By using pre- and post-harvest inventory and forest depletion spatial data analysis, woody biomass availability per square kilometre area for the whole research area is estimated. In Chapter 4, a road network optimization model is built to assist in planning woody biomass transportation and logistics for bioenergy production at a minimum cost in a sustainable way. Specifically, a minimum time and cost (or shortest distance) road network model was developed to transport woody biomass feedstock to the power generating stations; the minimum raster resolution that supplies consistent results at the regional scale was determined; and variable cost zones surrounding the power generating stations in the study area were established.

In Chapter 5, an integrated NLDP model is developed for procuring woody biomass from the FMUs surrounding the AGS in the most economical and sustainable way. The model determines the type and quantity of woody biomass, from depletion cells (each of 1 km^2 size), supplied to the AGS over a one-year horizon based on monthly electricity production by the AGS and computes the optimum monthly woody biomass procurement costs. Several scenario analyses were conducted to test the sensitivity of changes in key parameters, namely, harvesting factor, conversion efficiency, biomass moisture content and per unit biomass processing costs on woody biomass feedstock procurement costs. In Chapter 6, two optimization models (cost minimization and profit maximization) based on LP are developed and applied to analyze the impact of inter-power plant competition for the available biomass feedstock on cost structures and gross margins of each of the four major power plants. The models select the optimum quantity of each type of biomass (FHR and UW) from each depletion cell, subject to the constraints of woody biomass availability in each cell and demand of each of the four power plants. A number of scenarios were run to study the impact and sensitivities of changes in parameters relevant to transportation cost, processing technology, types and prices of woody biomass feedstock.

Finally, Chapter 7 is the summary of the research. In this chapter main findings and significance of the research are discussed, the implications of the study are concisely described, and some important future directions of study are suggested.

Chapter 2

Data sources for research on woody biomass supply chain for energy production in northwestern Ontario[1]

2.1 Introduction

Proper data is one of the most important components of any research, and procuring the desired data within given time and budget constraints is necessary to make the research successful. The use of various data and data collection activities are mainly related to the objectives of the research (Jensen *et al*. 2005). Data accuracy should be maintained in the process of bringing different types of data from different sources through a reconciliation process. The reconciled data further needs to be produced in a workable format to help make the research internally and externally valid.

Of the two data sources – primary and secondary – the secondary data is generally considered as ‘collated data in context’. In this context, bad sources of information may cause more harm than good, and in the situation of many sources having an excessive amount of data, filtering out the bad information and exploiting the good data is the wise strategy to follow for a successful research endeavor (Hutchinson and Warren 2001).

Cognizant of the fact that various data sources and data relating to biomass supply chains are available in different formats and extent, research on woody biomass supply

[1]A version of this chapter was published.
Alam, M.B. and Pulkki, R. 2011. Data Sources for the Research on Wood Biomass Supply Chain for Energy Production in Northwestern Ontario. European Journal of Scientific Research, 49(2):152-167.

chains for energy production in northwestern Ontario (NWO) needs to be specific in selecting and collecting the right data from different primary and secondary sources. Further, the collected data are required to be in a workable format for different software packages (e.g. Visual Basic, GAMS). In general, ArcGIS is used to compile, clean and analyze spatial data to prepare text database files. Hawth's Tools (Beyer 2004) are also used in ArcGIS to analyze data. Visual Basic or other high level computer programming languages can be used to write various heuristics and simulation models for solving the transport network problems using the text files created by Geographic Information System (GIS) software.

Research in woody biomass supply chain modeling for bioenergy production is complex and data sources, pros and cons of the data input methods, and related computer software need to be specified carefully. In this context, the objective of this study is to explore different reliable data sources and suggest workable data formats for modeling the woody biomass supply chain for energy production in NWO. This paper aims at providing detailed background information regarding the input data sources and methods for further modeling work in this thesis.

2.2 Major Data Sources

The research area covers the following 18 Forest Management Units (FMUs) of NWO: (1) Crossroute Forest, (2) Sapawe Forest, (3) Dog River Matawin Forest, (4) Whiskey Jack Forest, (5) Kenora Forest, (6) Lac Seul Forest, (7) Lakehead Forest, (8) Lake Nipigon Forest, (9) Armstrong Forest, (10) Black Sturgeon Forest, (11) Caribou Forest, (12) Wabigoon Forest, (13) English River Forest, (14) Spruce River Forest, (15) Trout

Lake Forest, (16) Dryden Forest, (17) Red Lake Forest, and (18) Ogoki Forest. There are two main sources of data - GIS and field inventory data. Following are the main GIS data sources relating to these FMUs:

1. Forest Resources Inventory (FRI) data of FMUs
2. Forest depletion data of FMUs, and
3. Forest Management Planning (FMP) data of FMUs.

All the above data are in shape files. The projected coordinate system is NAD 1983 UTM Zone 15N. FRI data covers the shape files of forest cover, roads and lakes/water. Forest depletion data contains the information of forest depletion mainly by timber logging from 2002-2003 to 2008-2009 in shape files. FMP data contains the forest harvest plan information for the next five years, 2009-2014.

The shape files were originally created using Ontario Base Maps (OBM), aerial photographs and field inventories (OMNR 2007a; OMNR 2009). Generally, the scale used to prepare maps for northern Ontario is 1:20,000 (Morgan 2008). The FRI layer preparation procedure can be described as follows (OMNR 2007a; OMNR 2009; Sapic 2009):

- Data compilation conducted from the base data, such as administrative layer, and roads, lakes and stream layers;
- Interpretation of aerial photographs and images of forest areas;

- Conducting surveys in the field to ground truth the aerial photographs and images, and also to collect other relevant data to delineate and classify the area within a FMU;
- All of the above information was incorporated to prepare the FRI layer;
- Two types of attributes are available in FRI, such as spatial and tabular attributes;
- The production rotation cycle of the FRI was for a period of 20-25 years.

In the new FRI, the production cycle of 10 years is being used instead of 20-25 years. Now the planning is on a continuous basis instead of the previously used periodic planning. The FRI needs to be updated at the start of each new FMP (every 10 years) to reflect all changes to the forests in each FMU. The changes to the forests could happen by forest depletions due to harvest or natural causes (e.g., blowdowns, wildfire, insects and diseases). Forest renewal and tending activities could also facilitate accruals in the forests (OMNR 2007a; OMNR 2009).

Base layers and FRI layers were originally used to prepare FMP layers. Planning for the next 10 years is incorporated in this layer according to the management plan for the FMUs. There are two phases in the management plan - 1st five year plan and 2nd five year plan. The main information available in this layer, which is relevant to this research, is the plan for the forest depletion. To prepare the depletion layer an FMP layer is mainly used, and the information about the actual depletion is available in this layer, e.g., forest depletion 2002-2003 to 2008-2009.

Relevant data were obtained for this research from different sources. Abitibi-Bowater Inc., Thunder Bay provided the FRI data, forest depletion data and FMP (forest management plan) data for the following FMUs: Crossroute Forest, Dog River Matawin Forest, Black Sturgeon Forest, English River Forest and Spruce River Forest (Abitibi-Bowater Inc. 2009). GreenForest Management Inc., Thunder Bay provided the FRI data, forest depletion data and FMP data for the Sapawe Forest (GreenForest Management Inc. 2009). Greenmantle Forest Inc., Thunder Bay provided the FRI data, forest depletion data and FMP data for the Lakehead Forest (Greenmantle Forest Inc.2009). The rest of the data were collected from the Ontario Ministry of Natural Resources (OMNR - OMNR 2010). The spatial data for the Wabigoon Forest are in the form of text files from Ride (1998), which is the only source of data for this FMU. Further, pre-harvest forest inventory, post-harvest cutover survey and slash pile measurements were conducted during the summers of 2008 and 2009 in different blocks of the Crossroute Forest.

A road network map for NWO, in a text file format was compiled during this study and contains five road classes. The grid codes assigned for the five road classes are as follows: Highway-I - 1, Highway-II - 2, and primary - 3, secondary - 4 and tertiary/ operational – 5 forest roads. The cell size of these text files is 1000 m x 1000 m.

2.3 Data Preparation and Analysis

2.3.1 Raster Database

ArcGIS and Hawth's Tools were used to prepare the workable databases for this research. Raster grids of 1 km^2 cells were prepared; then ASCII (.txt) files were created from the raster grids. Each grid cell represents only one type of feature. But when only a small portion of the cell contains a particular type of feature then the decision making to assign a feature to the cell becomes difficult (Nichols 2004). Therefore, for different types of features different data input methods were followed (Table 2.1).

Table 2.1 Data input methods (ESRI 2009).

Layer	Method	Description
Roads	Presence/absence	Grid code (1-5) is assigned depending on the presence of road types. If no road is present 9 (grid code) is assigned.
Landuse class	Dominant type	Grid code entity is assigned which occupies more than 50% area of the cell.
Forest depletion	Percent occurrence	The grid code is assigned according to the percent of cell area depleted by forest harvesting.

Three grid layers (roads, landuse class and forest depletion) were created using appropriate data input methods. To create the road network layer the presence/absence method of data input was followed. Each grid cell is assigned a particular grid code for the presence of a particular type of road in the cell, such as grid code 1 is assigned to Highway-I, grid code 2 is assigned to Highway-II and so on (Table 2.2). When there is no road present in a cell grid code 9 is assigned.

Table 2.2 Road classification

Road class	Road type
1	Highway-I
2	Highway-II
3	Primary forest road
4	Secondary forest road
5	Tertiary/operational forest road

The dominant-type method of data input was used to assign grid codes to the features of the landuse class layer. In this method any feature which occupies more than 50% of the cell area, represents the cell. For every feature type there is a particular grid code (Table 2.3).

Table 2.3 Grid codes for different forest landuse classes

Landuse class	Landuse type
1	Productive forest in Whiskey Jack FMU
2	Productive forest in Kenora FMU
3	Productive forest in Lac Seul FMU
4	Productive forest in Lakehead FMU
5	Productive forest in Ogoki FMU
6	Productive forest in Caribou FMU
7	Productive forest in Wabigoon FMU
8	Productive forest in Spruce River FMU
9	Productive forest in Dryden FMU
A	Productive forest in Armstrong FMU
B	Productive forest in Black Sturgeon FMU
C	Productive forest in Crossroute FMU
D	Productive forest in Dog River FMU
E	Productive forest in English River FMU
N	Productive forest in Lake Nipigon FMU
R	Productive forest in Red Lake FMU
S	Productive forest in Sapawe FMU
T	Productive forest in Lake Nipigon FMU
W	Lake/water in FMUs
O	Other landuse in FMUs

For the forest depletion layer, the percent-occurrence method was used to assign a grid number to the cells depending on the percentage of the cell area being depleted by forest harvesting during 2002-2009, and also the percentage of the cell area that is expected to be depleted within the next 5 years according to the forest management plans of the particular Sustainable Forest Licence (SFL) holders of the FMUs. The grid codes for the forest depletion layer are illustrated in Table 2.4.

Table 2.4 The grid codes for the different percentage of cell area depletion.

Grid code	Depletion percent of cell area
1	Cell area depletion is 100% (1 km^2)
2	Cell area depletion is ≥ 80% to <100%
3	Cell area depletion is ≥ 60% to <80%
4	Cell area depletion is ≥ 40% to <60%
5	Cell area depletion is ≥ 20% to <40%
6	Cell area depletion is > 0% to <20%
7	Cell area depletion is 0% (no depletion)

To assign codes for the road network in the Wabigoon Forest the two text files from Ride (1998) were converted into raster files first. These raster files were converted to the feature files, and then the feature files were converted into a grid. The road network for this forest was reclassified from 4 classes into 5 classes, and the grid codes given to the different road classes accordingly (Table 2.2).

Microsoft's Excel software was used for data analysis of field inventory data, which were collected by conducting forest inventory on the Crossroute Forest. Visual Basic software was used for analysis of data which had already been made workable by ArcGIS. Visual Basic software was used to develop the woody biomass supply chain model for energy production (Wang 1998; MSDN 2009).

2.3.2 Consequences of Using 1 km² Grid

The grid of 1 km x 1 km was created for every layer. The roads which, pass within a distance of 1000 m (or 1 km) touch each other in the grid layer of roads when the grid layer is created from road network shape files. This makes a link in the network though in reality there is no link. In this case it is necessary to adjust the coding of grid cells manually to get rid of the links which are not present in reality (Figures 2.1-2.3).

Figure 2.1 shows the actual road, Figure 2.2 illustrates the road links when all cells are included, and Figure 2.3 shows the manually adjusted cells for network integrity. While manually adjusting the road network it is necessary to keep the deviation of the network at a minimum level (Nichols 2004).

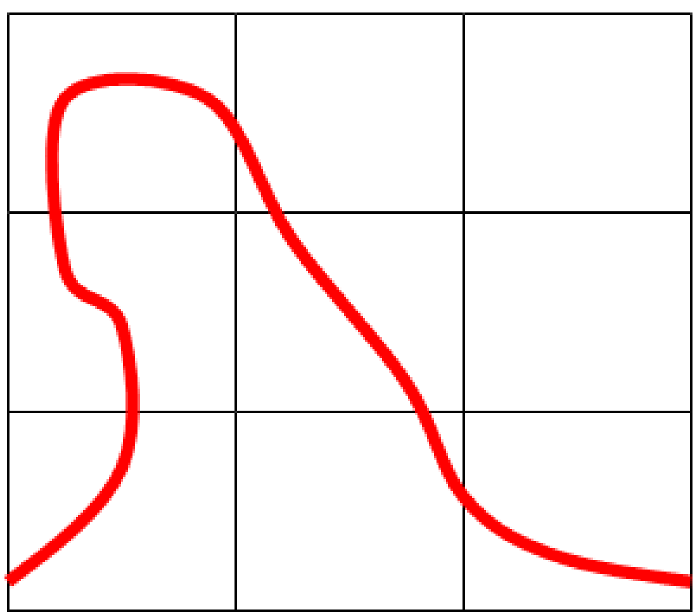

Figure 2.1 Actual road (Nichols 2004).

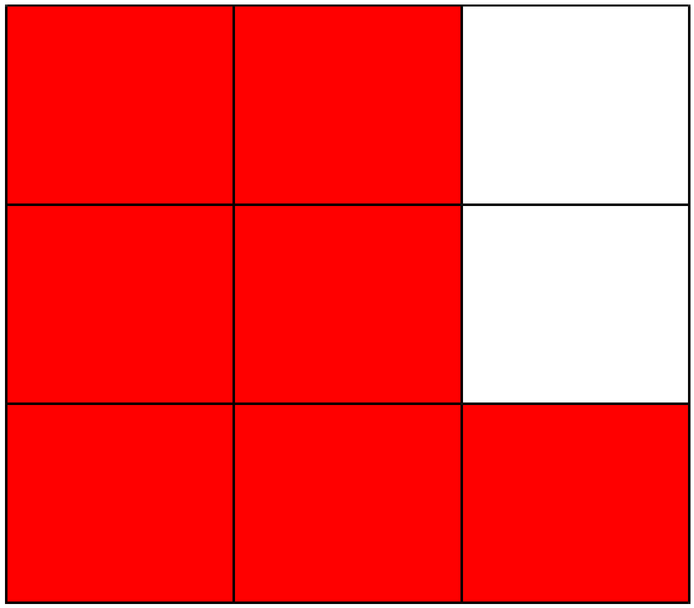

Figure 2.2 All cells included which are touched by actual roads (Nichols 2004).

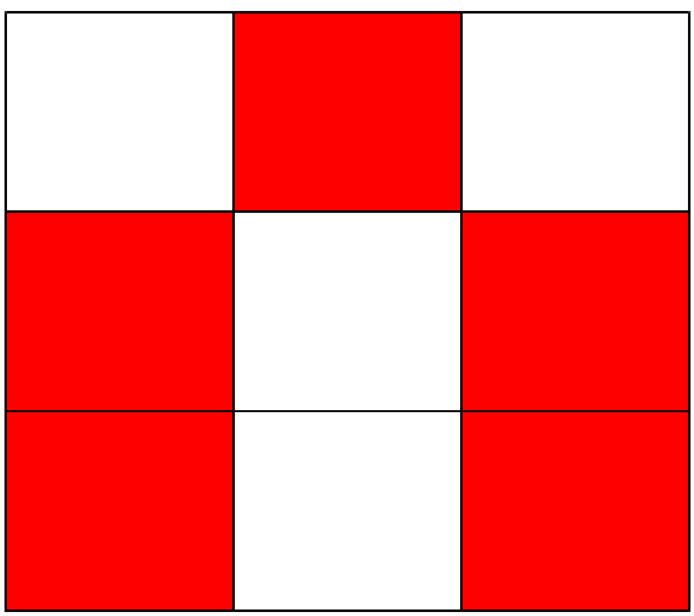

Figure 2.3 Road codes are manually adjusted for network integrity (Nichols 2004).

In the road network the higher-class road can touch a lower-class road on more than one side. However, a lower-class road must not touch the higher-class road on more than one side. When the lower-class road touches a higher-class road on more than one side the grid cells must be adjusted to maintain the road network integrity (Nichols 2004). Figure 2.4 shows the incorrect road intersection between two different classes of roads in which a lower-class road (secondary road) touches a higher-class road (primary road) on both sides.

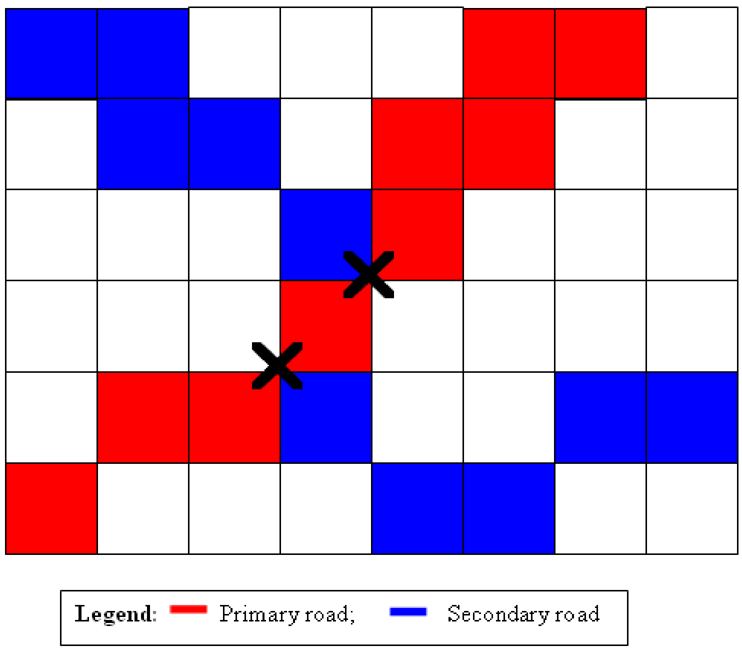

Figure 2.4 Incorrect road intersection between two different classes of roads (Nichols 2004).

Figure 2.5 shows the correct road intersection between two different classes of roads in which a lower-class road (secondary road) touches a higher-class road (primary road) on one side only.

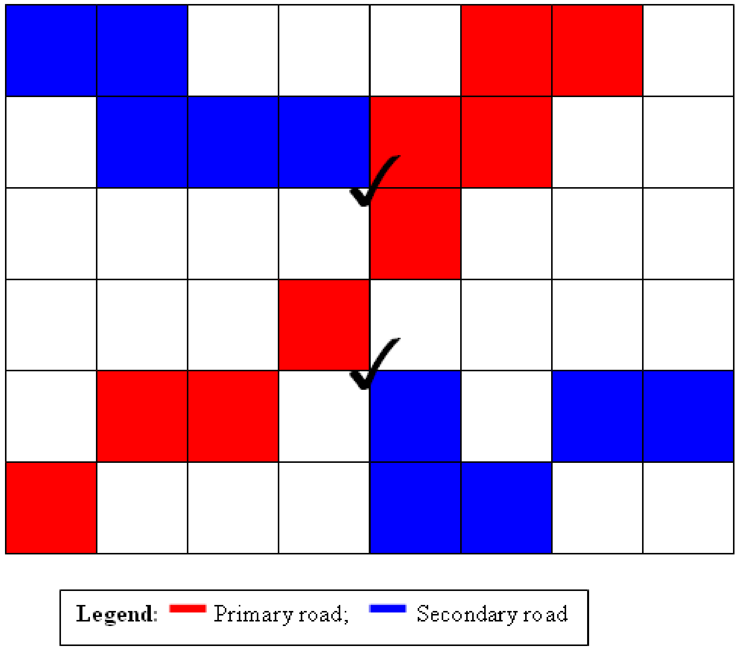

Figure 2.5 Correct road intersection between two different classes of roads (Nichols 2004).

Raster cells can be different sizes depending on the requirement of the resolution. Depending on the representation of the features within the surface the raster cell can be large or small, such as 1 km^2, 100 m^2, 1 m^2, etc. Figure 2.6 illustrates how a raster dataset at various cell sizes can represent one simple polygon feature (ESRI 2009).

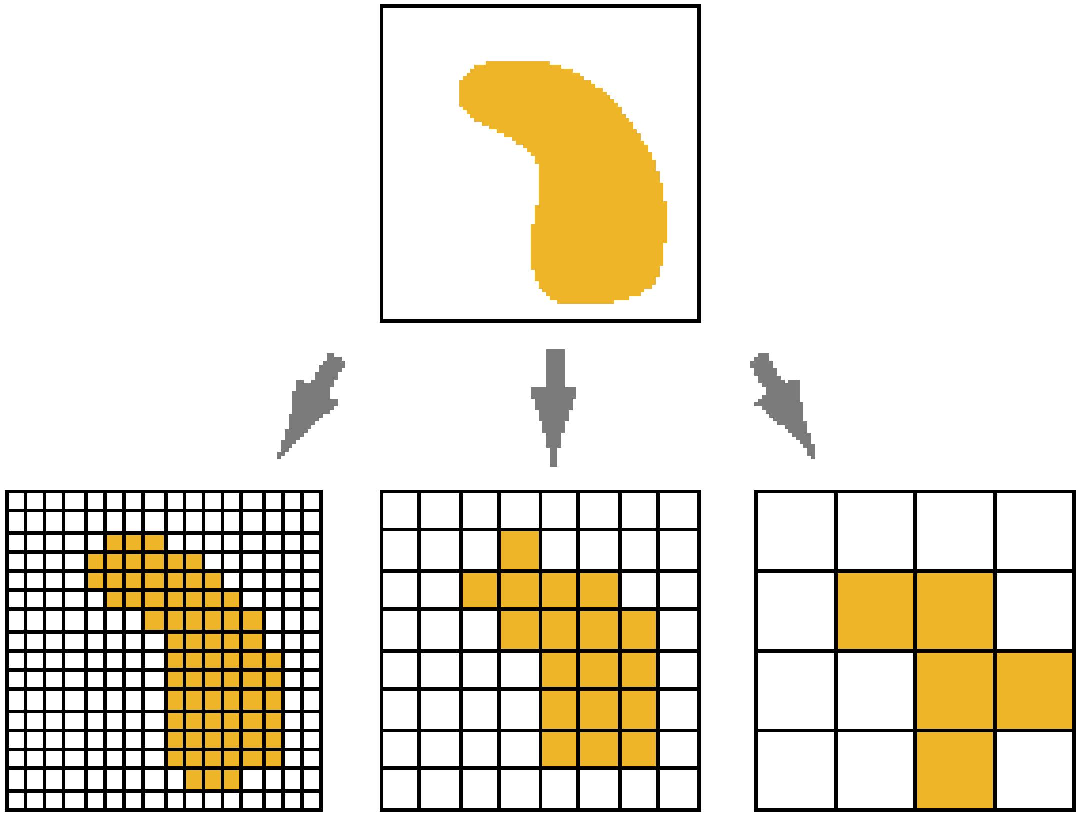

Figure 2.6 A simple polygon feature is represented by a raster dataset at various cell sizes (ESRI 2009).

When a smaller cell size is used a smoother, fine and more detailed raster is created. But due to the use of smaller cell sizes a greater number of cells is required to be created. It will take a longer time to process and larger storage space is required. When larger cells are used it results in a very coarse raster, and there is an increased chance of information loss. It is quite impossible to represent fine features or patterns within the surface while using larger cells (ESRI 2009). Figure 2.7 shows how classification errors occur when the size of the grid cell is larger than the features which are being mapped.

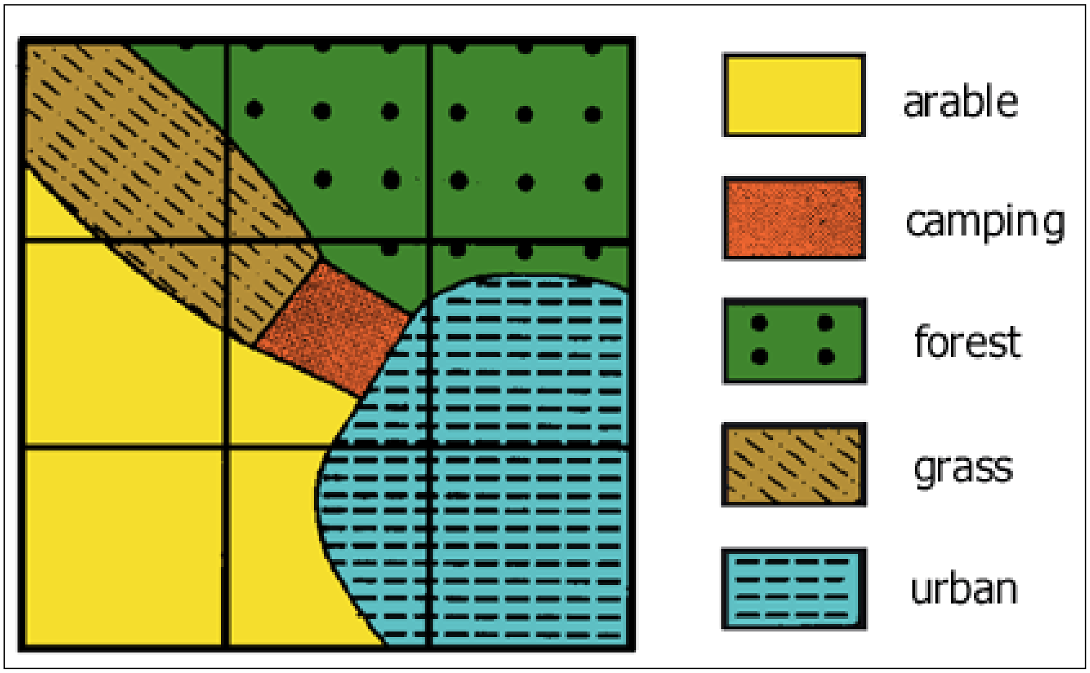

Figure 2.7 Classification errors occur when the size of the grid cell is larger than the features which are being mapped (Burrough.1986; Ellis 2001).

When we use the raster cell of 1 km^2 to create a road network it means the width of a cell is 1 km, but the width of a road with right-of-way in reality might be just 20 to 30 m. In this case the rest of 970-980 m of the cell width is not representing the road width in the real world. When many roads exist within 1 km we cannot show more than one road within the 1 km^2 area of the cell, resulting in loss of road information. Similarly, grid codes for different forest landuse classes are assigned by the dominant-type method by assigning the grid code for a particular cell for the feature which occupies more than 50% of the area of the cell (Tables 2.1 and 2.3), however, other features which are present (but not dominant) in reality within the extent of this cell are not assigned a grid code (Figure 2.7). So, to make the raster grids as realistic as possible three separate layers of road network, forest landuse class and forest depletion were prepared using three separate methods of data inputs (Table 2.1) by using a cell size of 1 km^2 within time limits and budget constraints.

2.4 Biomass Estimates and New Provincial FRI

2.4.1 Field Inventory

We conducted two types of field inventories (pre- and post-harvest forest inventory) to estimate stand volumes and biomass availability in a typical FMU of NWO, the Crossroute Forest. The pros and cons of the inventory data are contrasted with the new FRI in the later section.

2.4.1.1 Pre-harvest forest inventory

The pre-harvest inventory was conducted in different forest blocks in the Crossroute FMU during the summer of 2008 and 2009. By using a prism of 2 basal area factor (BAF), point sampling was conducted to collect data in the field. A systematic grid of 200 m x 50 m was followed to conduct the inventory in the stand (Figure 2.5).

The ratio of count plots and measure plots was 3:1. The measure plots are distributed in the forest stand at 200 m intervals (i.e., 1 measure plot per 4 ha). The count plots were applied at 50 m intervals between the measure plots on the grid line. Figure 2.8 shows the allocation of count plots and measure plots in the grid. In general there is no maximum limit or minimum requirement of the number of plots applied in timber cruising (Kurikka 2008; SFISL 2011). However, more plots may be used in small blocks to get a better estimate of the forest phenomena being measured. In the count plots the following attributes of the forest were collected: header information, such as crew names, date, basemap, block number, plot number and plot type; plot location (easting and northing); tree number; tree species; diameter; and tree condition.

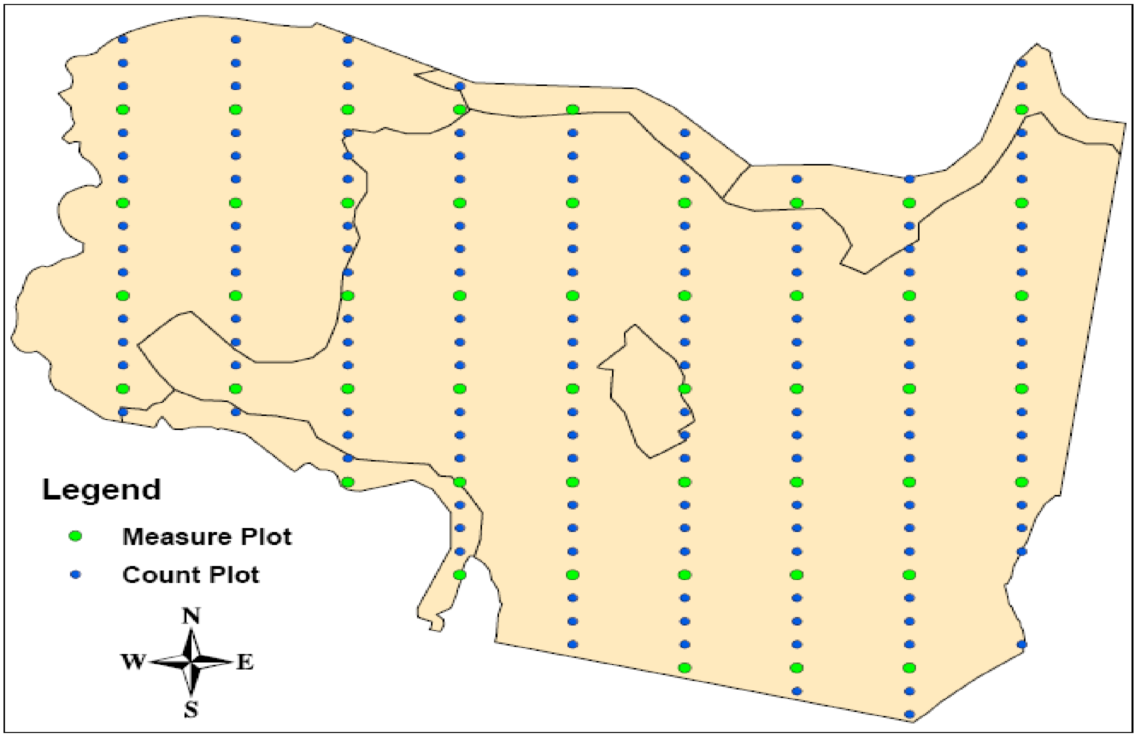

Figure 2.8 200 m x 50 m point survey grid in a block of Crossroute Forest (SFISL 2011).

In measure plots all the above attributes mentioned for count plots were collected. In addition the following attributes of forest were also collected: heights of some trees were measured and the heights of the rest of the *in-trees* of the plot were estimated; age of one tree, which represents the working group species, was measured.

The results of the pre-harvest inventory in the Crossroute Forest are shown in Table 2.5. The species composition, age and volume ($m^3 \cdot ha^{-1}$) of different blocks in this FMU are shown (Table 2.5). The net merchantable volume in this FMU varies from 52

$m^3 \cdot ha^{-1}$ to 178 $m^3 \cdot ha^{-1}$. According to this pre-harvest sampling the average net merchantable volume of the Crossroute Forest is 109 $m^3 \cdot ha^{-1}$ (Table 2.5).

Table 2.5 Stand description by blocks in Crossroute Forest from pre-harvest inventory.

Block Number	Species Composition*	Age (year)	Volume ($m^3 \cdot ha^{-1}$)			
			Gross	Merchantable	Net	UW
71430	Pt45 Mr16 Pj16 Bf7 Bw6 CE4 Sb3 Sw3	61	186	116	112	126
72219	Pt67 Pb23 Bw4 Ab3 Sw3	59	175	53	52	171
72801	Pj53 Sb38 Bw9	69	192	111	103	9
72805	Pj51 Sb45 Sw3 La1	80	212	158	147	2
71093	Pj55 Sb38 Bf7	68	228	66	62	0
71579	Sb31 Bf18 Bw16 Mr15 Pw10 Pt7 Pj3	69	146	192	178	82
Average		68	190	116	109	65

*Pt = trembling aspen, Mr = red maple, Pj = jack pine, Bf = balsam fir, CE = white cedar, Sb = black spruce, Sw = white spruce, Pb = balsam poplar, Bw = white birch, La = larch and Pw = white pine, Merch = merchantable, Net = Net merchantable, and UW = underutilized wood. Numbers with each species indicate the percentage of volume of that species available in the block.

Pre-harvest inventories conducted by Reynolds *et al.* (2008) in the Black Sturgeon Forest show an average net merchantable volume of 108.60 $m^3 \cdot ha^{-1}$ (Table 2.6) which is similar to the Crossroute Forest study. Due to the influence of different factors including species composition and age, the stand volume ($m^3 \cdot ha^{-1}$) varies by block in each of the two FMUs (Tables 2.5 and 2.6).

Table 2.6 Stand description by block in the Black Sturgeon Forest (Reynolds *et al.* 2008).

Block Number	Species composition*	Age (Year)	Net Merchantable Volume ($m^3 \cdot ha^{-1}$)
5334	Sb43 Po27 Bw26 Pj3 Sw1	Po44	121.93
5336	Sb30 Po26 Pj22 Bw20 Bf2	Po74 Sb79	103.35
5354	Sb49 Pj30 Po18 Bw3	Sb114 Pj64 Po54	134.10
5384	Sb60 Po23 Bw15 Pj2	Sb69 Po74	89.50
5875	Sb41 Bw32 Po23 Bf4	Sb69 Bw79 Po69	94.10
Average			**108.60**

*Po = poplar, Pj = jack pine, Bf = balsam fir, Sb = black spruce, Sw = white spruce and Bw = white birch. Numbers with each species indicate the percentage of volume of that species available in the block.

2.4.1.2 Post-harvest forest inventory

Harvestable biomass availability can be accurately estimated by using post harvest forest inventory. By doing cut-over sampling and measuring slash piles the amount of biomass left in the forest after harvesting can be determined. The techniques of post-harvest forest sampling are discussed in detail in Sorenson (2007), Bilyk (2009), Kurikka (2008), Reynolds *et al.* (2008) and Gautam (2010).

Post-harvest forest inventory studies were conducted in 2008 and 2009 in the Crossroute Forest. The estimates of total biomass from two post-harvest forest inventories are shown in Figures 2.9 and 2.10, respectively.

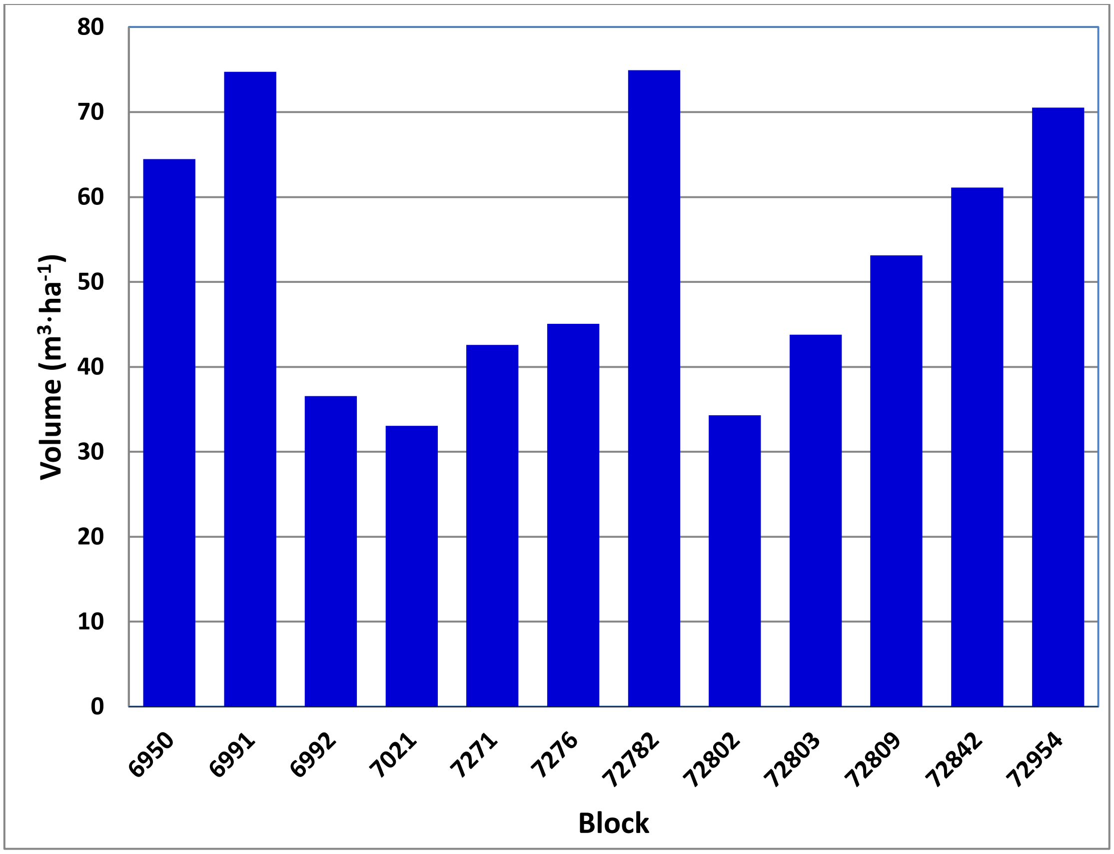

Figure 2.9 Cut-over residues in the Crossroute Forest in 2008 (Bilyk 2009).

The average cut-over residues in the Crossroute Forest without fine woody material is estimated at 60.4 $m^3 \cdot ha^{-1}$. Post-harvest inventories conducted by Reynolds *et al.* (2008) in the Black Sturgeon Forest show similar results.

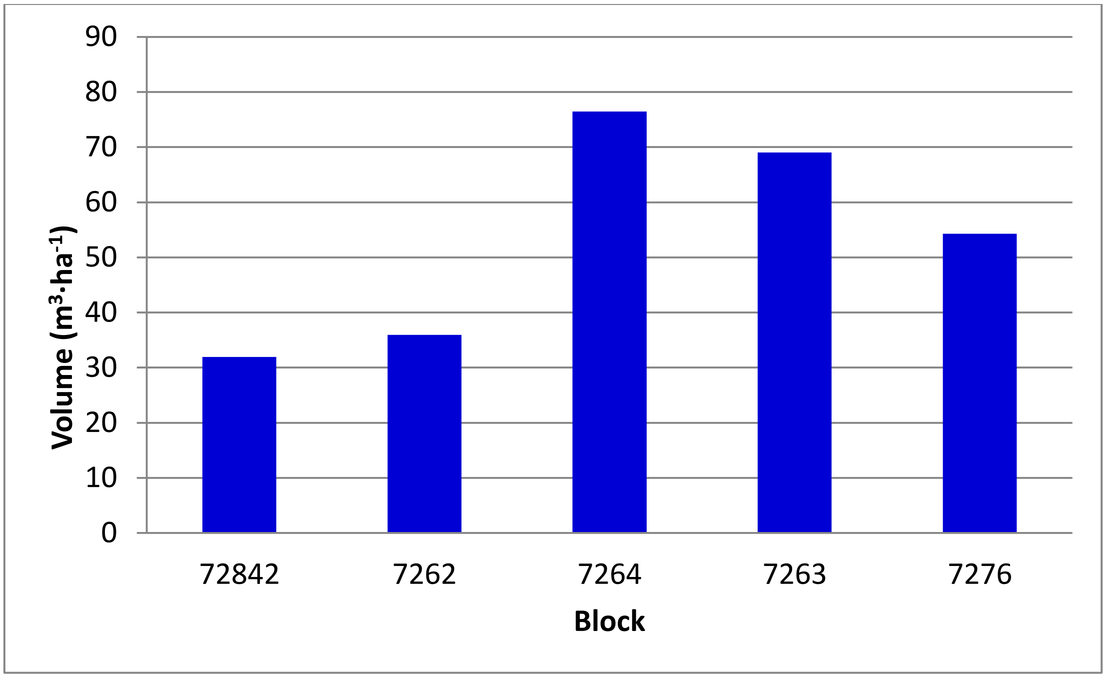

Figure 2.10 Cut-over residues in the Crossroute Forest in 2009.

2.4.2 New Provincial FRI in Ontario

FRI describes all areas within a FMU (OMNR 2007a). FRI information is used for forest management planning. The new FRI program is using a 10 year production cycle and an ecologically-based continuous inventory. In the new FRI, information about all lands within the Area of the Undertaking will be available. The OMNR is responsible to create and provide the FRI, and the Licensee is responsible to maintain and update the FRI continuously during the 10-year cycle (OMNR 2007a; OMNR 2009).

The main data sources that are being used in the process of preparing new FRI are: past and present records, maps, photographs, surveys, operational field cruises, sample plots, etc. (OMNR 2009). The major information available in the Polygon Forest layer of the FRI relevant to this research can be listed as follows: area; polygon types (productive forest, brush and alder, treed wetland, water, etc.); year of source; source of update; stage of development; year of last depletion/disturbance; overstorey year of origin; overstorey species composition; overstorey leading species; overstorey age; overstorey height; overstorey crown closure; overstorey site index; and overstorey site class (OMNR 2007a).

According to the new provincial FRI for Ontario, the FRI data will be readily available in a standardized format (OMNR 2009). The SFL holders should maintain and update the FRI continuously once they start using the new FRI. A sample of the FMP database for a typical block in one FMU is shown in Table 2.7. Further, Table 2.8 shows forest depletion information from which one can retrieve the estimate of available biomass. The depletion scenario presented in Table 2.8 is based on the FMP as shown in Table 2.7. It is expected that these databases can be obtained from the OMNR and forest companies in the future once the new FRI is completed. By interpreting the data from these sources, stand volume and biomass availability could be estimated at minimum cost. However, additional assessments could help determine biomass volume at local scales more accurately.

Table 2.7 Forest Management Planning (FMP) 2010-2020 for normal harvesting in Block 05_500 of Sapawe Forest (GreenForest Management Inc. 2009).

Stand Number	Area (ha)	FU	Age (yr)	Ht (m)	Stkg	SC	Species Comp	Volume (m^3)							
								Pj	Sb	La	Con. Sub tot.	Po	Bw	HW Sub tot.	Total
3f660156	0.4	CoMx1	85	56	3.2	1	Sb60 Pj30 Po10	14	28	0	42	5	0	5	47
3f666197	2	PjDom	95	11	6	2	Pj80 Bw10 Sb10	242	30	0	272	0	30	30	302
3f672203	0.4	SbLow	105	33	1.8	3	Sb100	0	26	0	26	0	0	0	26
3f673228	1	SbLow	105	11	0.6	3	Sb100	0	61	0	61	0	0	0	61
3f674235	2.1	PjDom	95	38	2	2	Pj80 Bw10 Sb10	263	33	0	296	0	33	33	329
3f690161	5.9	CoMx1	95	10	5.4	2	Pj50 Sb30 Po20	409	246	0	655	164	0	164	819
3f709222	15.3	PjDom	85	14	7.2	2	Pj70 Sb20 Bw10	1435	410	0	1845	0	205	205	2050
3f713268	0	CoMx2	95	13	0.5	2	Sb60 Bw30 Bf10	0	1	0	1	0	0	0	1
3f716174	2.3	SpDom	115	22	7	0	Sb90 La10	0	227	25	252	0	0	0	252
3f760218	0.1	PjDom	85	38	2	2	Pj70 Sb20 Po10	14	4	0	18	2	0	2	20
3f783277	1	CoMx2	85	18	1	2	Pj50 Po30 Bw10 Sb10	121	24	0	145	72	24	96	241
3f795321	0.7	PjDom	85	19	1	2	Pj70 Po20 Sb10	69	10	0	79	20	0	20	99
3f846236	35.1	PjDom	85	13	7	2	Pj80 Po10 Sb10	4179	522	0	4701	522	0	522	5223
3f878293	27.7	PjDom	85	38	2	2	Pj70 Bw10 Po10 Sb10	2889	413	0	3302	413	413	826	4128
3f898250	17.5	HwMx2	85	85	4	2	Bw40 Pj30 Po20 Sb10	466	155	0	621	311	621	932	1553
Total:	**112**							10101	2190	25	12316	1509	1326	2835	**15151**

Note: FU = forest unit, CoMx = conifer mix, PjDom = jack pine dominant, SbLow = black spruce lowland, SpDom = spruce dominant, HwMx = hardwood mix; Ht = height; Stkg = stocking; SC = site class; Comp = composition; Sb = black spruce, Pj = jack pine, Po = poplar, Bw = white birch, Bf = balsam fir and La = larch; Con. Sub tot. = conifer subtotal; HW Sub tot. = hardwood subtotal. Numbers with each species indicate the percentage of volume of that species available in the block.

Although data collection from secondary sources like these is less costly, there are some caveats of the information obtained through this method in terms of accuracy and completeness. For example, to determine a harvestable biomass factor with respect to the forest harvesting for the primary forest products, such as sawlog and pulpwood, a thorough post-harvest forest inventory is necessary, which is not available in the new FRI tables. However, the information about post-harvest biomass availability in the forest could be derived by tracking biomass truck movements using GPS, interpreting the bills of lading from the mill-gate scaling section, and using other available information about woody biomass for energy production from the companies.

Table 2.8 Depletion by clear-cut in Block 05_100 of the Sapawe Forest in 2007 (GreenForest Management Inc. 2009).

Stand Number	**Area (ha)**	**FU**	**Age (yr)**	**Ht (m)**	**Stkg**	**SC**	**Species Comp**	**Volume (m^3)**					
								Pj	**Sb**	**Con. Sub tot.**	**Po**	**HW Sub tot.**	**Total**
2a498966	31.3	PjDom	95	20	0.7	2	Pj80 Po10 Sb10	3115	389	3504	389	389	3893
2a555988	9.3	PjDom	85	20	0.6	2	Pj70 Sb30	674	289	963			963
2a572933	14.2	PjDom	95	18	1.3	2	Pj80 Sb20	2625	656	3281			3281
2a582975	2.8	SpUpl	85	14	0.8	1	Sb80 Pj20	66	263	329			329
Block Area:	**57.6**						**Block Volume:**	6480	1597	8077	389	389	**8466**

Note: FU = forest unit, PjDom = jack pine dominant, SpUpl = spruce upland; Ht = height; Stkg = stocking; SC = site class; Comp = composition; Sb = black spruce, Pj = jack pine, and Po = poplar; Con. Sub tot. = conifer subtotal; HW Sub tot. = hardwood subtotal. Numbers with each species indicate the percentage of volume of that species available in the block.

2.5 Conclusions

Proper planning is important to collect the right types and amount of data in time for a complex research endeavor. Otherwise the cost of the research project will increase due to the collection of irrelevant data. This can even go to the stage of project failure due to lack of relevant data, shortage of money and crossing the time limit of project completion. This study suggests that both the secondary and the primary data sources complement each other, and use of raster text files (with 1 km x 1 km grid) for road network, forest land use and forest depletion layers is appropriated for optimization models to analyze biomass supply chains for bioenergy production at the regional scale.

If woody biomass for energy use in NWO continues to develop to become a regular part of forest harvesting, the post-harvest field inventory data can be augmented from other sources. For example, the tracking of biomass truck movements using GPS, the interpretation of bills of lading from mill-gate scaling, and the use of other available information about biomass for energy production from the companies enrich the information about post-harvest biomass availability in the forest. Eventually, by developing biomass factors with respect to the harvest volume for primary forest products, the harvestable amount of available woody biomass can be estimated. Using this method costs can be minimized in research projects to determine more accurately woody biomass availability for the production of bioenergy in NWO.

Chapter 3

Woody biomass availability for bioenergy production using forest depletion spatial data in northwestern Ontario[2]

3.1 Introduction

Woody biomass is a competitive, low greenhouse gas (GHG) emission and renewable fuel that is replacing non-renewable fossil fuels for energy production all over the world (Gan and Smith 2006; Layzell *et al*. 2006; Meehan *et al.* 2010). The major biomass feedstock resources used for energy production are forest-based woody biomass, energy crops, agricultural crop residues, and urban wastes (McKenney *et al.* 2011). Although, the establishment of local sustainable bioenergy systems is globally desirable, there are apprehensions about sustainable supply of biomass feedstock in order to keep the bioenergy plants operational. In the last decade, a number of methods have been used to assess different types of biomass feedstock for bioenergy production under local conditions. For example, geographic information system (GIS)-based spatial estimation methods have been used for bioenergy feedstock assessment using land use maps and agricultural statistics in Japan (Yoshioka *et al.* 2005), in the Czech Republic (Lewandowski *et al.* 2006), in the European Union (Panoutsou *et al.* 2009), in the U.S. (Perez-Verdin *et al.* 2009), in Portugal (Viana *et al.* 2010), in Australia (Herr and Dunlop 2011), and in Romania (Scarlat *et al.* 2011). Tyndall *et al.* (2011) conducted forest inventories of low-value trees and interviewed large sawmill owners to assess

[2] A version of this chapter is in press for publication in the Canadian Journal of Forest Research.

biomass availability in the U.S. Cornbelt. A few studies have also assessed the supply costs of biomass using forest inventory and competing industry data (Voivontas *et al.* 2001; Stasko *et al.* 2011). All these studies found large variation in biomass availability and costs, depending on the method of assessment, type of biomass, cropping frequency, and yield under local conditions.

In Canada, similar variations in biomass availability for bioenergy production over different years have been found in Peace River region of Alberta (Stephen *et al.* 2010) and in southern Ontario (McKenney *et al.* 2011). Canada has 402 million ha of forest land that can fulfill 60% of the domestic renewable energy requirements, whereas at present woody biomass is only contributing to 6% of its energy production (Bradley 2006a). The Crown forests in Canada are managed by the provinces, by dividing these into geographic planning areas known as forest management units (FMU). Most of these FMUs are managed by individual forest companies under a sustainable forest licence (SFL). The quantity of forest biomass produced during the harvesting operation varies for each FMU depending on the type of forest and the harvesting methods and systems used (Pulkki 1978; Ride 1998). In addition, the availability of forest harvest residue (FHR) biomass, which is in the form of tree tops, branches and broken pieces left in the forest after harvesting commercial species, may vary from site to site within each FMU, if the harvesting operation is dispersed over a wide region (Wood and Layzell 2003). The woody biomass may also be collected from underutilized wood (UW) species, which are not commercially important to harvest for lumber and pulpwood production. The harvesting operations result in forest depletion of productive forest area, which can be accurately assessed using GIS techniques. The extent of forest depletion of productive forest area can be used for accurately assessing the availability of woody biomass from the FMUs.

As a case study, we assess the annual woody biomass availability for bioenergy production in northwestern Ontario (NWO) from 18 FMUs. There are three existing combined heat and power (CHP) plants and one proposed woody biomass-based power generating stations in NWO. The three existing CHP plants include: Abitibi-Bowater (recently renamed Resolute Forest Products) Thunder Bay Power Plant (ABTB), Abitibi-Bowater Fort Frances Power Plant (ABFF) and Domtar Dryden Power Plant (DDPP), with production capacities of 61 megawatt hours (electricity) (MW_e) and 16 megawatt hours (thermal) (MW_{th}), 50 MW_e and 61 MW_{th}, and 30 MW_e and 37 MW_{th}, respectively (Abitibi-Bowater Inc. 2011; McKinnon 2011). The proposed biomass based power plant is the Atikokan Generating Station (AGS). At present AGS is running with coal feedstock with production capacity of 230 MW_e. It is currently being converted from a coal-based to a biomass-based power plant. The annual biomass feedstock requirements of ABTB, ABFF, DDPP and AGS power plants are around 730,000 green tonnes (gt), 800,000 gt, 480,000 gt and 200,000 gt (with AGS operating at 10% of its capacity with woody biomass), respectively. Therefore, the total annual woody biomass feedstock requirement is about 2.2 million gt to run these four power plants. A study conducted by the Ontario Ministry of Energy (OME 2007) found that within a 500 km radius of the AGS, approximately 2.7 million oven dry tonnes (ODt) of woody biomass feedstock is available annually from FHR, UW and mill wood waste. However, the OME study is based on estimates of forest biomass availability using personal surveys and approximate methods. Moreover, as most sawmills are not operating at present, there is not much wood waste being generated. Reynolds *et al*. (2008) conducted a research on the feasibility of forest feedstock for bioenergy production from one FMU in NWO. No other study has ever attempted to quantify the woody biomass availability for all the four bioenergy stations in the region. We estimate the FHR and UW biomass availability per km^2 using pre- and post-harvest inventory and forest depletion data.

3.2 Study Area

The research area for this study consists of 18 FMUs (Armstrong Forest, Black Sturgeon Forest, Caribou Forest, Crossroute Forest, Dog-River Matawin Forest, Dryden Forest, English River Forest, Kenora Forest, Lac Seul Forest, Lake Nipigon Forest, Lakehead Forest, Ogoki Forest, Red Lake Forest, Sapawe Forest, Spruce River Forest, Trout Lake Forest, Wabigoon Forest and Whiskey Jack Forest), which fall in seven Ontario Ministry of Natural Resources (OMNR) districts (Dryden, Fort Frances, Kenora, Nipigon, Red Lake, Sioux Lookout and Thunder Bay) of northwestern Ontario (NWOPA 2007). The extent of research area is 167,184 km^2 (324 km (N-S) x 516 km (E-W)). The four power plants (ABTB, ABFF, AGS and DDPP) and the 18 FMUs are shown in Figure 3.1.

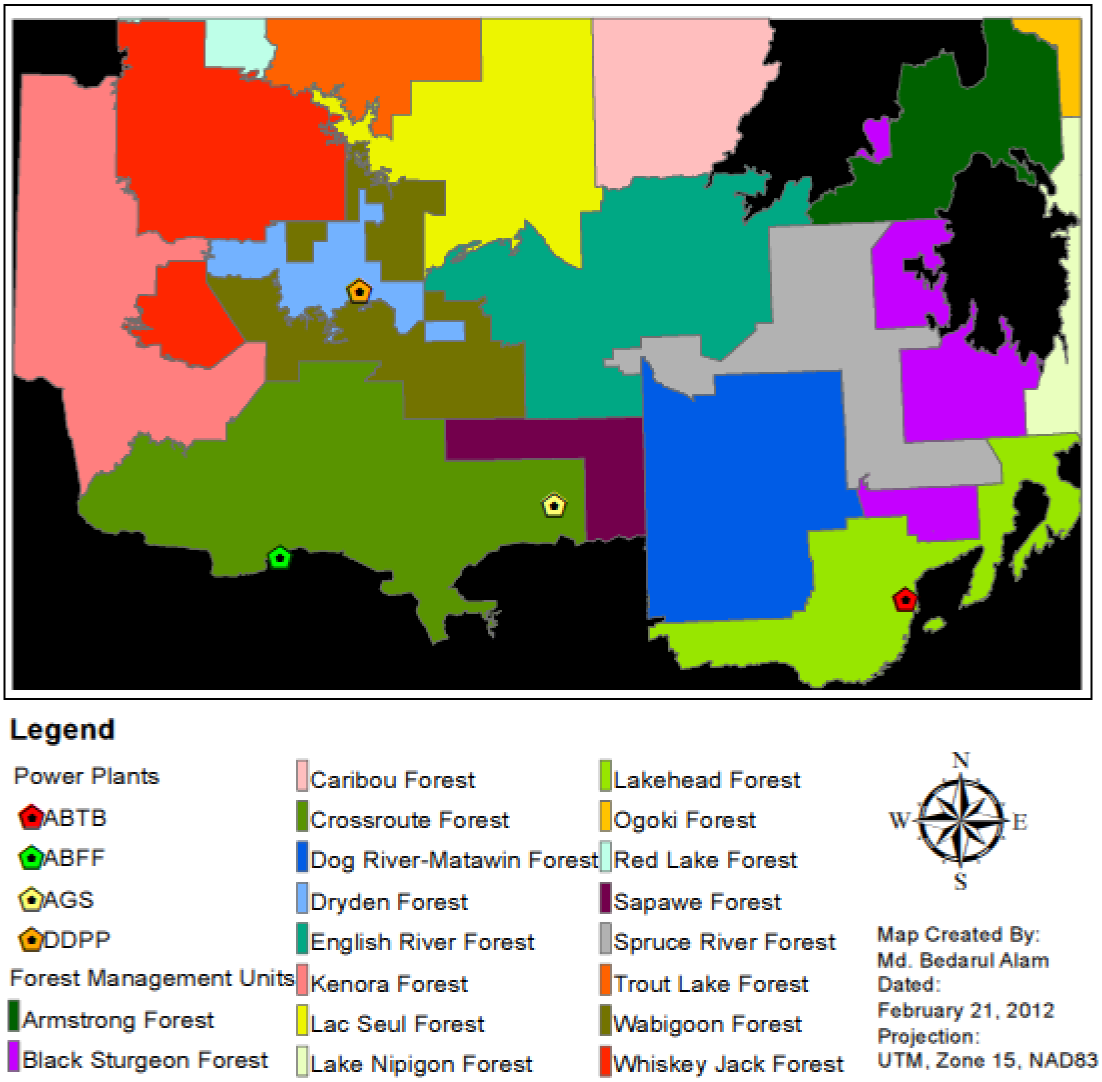

Figure 3.1 Locations of 18 FMUs and 4 power plants in the research area (324 km (N-S) x 516 km (E-W) extent) in northwestern Ontario (NWO).

The study area is in the Boreal forests and is dominated by upland coniferous and mixedwood forests (OMNR 2011). The most common tree species available in these northwestern Ontario FMUs are: balsam fir (*Abies balsamea* (L.) Mill.), balsam poplar (*Populus balsamifera* L.), black spruce (*Picea mariana* (Mill.) Britton, Sterns & Poggenburg), jack pine (*Pinus banksiana* Lamb.), red pine (*Pinus resinosa* Sol. ex

Aiton), tamarack (*Larix laricina* (Du Roi) K. Koch), trembling aspen (*Populus tremuloides* Michx.), white birch (*Betula papyrifera* Marsh.), white pine (*Pinus strobus* L.), and white spruce (*Picea glauca* (Moench) Voss). The forest is sustainably managed using forest management planning on a 10-year cycle, applying growth and yield modeling over a 150-year horizon. The average rotation age of trees is 80 years in the study area (OMNR 2010). The harvesting systems and methods used in the FMUs include: (i) Feller-Buncher/Grapple-Skidder/Roadside-Delimber/Slasher system (conventional Full-Tree to Roadside, Shortwood-to-Mill method), (ii) Single-Grip Harvester/Forwarder system (Cut-to-Length method), (iii) Feller-Buncher/Skidder/Delimber-Debarker-Chipper system (Full-Tree to Roadside, Chip-to-Mill method), and (iv) Feller-Buncher/Grapple-Skidder/Stroke Delimber system (Full-Tree to Roadside, Tree-Length-to-Mill method) (Ride 1998). The use of biofibre (FHR and UW) and its recording is very recent in Ontario as it was mainly sawmill residues and pulpmill wastes that were used for energy (mainly heat) production. The expansion of the combined heat and power (CHP) plants at the pulp mills has only been a recent phenomenon in Ontario; as a result there are no long-term official provincial statistics available on biofibre use.

3.3 Methods

The acronyms used in this paper are described in the Acronyms section of this dissertation (p. xiv). The flow chart in Figure 3.2 describes the methodology used for this study. The pre- and post-harvest inventory was only conducted in one FMU in the western part of the study area but paralleled that by Reynolds *et al*. (2008) done in the eastern part. We could then compare our data of pre- and post-harvest inventory with that found by Reynolds *et al.* (2008). We found that our results were very similar to those reported in that study. The results were also very similar to other studies done by FPInnovations (e.g., Kapuskasing) but unfortunately only recorded in unpublished literature. At this point we have not yet conducted pre- and post-harvest inventory in other FMUs. In the future this could be done to add to the confidence in the data.

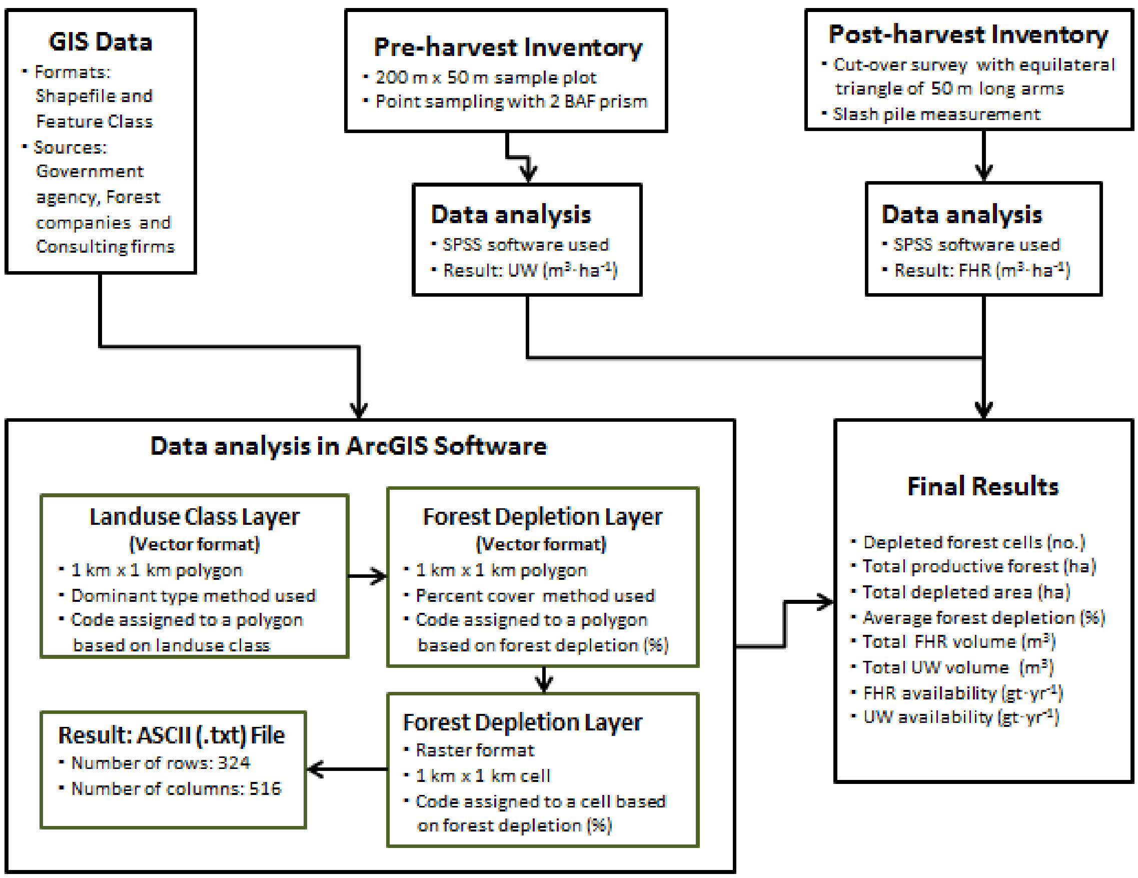

Figure 3.2 Flow-chart of assessing woody biomass availability.

The western pre-harvest inventory was conducted in the Crossroute Forest during the summer of 2008, where harvesting operation had been planned for the coming winter season. A systematic grid of 200 m x 50 m was laid in different blocks of the FMU to conduct the pre-harvest inventory using a prism with a basal area factor (BAF) of 2 (Figure 2.8). The measure plots were placed in each forest stand at 200 m intervals, and the count plots were placed at 50 m intervals (Figure 2.8). This resulted in a ratio of count plots to measure plots of 3:1 (SFISL 2011). The attribute data collected for count plots included: crew information, date, basemap, block number, plot number, plot type, plot location, tree number, tree species, diameter and condition of tree. For measure plots, in addition to the attributes' data for count plots, height and age of trees that represent the working group species were also measured. The heights of the remaining trees in the plot were estimated.

Post-harvest inventories within the same FMU were conducted in the summers of 2008 and 2009. The amount of biomass left in the forest after harvesting was determined using cutover sampling and measuring slash piles (Bilyk 2009). The post-harvest cutover survey was conducted using the line intersect method in triangular plots (each side of the triangle being 50 m). The triangular plots were located along transect lines in the harvest block on a 100 m x 100 m grid. All downed coarse woody material (CWM) over 7.5 cm diameter outside bark (DOB) along each line was recorded. The fine woody material (FWM) with the DOB between 7.5 and 2.5 cm was also tallied on every third transect of each triangle. One point sampling was done at each vertex of the triangle using a prism of 2 BAF, and data for type of species, diameter at breast height (DBH) and heights of the trees were collected. The volume of chipper-debris piles was estimated by measuring the average length, width and depth of each pile using two long poles and a cord[3]. The data collected from pre-harvest inventory was analyzed using local volume tables (Luckai 2011; MNDMF 2011) and the data from post-harvest inventory was analyzed using SPSS version 18.0 software. Some equations used for data analysis are as follows.

Equation (1) was used to estimate the volume of downed woody material (both the CWM and the FWM) in the triangular plot (Nemec and Davis 2002; Bilyk 2009).

$$V_d = \frac{\pi}{2L} \sum_{j=1}^{m_i} \frac{A_{ij}}{\cos \lambda_{ij}} \qquad (1)$$

Where:

V_d = volume of downed woody material, $m^3 \cdot ha^{-1}$

L = length of sampling unit (150 m)

i = transect line

j = piece number

m_i = number of pieces that intersect the transect line

a_{ij} = cross-sectional area (cm^2) of j^{th} piece at the intersection with i^{th} transect line

λ_{ij} = the acute angle between j^{th} piece and horizontal at i^{th} transect line

Equation (2) was used to estimate the volume of woody biomass in the beehive type of forest harvest residue pile (V_b) in the cut over (Bilyk 2009).

$$V_b = H * 0.5N * 0.5E \qquad (2)$$

[3] The techniques of post-harvest forest sampling are discussed in detail in Sorenson (2007), Bilyk (2009), Kurikka (2008) and Reynolds *et al.* (2008).

Where:

V_b = Volume of FHR pile of bee hive type (m^3)

H = Height of pile (m)

N = Width of pile from north to south direction (m)

E = Width of pile from east to west direction (m)

Equations (3) and (4) were used to calculate the volume of FHR (V_r) and UW (V_u) in a forest cell.

$$V_r = A_c * R_i * F_r \qquad (3)$$

Where:

V_r = Volume of harvest residue in a forest cell (m^3)

A_c = Area of a forest cell (km^2)

R_i = Forest depletion (or forest residue area) in a forest cell (%)

F_r = Volume factor of forest harvest residue (m^3/km^2)

$$V_u = A_c * U_i * F_u \qquad (4)$$

Where:

V_u = Volume of underutilized wood in a forest cell (m^3)

U_i = Underutilized wood area in a forest cell (%)

F_u = Volume factor of underutilized wood (m^3/km^2)

In this paper, we conservatively assumed that 67% of logging residues are harvestable, leaving sufficient material on-site for maintaining forest health. The use of 67% of logging residue is based on past literature related to conditions found in northern Ontario. In our literature review, we found that Borjesson (2000), and Gan and Smith (2006) used a 70% residue recovery rate; Kerstetter and Lyons (2001) estimated a logging residue recovery rate from 70% to 97%; Ranta (2004) estimated an economic woody biomass recovery rate of 65%; Nurmi (2007) determined a logging residue recovery from 66.8% to 78.7%; and FPInnovations FERIC (2008) indicated that 67% woody biomass is recoverable. At present four main tree species (balsam fir, black spruce, jack pine and white spruce) are mostly used for commercial production of lumber and pulpwood in NWO. Other available tree species in the FMUs of the research area are assumed as candidates to be used as UW for bioenergy production. Based on our experience we also conservatively assumed that 67% of theoretically available UW are technically harvestable. Equations (5) and (6) were used to calculate total theoretical and technically available woody biomass in the whole research area.

$$V_t = \sum_{i=1}^{n}\left(\sum_{i=1}^{n_i} V_r + \sum_{i=1}^{n_i} V_u\right) \qquad (5)$$

Where:

V_t = Total theoretical availability of woody biomass in whole research area (m^3)

n_i = Total number of forest cells in each grid code type (i = 1, ...,7)

n = Total number of forest cells in whole research area

$$V_a = \sum_{i=1}^{n}\left(\sum_{i=1}^{n_i} V_r * H_r + \sum_{i=1}^{n_i} V_u * H_u\right) \qquad (6)$$

Where:

V_a = Total technical availability of woody biomass in whole research area (m^3)

H_r = Harvesting factor for forest harvest residue (assumed to be 0.67)

H_u = harvesting factor for underutilized wood (assumed to be 0.67)

Equation (7) was used to find the total woody biomass availability (gt) in the research area.

$$B_a = V_a * F_w \qquad (7)$$

Where:

B_a = Total woody biomass availability in whole research area (gt)

F_w = Conversion factor of woody biomass from volume to weight (1 m^3 = 0.876 gt)

GIS data in Shapefile and Geodatabase formats were collected from OMNR, SFL holders and consultant companies (OMNR 2007a; OMNR 2009; Abitibi-Bowater Inc. 2009; Greenmantle Forest Inc. 2009; GreenForest Management Inc. 2009; LIO 2010). ArcGIS software was used to prepare a spatial database in text format for the research area (167,184 km^2) (Burrough1986; Ellis 2001; Jensen *et al.* 2005; ESRI 2010). The vector grid was first converted to a raster layer, which was used to generate an ASCII (text) file. A cell usually represented only a single feature, however, when only a small portion of the cell contained a particular type of feature, the decision making to assign a feature to the cell became difficult (Nichols 2004). Therefore, different data input methods were used for different types of features to convert Shapefiles and Geodatabases (original spatial data) to a workable format (ASCII file). Two main spatial layers, forest landuse layer and forest depletion layer, were prepared using a grid size of 1 km^2 (1 km x 1 km). The forest landuse layer was prepared using the dominant type of data input method (ESRI 2010). In this method, grid code entity was assigned to the feature having more than 50% area of the cell. Code numbers were assigned to each grid cell for different landuses in the forest. The forest depletion layer was prepared using the percent occurrence data input method (ESRI 2010). In this method, code numbers 1-7 were assigned to the grid cell depending on depletion percentage in the cell within productive forest. This yielded more representative information on forest depletion in different geographic locations in the study area. The grid codes assigned for the cells of depletion in productive forest are shown in Table 3.1. The grid codes assigned for the depleted forest cells are as follows: 1 is 100% (100 ha) depletion, 2 is >= 80% to <100% depletion, 3 is >= 60% to <80% depletion, 4 is >= 40% to <60% depletion, 5 is >= 20% to <40% depletion, 6 is > 0% to <20% depletion and 7 is 0% depletion. The other codes used for this layer were 8 (lake/water) and 9 (other landuse). Forest depletion in the research area was estimated using these layers and inventory data. The forest depletion data was then used to assess the availability of biomass in the 18 FMUs. The types and amount of woody biomass availability in each of the forest cells depends on the percentage of depletion of the forest cells. For example, if 100% of the area of a cell is depleted, 100% FHR is available and 0% UW is available in this cell, and if 90% of the area of a cell is depleted, 90% FHR is available and 10% UW is available in this cell. If a cell is 0% depleted, no FHR is available (Table 3.1). An assumption in this study is that for a cell having 0% depletion, although UW is available it is not harvested. We also compared the results of our study, which was focused in the western part of NWO, with that of Reynolds *et al*. (2008) that was conducted in the Black Sturgeon Forest, a FMU located in the eastern part of the study area (Figure 3.1).

Table 3.1 Grid code assigned to depleted cells in productive forests.

Grid Code	Depleted area of forest cell (%)	FHR[*] availability in a forest cell (%)	UW[**] availability in a forest cell (%)
1	100% (100 ha)	100% (100 ha)	0%
2	>= 80% to <100%	>= 80% to <100%	> 0% to <20%
3	>= 60% to <80%	>= 60% to <80%	>= 20% to <40%
4	>= 40% to <60%	>= 40% to <60%	>= 40% to <60%
5	>= 20% to <40%	>= 20% to <40%	>= 60% to <80%
6	> 0% to <20%	> 0% to <20%	>= 80% to <100%
7	0%	0%	100%

[*]FHR = forest harvest residue, [**]UW = underutilized wood

3.4 Results and Discussion

The analyses of pre-harvest inventory (species composition, age and net merchantable volume in each block planned for harvesting) in the Crossroute Forest show that the stand volume varies from block to block in the FMU due to the influence of factors such as species composition and age. The net merchantable volume in this FMU was found to vary from 52 $m^3 \cdot ha^{-1}$ to 178 $m^3 \cdot ha^{-1}$ and the average net merchantable volume of the Crossroute Forest was found to be 109 $m^3 \cdot ha^{-1}$. The average gross, merchantable and UW volume were found to be 190 $m^3 \cdot ha^{-1}$, 116 $m^3 \cdot ha^{-1}$ and 65 $m^3 \cdot ha^{-1}$, respectively (Table 2.5). In this forest 36% of trees fall under the category of UW which constitutes 38% of the volume of wood. Therefore, the results of pre-harvest inventory determined that on average the theoretical UW availability in FMUs of NWO is at least (conservatively) 60 $m^3 \cdot ha^{-1}$. The results of post-harvest forest inventory are shown in Tables 3.2 and 3.3. The average cut-over residues in the Crossroute Forest with FWM was found to be 61.6 $m^3 \cdot ha^{-1}$, and without FWM was found to be 60.4 $m^3 \cdot ha^{-1}$, respectively (Table 3.2). Standing tree volume ($m^3 \cdot ha^{-1}$) in the Crossroute Forest cut-overs is shown in Table 3.3. The average gross volume, merchantable volume, net volume and dead volume of standing trees found were 14.6 $m^3 \cdot ha^{-1}$, 8.5 $m^3 \cdot ha^{-1}$, 7.7 $m^3 \cdot ha^{-1}$ and 2 $m^3 \cdot ha^{-1}$, respectively (Table 3.3).

Table 3.2 Cut-over residues in Crossroute Forest of northwestern Ontario (NWO).

Block Number	Cover Type	Volume of CWM* ($m^3 \cdot ha^{-1}$)	Volume of FWM** ($m^3 \cdot ha^{-1}$)	Volume of residues in roadside piles ($m^3 \cdot ha^{-1}$)	Total volume of residues without FWM ($m^3 \cdot ha^{-1}$)	Total volume of residues with FWM ($m^3 \cdot ha^{-1}$)
6950	Conifer	64.46	1.63	0.00	64.46	66.09
6991	Hardwood	74.75	1.95	0.00	74.75	76.69
6992	Hardwood	36.55	1.24	0.00	36.55	37.79
7021	Conifer	33.05	1.61	24.20	57.25	58.86
7262	Mixed	35.95	0.00	0.00	35.95	35.95
7263	Mixed	69.01	0.00	0.00	69.01	69.01
7264	Mixed	76.45	0.00	0.00	76.45	76.45
7271	Conifer	42.59	1.81	0.00	42.59	44.40
7276	Hardwood	45.06	1.22	27.80	72.86	74.08
72782	Conifer	74.93	1.51	0.00	74.93	76.44
72802	Conifer	34.31	0.71	0.00	34.31	35.02
72803	Conifer	43.79	1.83	0.00	43.79	45.62
72809	Conifer	53.11	0.80	0.00	53.11	53.91
72842	Hardwood	61.11	1.73	37.92	99.02	100.76
72954	Hardwood	70.51	1.72	0.00	70.51	72.23
Average		54.38	1.18	5.99	60.37	61.55

*CWM = coarse woody material, **FWM = fine woody material.

Table 3.3 Standing tree volume in cut-over of Crossroute Forest in NWO.

Block Number	Standing in Cut-over ($m^3 \cdot ha^{-1}$)			
	Gross	Merchantable	Net	Dead
6950	5.8	0.0	0.0	5.8
6991	35.9	17.4	14.0	17.1
6992	12.7	6.5	6.5	0.0
7021	12.1	8.3	8.3	0.0
7271	14.5	8.8	8.8	0.0
7276	19.5	11.0	10.1	0.0
72782	3.1	0.3	0.3	0.0
72802	12.1	5.7	4.7	1.0
72803	0.0	0.0	0.0	0.0
72809	10.1	4.8	4.8	0.0
72842	15.6	12.2	9.8	0.0
72954	34.3	26.9	24.7	0.0
Average	14.6	8.5	7.7	2.0

Reynolds *et al.* (2008) presented similar results in their study in the Black Sturgeon Forest, where 43% of measured trees were under the UW category. For example, they found that gross merchantable volume, merchantable volume and net merchantable volume of wood in the Black Sturgeon Forest were 189 $m^3 \cdot ha^{-1}$, 116 $m^3 \cdot ha^{-1}$ and 109 $m^3 \cdot ha^{-1}$, respectively. They also found that the net merchantable volume in their study areas varied from 94 $m^3 \cdot ha^{-1}$ to 134 $m^3 \cdot ha^{-1}$. The variation of net merchantable volume in our study is more as compared to Reynolds *et al.* (2008), because the Crossroute Forest is a much larger area and has a larger variation in species as compared to the Black Sturgeon Forest. Also Reynolds *et al.* (2008) looked at sample stands in a limited geographic area, while our study looked at compartments over a much larger area. Therefore, the results of post-harvest inventory show that on average the theoretical availability of FHR in FMUs of NWO is approximately 60 $m^3 \cdot ha^{-1}$. However, due to the existence of technical limitations it is not possible to harvest all woody biomass from the forest (Viana *et al.* 2010). By using 0.67 harvesting factor the technical availability of each type of woody biomass becomes 40.2 $m^3 \cdot ha^{-1}$; this matches in-field anecdotal experience of an average one truck-load of biomass per hectare harvested. After harvesting there is still sufficient material on-site to meet the Ontario Forest Management Guide for Natural Disturbance Pattern Emulation (OMNR 2002). Depending on the depletion percent of forest cells, the amounts of theoretically and technically available FHR and UW in a forest cell (1 km^2 area) are shown in Table 3.4. For example, if a cell is 100% depleted, the theoretical availability and technical availability of FHR are 6000 m^3 and 4020 m^3, respectively in this cell, and there is no UW available. Converting these into green tonnes (1 m^3 = 0.876 gt), the theoretical and technical availability of each type of woody biomass in the FMUs of NWO are 52.56 $gt \cdot ha^{-1}$ and 35.21 $gt \cdot ha^{-1}$, respectively.

Table 3.4 Theoretical and technical (assuming 67% recovery) biomass availability (m^3) in a forest cell (1 km x 1 km or 100 ha).

Grid Code	Cell area depletion (%)	Area of UW in a cell (%)	Theoretically available biomass in a cell (m^3)			Technically available biomass in a cell (m^3)		
			FHR	UW	Total	FHR	UW	Total
1	100% (100 ha)	0%	6000	0	6000	4020	0	4020
2	>=80% to <100%	> 0% to <20%	5400	600	6000	3618	402	4020
3	>=60% to <80%	>=20% to <40%	4200	1800	6000	2814	1206	4020
4	>=40% to <60%	>=40% to <60%	3000	3000	6000	2010	2010	4020
5	>=20% to <40%	>=60% to <80%	1800	4200	6000	1206	2814	4020
6	>0% to <20%	>=80% to <100%	600	5400	6000	402	3618	4020

The results of the forest landuse spatial layer analysis are shown in Figure 3.3. It was found that out of a total area of 16,718,400 ha, productive forests cover 10,006,200 ha, water/lakes cover 2,661,500 ha and the area under other landuse category was 4,050,700 ha. That means productive forest consists of about 59.8 % of total land area in NWO.

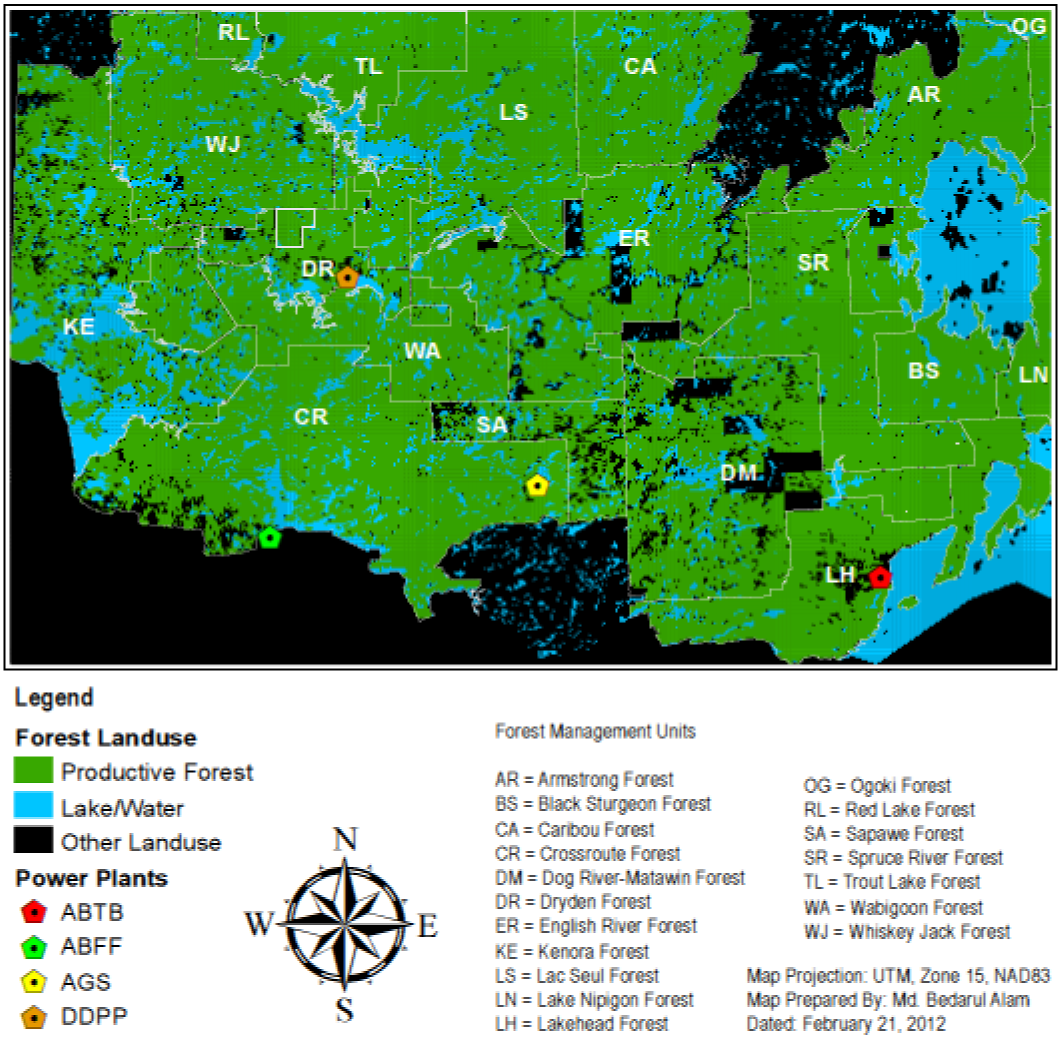

Figure 3.3 Forest landuse classes in 18 forest management units of NWO.

The forest depletion from 2002 to 2009 in 18 FMUs of NWO along with the location of the four bioenergy generating stations are shown in Figure 3.4. The total forest depletion area over the period (2002 to 2009) was found to be 426,070 ha. The annual average forest depletion was found to be 60,867 ha, which is 0.61% of the productive forest area under study.

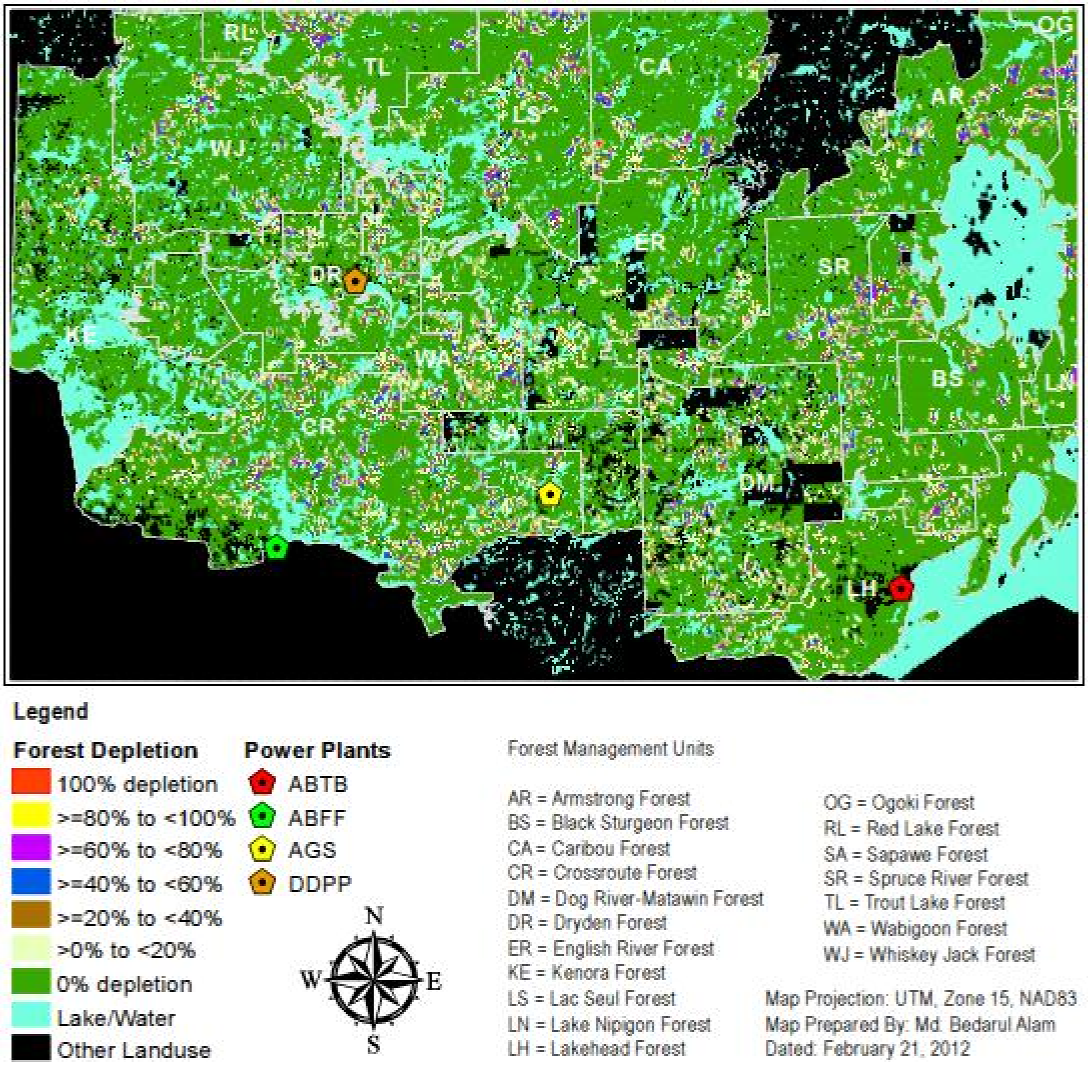

Figure 3.4 Forest depletion in productive forests of NWO (from 2002 to 2009).

The theoretical and technical availability of woody biomass (gt) in productive forests as a result of forest depletion from 2002 to 2009 in each category (grid code) of forest depletion are shown in Table 3.5. The theoretically available FHR and UW over this period were found to be over 22 million gt and 79 million gt, respectively. The technically available FHR and the UW over this period were over 15 million gt and 53 million gt, respectively. Therefore, the annual average theoretically available FHR and

UW were approximately 3.2 million gt and 11.3 million gt, respectively. By using a harvesting factor of 0.67, the annual average technical availability of FHR and UW were about 2.1 million gt and 7.6 million gt, respectively. We observed that there were differences in annual forest depletion over the seven year historic period (2002 to 2009) (Table 3.5). The lowest annual depletion occurred in 2002-’03 (40,040 ha). From then the amount of forest depletion gradually increased. The highest annual depletion was found in 2005-’06 (74,140 ha). Then annual forest depletion started to gradually decrease. Eventually, in 2008-’09 the amount of forest depletion began to slightly increase (Table 3.5).

Table 3.5 Theoretical and technical woody biomass availability (gt) in productive forest as a result of forest depletion from 2002 to 2009 assuming 67% technical availability.

Depletion year	Forest cells depleted under different codes (no.)						Total cells (no.)	Total depleted area (ha)	Total FHR availability (gt)		Total UW availability (gt)	
	1	2	3	4	5	6			Theoretical	Technical	Theoretical	Technical
2002-'03	0	3	61	194	422	1,314	1,994	40,040	2,104,502	1,410,017	8,375,962	5,611,894
2003-'04	5	14	75	265	583	1,603	2,545	53,780	2,826,677	1,893,873	10,549,843	7,068,395
2004-'05	2	14	118	310	691	1,857	2,992	64,520	3,391,171	2,272,085	12,334,781	8,264,303
2005-'06	0	28	107	396	839	1,916	3,286	74,140	3,896,798	2,610,855	13,374,418	8,960,860
2006-'07	1	18	126	347	731	1,762	2,985	67,440	3,544,646	2,374,913	12,144,514	8,136,824
2007-'08	0	19	123	312	657	1,636	2,747	61,990	3,258,194	2,182,990	11,180,038	7,490,625
2008-'09	0	18	123	368	648	1,609	2,766	64,160	3,372,250	2,259,407	11,165,846	7,481,117
Total	8	114	733	2,192	4,571	11,697	19,315	426,070	22,394,239	15,004,140	79,125,401	53,014,019

The research findings show that there is sufficient FHR and UW biomass feedstock available in NWO to run the four major power generating plants sustainably. Reynolds *et al.* (2008) also stated that there is enough FHR to produce bioenergy in NWO sustainably based on their inventory in the Black Sturgeon Forest. However, their study did not take into account four power generating stations and biomass availability from 18 FMUs. The species composition across the FMUs in the research area is almost similar (OMNR 2011).

As the forest inventory conducted by Reynolds *et al.* (2008) in the Black Sturgeon Forest (in the eastern part of research area) and our forest inventory in Crossroute Forest (in the western part of research area) found similar residue volumes we assume for the purpose of this study that there is no major difference in woody biomass availability per hectare harvested between eastern and western parts of the study area. In the future as additional similar pre- and post-harvest studies are conducted better precision in the data can be developed. Woody biomass feedstock from some areas (which are farther from power plants) in the research area will not be economically available due to cost resulting from excessive transport distances.

The government of Ontario maintains the forest resource inventory (FRI) data for the purpose of forest management planning (FMP). According to the new provincial FRI guidelines of Ontario, the FRI data will be readily available in a standard format. The SFL holders will be required to maintain and update FMP information continuously and this data will be available from the year 2015 onward (OMNR 2010). The FMP data along with FRI database and forest landuse classification will be helpful in compiling information about the forest depletion rate. By interpreting the data from OMNR and forest companies, the stand volume ($m^3 \cdot ha^{-1}$) can also be derived without pre-harvest forest inventory (Alam and Pulkki 2011). As the biomass harvesting becomes a regular part of business in NWO, biomass availability can be better derived by tracking biomass trucks with GPS, by interpreting the bills of lading from mill-gate scaling and other available information about biomass for energy production from the companies. The harvestable amount of available woody biomass can be estimated by using a biomass availability factor (that could be developed by following time series trends) with the harvest volumes for the primary forest products (Alam and Pulkki 2011). Therefore, our study helps in more accurately assessing the available woody biomass around power plants on an annual basis. Accurately estimating woody biomass availability is an important issue for successful bioenergy deployment, for current and future planning and for investment opportunities in bioenergy based businesses (Panoutsou *et al.* 2009). The four bioenergy generating plants will not only help distribute costs over a broader base including forest harvest residues as a raw material, but also reduce greenhouse gas emissions. In addition, this initiative will improve the competitiveness of the forest industries as forest industries can make profit from supplying woody biomass from the FMUs to power plants on a regular basis. As the power plants have the advantages of favourable locations there is a potential for trans-boundary woody biomass feedstock sourcing. For example, with proper contracts woody biomass feedstock can be collected from Manitoba, as well from Minnesota.

3.5 Conclusions

Canada has the advantage of having vast renewable forest resources as compared to other countries. A portion of these renewable resources could be utilized for providing a sustainable supply of bioenergy. However, an accurate assessment of the availability of woody biomass and its quality is essential before switching over from fossil fuels to bioenergy alternatives for power generation. In this study, we used pre- and post-harvest forest inventory data along with forest depletion spatial data analysis to more accurately assess the availability of forest harvest residue and underutilized wood for four bioenergy generating stations in northwestern Ontario. It was found there is enough woody biomass available from FHR and UW in the FMUs of northwestern Ontario to sustain bioenergy production at the four power generating stations. Only 67% of logging residues are considered harvestable, leaving sufficient material on-site to maintain forest health. The use of only 67% of logging residue is based on our calculations of the common practice for collection of harvest residues in northern Ontario and also based on the information on biomass recovery rates in the literature. The methodology of this study could be applicable as a template across Canada and abroad.

The forest industries should make woody biomass collection and processing from FHR and UW an integral part of the harvesting of wood destined for pulp, paper, lumber and higher value products, in order to make biomass procurement most efficient. One of the limitations of this study is the assumption of availability of UW for harvesting, although we feel that our estimates on UW availability are conservative. As more data becomes available through Ontario's enhanced forest resource inventory and with more experience in biomass harvesting, this shortcoming can be alleviated. In addition, in order to quantify the feedstock supply risk for bioenergy production, it is important to determine inter-year variability in woody biomass availability. Alternate feedstock sources for the biomass based power plants must be identified to supply woody biomass feedstock in low yield years. More research also needs to be done on optimizing the entire wood supply chain to ensure maximum value is obtained from the forest resources.

Chapter 4

Road network optimization model for supplying woody biomass feedstock for energy production in northwestern Ontario[4]

4.1 Introduction

The road network optimization problem involves the optimal decision on the choice of route in response to the given demand for transporting material from each source to each destination. It has emerged as an important area for research in handling effective transport planning, because the demand for transportation of material on the roads is growing, while resources available for expanding the system capacity remain limited. Optimized transport over the road network plays a vital role in bioenergy production, as woody biomass is bulky and of low value. Thus, transportation and logistics play a vital role for making emerging biomass-based renewable energy businesses efficient and profitable (Searcy *et al.* 2007; Gold and Seuring 2011). The increased cost of non-renewable fossil energy and its effect on climate change through greenhouse gas (GHG) emissions has led to some cutting-edge research in renewable bioenergy production systems (Campbell and Duncan 1997; Zhu *et al.* 2011). However, there is little research focused on formulation and solution procedures in woody biomass supply chain optimization for power generation.

The mathematical models and algorithms developed for biomass transportation focus either on cost calculation or optimal location of bioenergy power plants. For

[4]A version of this chapter has been submitted to The Open Forest Science Journal for publication.

example, Singh *et al.* (2010) developed a mathematical model for collecting and transporting agricultural biomass feedstock from fields to a biomass-based power plant in Punjab, India. They compared the unit cost of biomass transportation for two modes of transport (truck and tractor with wagon) and three types of agricultural biomass (loose biomass, baled biomass and briquetted biomass). Velazquez-Marti and Fernandez-Gonzalez (2010) formulated a mathematical algorithm to optimally locate biomass-based power plants in Spain by minimizing transportation costs, under the constraint that all the bioenergy produced by the biomass-based power plant is used. They used the mathematical model to select power plant location points on the map that minimize transportation cost under the given constraints.

Transportation models for efficient and effective biomass supply logistics for bioenergy production face a number of other challenges in model formulations (Zhu *et al.* 2011). A crucial decision of the road network optimization problem is the full capacity utilization of existing roads (primary and secondary) and/or the addition of new links (tertiary forest roads). Such a decision is referred to as the network design problem, which determines the optimal decision variables (e.g. full capacity utilization and/or new link additions) so as to minimize a specific network performance index (e.g. total travel time or generalized cost), while accounting for different route characteristics in the network. The generalized cost of energy recovery from woody biomass mainly depends on the logistics cost of supplying biomass feedstock to the power plants (Yoshioka *et al.* 2002; Edward *et al.* 2007; Searcy *et al.* 2007). Using four different feedstocks (forest fuel, straw, miscanthus and short rotation coppice), Allen *et al.* (1998) found that biomass logistics costs (transport, storage and handling) constitute a significant part of the total costs of the biomass supply chain. In addition Nichols *et al.* (2006), in their study on provincial road conditions and round wood timber transport in South Africa, found that road type and conditions also have a substantial effect on transportation costs.

Spatial data analysis techniques are often used to find shortest distance in road network problems. Geographic Information Systems (GIS) have been used to compile, clean and analyze all types of spatial data and to build raster spatial databases of road networks for supplying woody biomass for energy production (Burrough 1986; ESRI 2010; ESRI 2011). In raster format, the geographic location of each cell is determined by a single attribute, its position relative to the point of origin (bottom left corner) of the cell matrix, and no other geographic coordinates are required to be stored (Buckley 1998; Husdal 1999; ESRI 2010). This technique of data storage in raster format makes the data analysis much easier in network optimization models and has allowed the development of efficient solution techniques for solving very large cyclic network problems (Pulkki 1994 and 1996). The raster format is also better than the vector format, as it works even in areas where predefined paths do not exist and many attribute layers are not available (Husdal 1999).

Hawth's Tools (Beyer 2004) are further used in ArcGIS to analyze spatial data (Jensen *et al.* 2005; ESRI 2010). The sources and destinations of the network are identified in a GIS based system for biomass logistics and transport optimization (Perpiña *et al.* 2009; Velazquez-Marti and Fernandez-Gonzalez 2010). The nodes of network structure as biomass sources, storage locations or biomass-based power plants are connected through arcs in the network. The combination of ArcGIS and Visual Basic has been applied for spatial road network analysis (Jensen *et al.* 2005; MSDN 2009; ESRI 2010; Microsoft 2010; ESRI 2011). Kanzian *et al.* (2009) performed scenario analyses for regional energy wood logistics for optimizing fuel supply by combining GIS and LP. Geijzendorffer *et al.* (2008) used a combination of GIS-BIOLOCO tools for designing and assessing the effectiveness of biomass delivery chains at regional levels based on biomass availability, logistics, costs, and spatial and environmental conditions. Further, several database layers for roads can be developed in ArcGIS, using a precedence/absence type of data input method (Nichols 2004). These database layers help in finding the minimum time (or shortest distance) in road network models and establishing variable cost zones around power generating plants.

There are three existing, plus one coal plant currently being converted, major woody biomass consuming power generating plants in northwestern Ontario (NWO) west of Lake Nipigon. The general purpose of this research is to build a road network optimization model to assist in planning woody biomass transportation and logistics for bioenergy production at a minimum cost in a sustainable way. The specific objectives of this study are: (i) to develop a minimum time and cost (or shortest distance) road network model to transport woody biomass feedstock to the power generating stations; (ii) to determine the minimum raster resolution that supplies consistent results at a regional scale; and (iii) to establish variable cost zones surrounding the power generating plants in NWO. ArcGIS was used to develop raster-based spatial database layers of the road network. The raster spatial data for the region was combined with the raster network optimization model (Pulkki 1994 and 1996) programmed in Visual Basic to optimize the road network transportation with the objective of minimum time and cost (or shortest distance), under the constraints of highway-I, highway-II, and primary, secondary and tertiary forest road classes. Tests of different resolutions on accuracy of time and distance optimization with the model were conducted. First, a higher resolution test on a smaller area was performed. Second, we moved to a larger area to determine if we could go to a coarser resolution on a broader scale from the point of processing time and accuracy. Finally, six variable cost zones surrounding each power generating station were established.

4.2 Methodology

4.2.1 Research Area

The research area for this study (Figure 3.1) consists of 18 Forest Management Units (FMUs) in NWO covering an area of 167,184 km^2 (324 km (N-S) x 516 km (E-W)). Twelve FMUs (Armstrong Forest, Black Sturgeon Forest, Crossroute Forest, Dog-River Matawin Forest, Dryden Forest, English River Forest, Kenora Forest, Lakehead Forest, Sapawe Forest, Spruce River Forest, Wabigoon Forest, and Whiskey Jack Forest) are completely within the research area, whereas six FMUs (Caribou Forest, Lac Seul Forest, Lake Nipigon Forest, Ogoki Forest, Red Lake Forest, and Trout Lake Forest) are partially within the research area. Woody biomass from these FMUs will be supplied to four biomass-based power plant developments (Abitibi-Bowater Thunder Bay Power Plant (ABTB); Abitibi-Bowater Fort Frances Power Plant (ABFF); Atikokan Generating Station (AGS); Domtar Dryden Power Plant (DDPP) (Figure 3.1). ABTB, ABFF and DDPP are combined heat and power (CHP) generating plants and AGS is only a power (electricity) generating plant.

4.2.2 Data Source

Two types of data (field inventory and GIS) were used for this study. Field inventory data on woody biomass availability from two FMUs – one in the eastern part (Black Sturgeon Forest) and another in the western part (Crossroute Forest) of the research area – were applied over the region. GIS data were obtained for the road network in two formats (Shapefile and Geodatabase). Road network data of some FMUs (Crossroute Forest, Dog River Matawin Forest, Dryden Forest, English River Forest, Kenora Forest, Lac Seul Forest, Red Lake Forest, Sapawe Forest, Trout Lake Forest, Wabigoon Forest, and Whiskey Jack Forest) were available in a projected coordinate system of NAD 1983 UTM Zone 15N, and for some FMUs (Armstrong Forest, Black Sturgeon Forest, Caribou Forest, Lake Nipigon Forest, Lakehead Forest, Ogoki Forest, and Spruce River Forest) in a projected coordinate system of NAD 1983 UTM Zone 16N. The whole database was converted to a coordinate system of NAD 1983 UTM Zone 15N for uniformity before further analysis. The road network data of the Black Sturgeon Forest, Crossroute Forest, Dog River Matawin Forest, English River Forest and Spruce River Forest were provided by Abitibi-Bowater Inc., Thunder Bay (Abitibi-Bowater Inc. 2009); road network data of the Sapawe Forest were provided by GreenForest Management Inc., Thunder Bay (GreenForest Management Inc. 2009); whereas road network data of the Lakehead Forest were provided by Greenmantle Forest Inc., Thunder Bay (Greenmantle Forest Inc. 2009). The road network data for rest of the FMUs were collected from Land Information Ontario (LIO 2010) and OMNR (OMNR 2010).

4.2.3 Data Input and Analysis

The flow chart in Figure 4.1 shows details of data input and analysis for GIS and aspatial data used for this study.

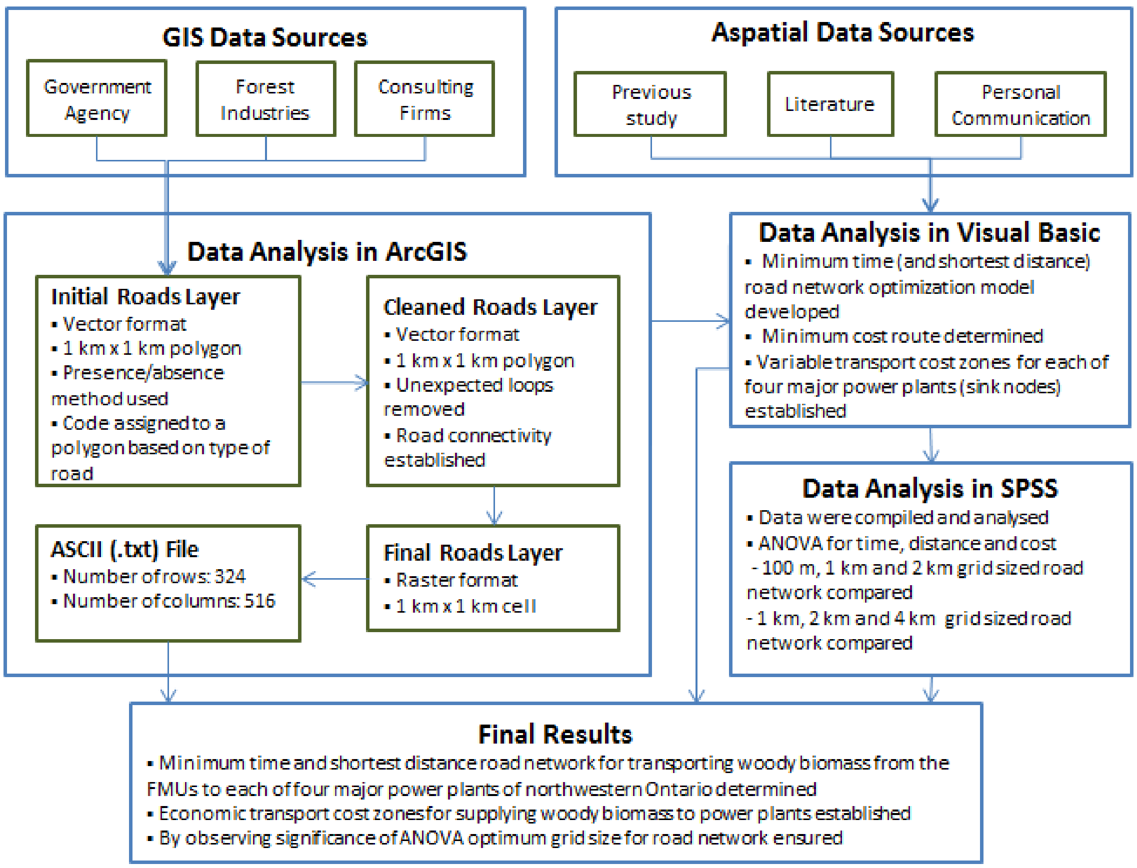

Figure 4.1 Flow chart of GIS-based road network optimization model.

The GIS shapefile and geodatabase for the road network are in vector format. ArcGIS was used to convert these databases from vector format into an easily workable database for this study (ESRI 2010; ESRI 2011). These vector road network data were first converted into raster format of 1 km^2 (1 km x 1 km) grid cells. The size of raster cells depends on the resolution requirements. A raster cell could be smaller than 1 km^2

(e.g. 100 m^2, 1 m^2), however, smaller cell size requires a large number of cells and a much greater time to process the information.

Figure 2.6 illustrates how a raster dataset of various cell sizes represents a polygon feature (ESRI 2009). The raster grids were then transformed to ASCII (.txt) files, with each cell representing a feature. A grid code could be easily assigned to a cell, if it contains only one type of feature. However, the decision making to assign a grid code to the cell became difficult when only a small portion of the cell contained a particular feature (Figure 2.7). Therefore, different data input methods were used for different types of features (Nichols 2004). For example, grid codes were assigned to the cells for road layer data input using the presence/absence method (ESRI 2010; ESRI 2011) and the grid codes 1, 2, 3, 4 and 5 represent highway-I, highway-II, and primary, secondary and tertiary (operational) forest roads, respectively. If no roads are present, grid code 9 is assigned to the cell (Figure 4.2).

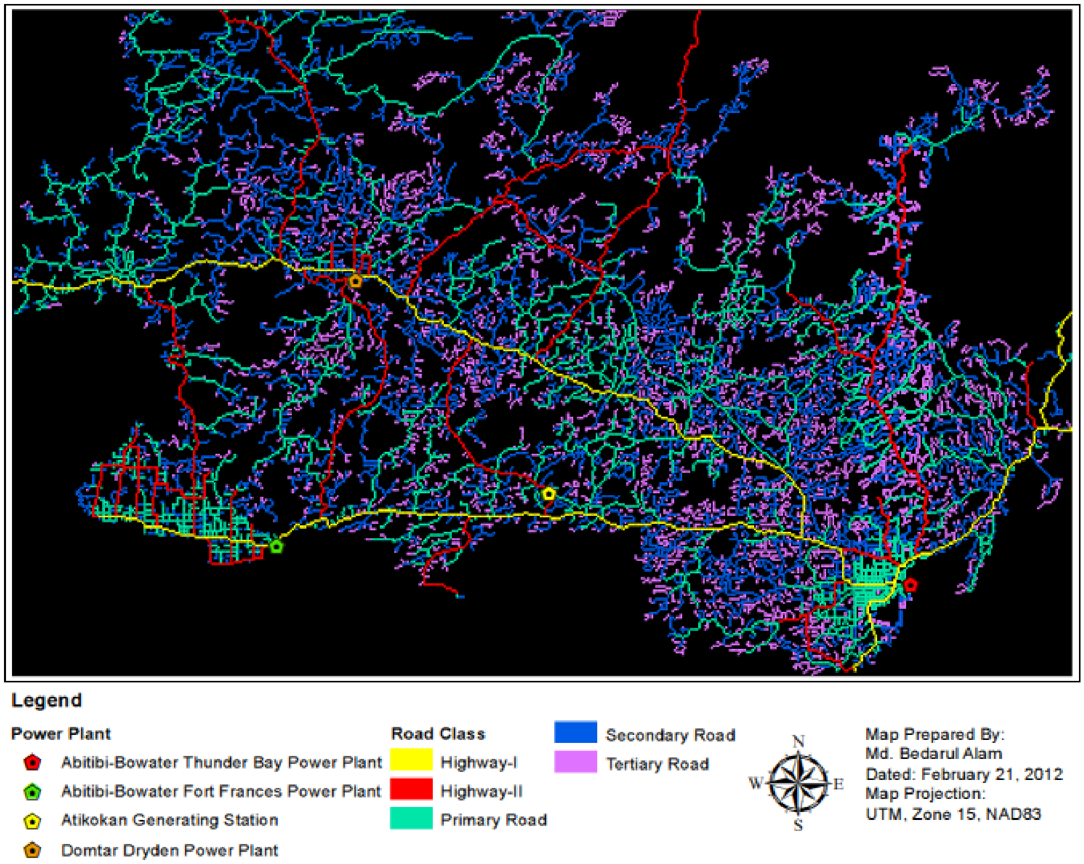

Figure 4.2 Road network in northwestern Ontario (NWO) for the extent of 324 km (N-S) x 516 km (E-W).

The roads passing within a distance of 1 km touch each other in the grid layer. This creates a link in the road network, though in reality there is no link. The coding of grid cells is adjusted manually to eliminate links, which are not present on the ground (Alam and Pulkki 2011). However, deviations in the network were kept to a minimum during manual adjustment of the road network. In the road network, a higher-class road could touch a lower-class road on more than one side. But a lower-class road could not touch the higher-class road on more than one side. When the lower-class road touches a higher-class road on more than one side, the grid cells are adjusted to maintain the road network integrity (Nichols 2004). Figure 2.4 shows the incorrect road intersection between two different classes of roads in which a lower-class road (secondary road) touches a higher-class road (primary road) on both sides. Figure 2.5 shows the correct road intersection between two different classes of roads in which a lower-class road (secondary road) touches a higher-class road (primary road) on one side only (Nichols 2004; Alam and Pulkki 2011).

The ASCII (.txt) files along with aspatial data were analyzed using a raster-based road network optimization model programmed in Visual Basic that minimizes time and cost (or shortest distance) for transporting woody biomass for energy production in NWO. Driving speeds of 90, 80, 60, 40 and 30 kilometres per hour ($km \cdot h^{-1}$) for empty vehicles, and 90, 70, 50, 30 and 20 ($km \cdot h^{-1}$) for loaded vehicles were used for highway-I, highway-II, and primary, secondary and tertiary (operational) forest roads, respectively. A load size of 50 m^3 for a woody biomass truck with 53 foot trailer with belly, which is equivalent to 43.8 green tonnes (gt) (1 m^3 = 0.876 gt), and an hourly rate of $85 (2009) for a biomass truck (with operator) were used in the model. In addition, a fixed time of 2.5 hours per trip for loading, unloading and delay was used. The previously developed raster layer of productive forests for the 18 FMUs is integrated with the road network layer to determine the minimum transportation cost of woody biomass from each forest cell to each of the four power plants (ABTB, ABFF, AGS and DDPP). Analysis of variance was used to determine the minimum raster resolution that supplies consistent results at a regional scale. Finally, variable cost zones for transporting woody biomass for energy production for each of the power generating plants were established.

4.2.4 Road Network Minimization Algorithm

The road network minimization algorithm was developed by incrementally determining cost between source node and all other nodes[5]. The cost from each source node to all other nodes were repeatedly compared and the least time and cost (or shortest distance) option was determined. The model then proceeds to the next node until the destination is reached. The road network minimization algorithm is a cyclic network because the loops are created by two-way traffic. If an arc is one-way the distance in the closed direction is set to infinity (Table 4.1).

Table 4.1 The cost (or distance) network matrix.

		To node					
		1	2	…	n-1	n	Summation (u_i)
From node	1	$d_{1,1}$	$d_{1,2}$	…	$d_{1,n-1}$	$d_{1,n}$	u_1
	2	$d_{2,1}$	$d_{2,2}$	…	$d_{2,n-1}$	$d_{2,n}$	u_2
	…	…	…	…	…	…	…
	n	$d_{n,1}$	$d_{n,2}$	…	$d_{n,n-1}$	$d_{n,n}$	u_n
	Summation (v_j)	v_1	v_2	…	v_{n-1}	v_n	

Let u_i denote the summation of time and cost (or distance) from node i to all other closest n nodes, and v_j the summation of time and cost (or distance) from all closest n nodes to the node j. The steps of the algorithm are described as follows:

Step 1: Initial Solution

- For start node (i=j=1) set $u_i = v_j = 0$;

[5] The minimization algorithm technique is based on details described in Taha (1982), Pulkki (1994) and Pulkki (1996).

- Provided an arc exists between any two nodes i and j, the value of $v_j = \min(u_i + d_{i,j})$ is computed, where $d_{i,j}$ is the time and cost (or distance) between nodes i and j;
- The value of v_j obtained in the previous step is retained and u_i is set equal to v_j for further computation in the network.

Step 2: Optimality Check

(a) Compute v_j-u_i for all j and i =1;

(b) If $d_{i,j} \geq v_j$-u_i for all j, then no shorter route can be found between i and j; otherwise set i = i + 1 and repeat sub-step (a) till i = n (last node). When i = n, go to Step 3;

(c) If $d_{i,j} < v_j - u_i$, compute and replace v_j with a new value, $v_j' = u_i + d_{i,j}$ and start afresh from sub-step (a);

Step 3: Least Time and Cost (or Shortest Distance) Path Determination

The values of v_j, obtained in Step 2, give the least time and cost (or shortest distance) from any node i to j in the network. In order to determine the least time and cost (or shortest distance) path in the network, the last ARC (n-1, n) of the chain must satisfy $u_{n-1} = v_n - d_{n-1, n}$ and the penultimate node n-2 must satisfy $u_{n-2} = v_{n-1} - d_{n-2, n-1}$. The process is repeated backwards (by repeatedly setting n = n-1), until node 1 in the minimum time and cost (or shortest distance) network is reached.

4.2.5 Calculating Transportation Distance, Time and Cost through Road Network

4.2.5.1 Transportation distance

There are 26,405 cells (1 km^2 each) containing a road in the research area of 167,184 km^2 (167,184 total cells). The transportation distance for carrying woody biomass per trip from a road cell (source node) to a power plant (sink node) through the road network is determined by Equation (1).

$$D_r = \sum_{t=1}^{5} R_r \quad (1)$$

Where,

r = road cells in the raster route (r = 1, 2, 3,…, 26405)

t = types of roads (t = 1, 2, 3, 4, 5)

R_r = distance between nodes

D_r = Transportation distance from the source node to sink node (distance is taken as 1 km if the route is along the cell wall and 1.4142 km if the route is along the cell diagonal)

4.2.5.2 Transportation time

Woody biomass transportation time per trip from a road cell (source node) to a power plant (sink node) through the road network is determined by Equation (2).

$$T_r = \frac{D_r}{\sum_{t=1}^{5} S_{er}} + \frac{D_r}{\sum_{t=1}^{5} S_{lr}} \quad (2)$$

Where,

T_r = Woody biomass transportation time (hours) from a road cell (source node) to power plant (sink node) through road network

S_e = speed (km·h^{-1}) of empty vehicle

S_l = speed (km·h^{-1}) of loaded vehicle

4.2.5.3 Transportation cost

The transportation cost of woody biomass per trip from a road cell (source node) to a power plant (sink node) through the road network is determined by Equation (3).

$$TC_r = VC_r + FC \tag{3}$$

Where,

TC_r = transportation cost ($·gt^{-1}) to transport woody biomass from a road cell (source node) to power plant (sink node) through the road network

VC_r = variable transportation cost ($·gt^{-1}) obtained from Equation (4)

$$VC_r = \frac{T_r \times P}{L \times f} \tag{4}$$

Where,

FC = fixed transportation cost ($·gt^{-1}) obtained from Equation (5)

$$FC = \frac{FT \times P}{L \times f} \tag{5}$$

Where,

P = payment rate ($\$\cdot h^{-1}$) for truck including operator (assumed = 85 $\$\cdot h^{-1}$)

L = load size (m^3) of woody biomass truck (assumed = 50 m^3)

f = Conversion factor for biomass from cubic metre to green tonne (1 m^3 = 0.876 gt)

FT = fixed time (h) for loading, unloading and delay per trip (assumed = 2.5 h)

4.2.6 Determining Minimum Raster Resolution

In order to determine the minimum raster resolution that supplies consistent results with reasonable processing time, analysis of variance was first conducted for trip time results for a 50 km (N-S) x 50 km (E-W) raster for five road network locations and three grid sizes (100 m x 100 m, 1 km x 1 km and 2 km x 2 km) (Figure 4.3). Then analysis of variance was also conducted for a bigger raster (160 km (N-S) x 240 km (E-W)) for five road networks and three grid sizes (1 km x 1 km, 2 km x 2 km and 4 km x 4 km) (Figure 4.4).

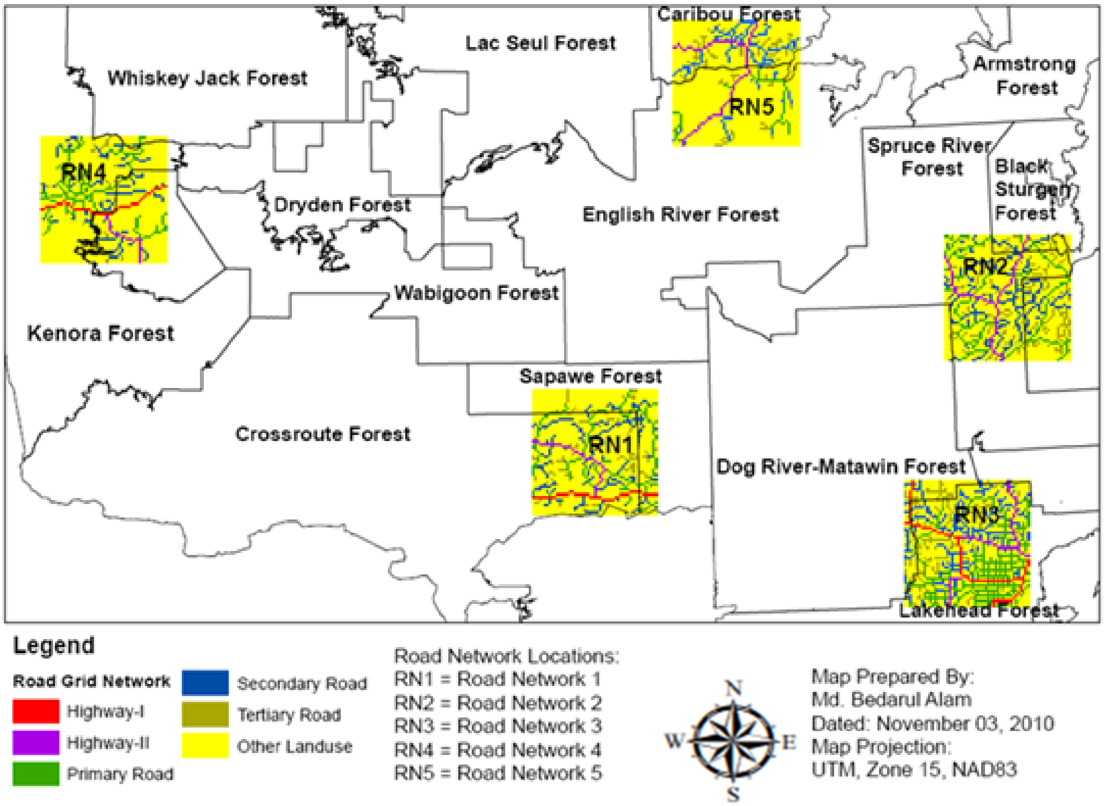

Figure 4.3 Locations of five road networks of 50 km (N-S) x 50 km (E-W) in extent within the research area.

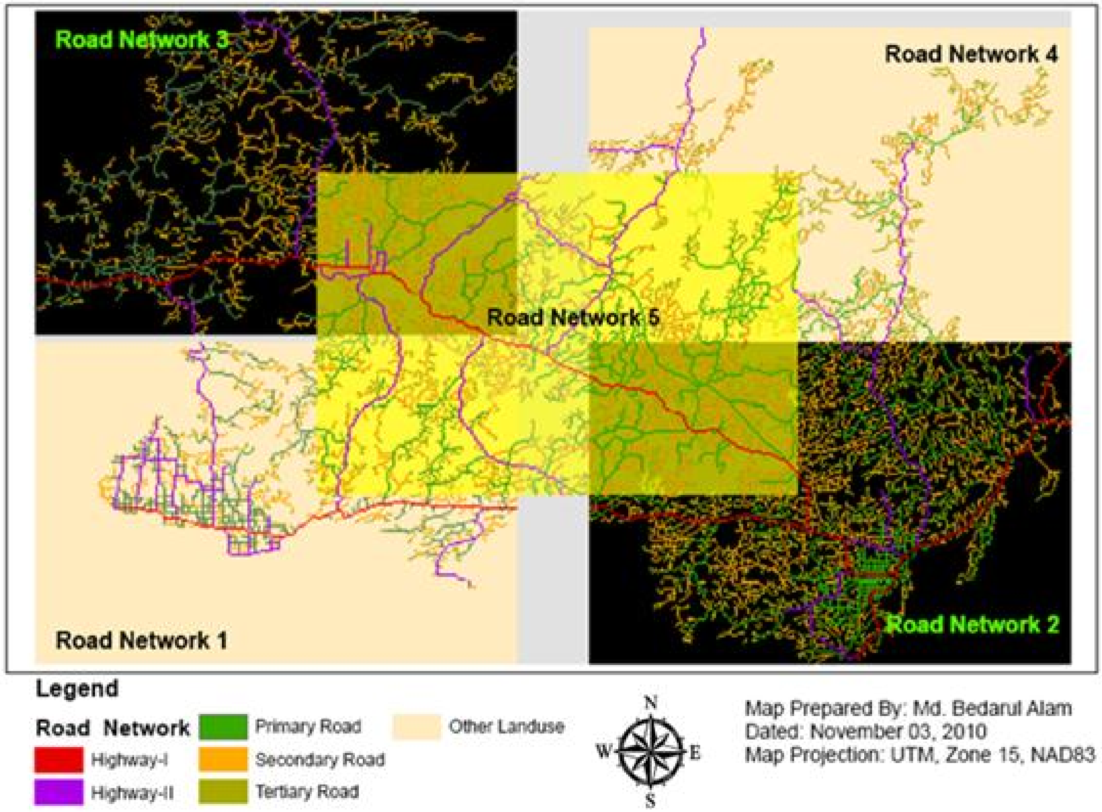

Figure 4.4 Locations of five road networks of 160 km (N-S) x 240 km (E-W) in extent within research area.

4.2.7 Variable Cost Zones

The transportation costs of woody biomass through the road network from source nodes to each sink node (power plant) were classified into variable transportation cost zones using integer codes (1, 2, 3, 4, 5 and 6 for variable transportation costs of 0-5, 5-10, 10-15, 15-20, 20-25 and 25-30 $\$\cdot gt^{-1}$, respectively). The variable transportation costs were developed for each power plant (ATTB, ABFF, AGS and DDPP).

4.2.8 Application of Road Network Model to Transport Woody Biomass

The road network model was integrated with the productive forest layer and depletion forest layer (grid cell with some harvesting from > 0% to 100% of its area) to determine time and cost of woody biomass transport from the entire productive forest area, as well as just from the cells with harvesting activities over the period 2002-2009, to any sink node (power plant). There are 100,061 cells (out of 167,184 cells) in productive forests and 19,315 forest cells in the harvested forest layers within the research area.

Not all productive forest or depletion cells are adjacent to a road cell. So in the model an offset value of 50 km was used to search for the nearest least cost road cell. A winding coefficient along with reduced loaded and unloaded driving speeds were applied to the straight line distance from the non-adjacent supply cell to the nearest least cost road cell to get the additional time required to move to the road. The minimum access time from the forest cells to the nearest road node is determined by Eq. (6).

$$T_a = \frac{\sqrt{W((RN_v - RN_1)^2 + (CN_h - CN_1)^2)}}{S_1} + \frac{\sqrt{W((RN_v - RN_1)^2 + (CN_h - CN_1)^2)}}{S_2} \quad (6)$$

Where,

T_a = Access time from the road cell r to forest cell m (hours)

W = winding coefficient applied to straight line distance (assumed = 1.38)

RN_v = row number of forest cell (v = 1, 2, 3, ..., 324)

RN_1 = row number of forest cell at road cell r

CN_h = column number of forest cell (h = 1, 2, 3, ..., 516)

CN_1 = column number of forest cell at road cell r

S_1 = speed of empty vehicle from road to forest (assumed = 20 km·h^{-1})

S_2 = speed of loaded vehicle from forest to road (assumed = 10 km·h^{-1})

The transportation time of woody biomass per trip from a forest cell (source node) to a power plant (sink node) can be determined by Equation (7).

$$T_c = T_r + T_a \tag{7}$$

Where,

T_c = time to transport woody biomass from a particular forest cell, c (source node, c = 1, 2, 3, …, 100,061) to power plant (sink node) in hours

Similarly, the transportation cost of woody biomass ($·gt^{-1}) from a forest cell (source node) to a power plant (sink node) can be determined by Equation (8).

$$TC_c = \frac{T_c \times P}{L \times f} + FC \tag{8}$$

Where,

TC_c = transportation cost to transport woody biomass from a particular forest cell (source node) to a power plant (sink node) in $·gt^{-1}

The minimum costs for transporting woody biomass from productive and depleted forests of an entire region (not necessarily just the cells needed for woody biomass) to four power plants (ABTB, ABFF, AGS and DDPP) were compared.

4.3 Results and Discussion

4.3.1 Transportation Distance, Time and Cost through Road Network

The results of the cost and time (or shortest distance) for transporting woody biomass obtained from the road network optimization model are presented in Table 4.2. The minimum time (or distance) for transporting woody biomass to each of the four power plants is zero, whereas the minimum cost is 4.85 $\$\cdot gt^{-1}$. This is because the model starts from the sink node (power plant) and the minimum value of time (or distance) in that case is taken as zero. However, some minimum fixed cost is being incurred even if we start from the sink node.

Table 4.2 Summary of optimized trip distance, time and transport cost from road cells (source nodes) to a power plant of woody biomass feedstock using road network model.

Power plant	Trip distance (km)			Trip time (hr)			Transport cost ($\$\cdot gt^{-1}$)		
	Mean	Median	Max	Mean	Median	Max	Mean	Median	Max
ABTB	273.54	267.38	605.17	7.14	6.96	17.49	18.71	18.35	38.79
ABFF	280.31	288.27	606.76	7.75	7.82	19.46	19.89	20.04	42.61
AGS	217.31	214.47	453.92	6.47	6.17	16.56	17.41	16.83	37.00
DDPP	228.12	220.35	540.10	6.38	6.21	18.07	17.23	16.90	39.92

In comparison with other power plants, the maximum trip distance, the median trip distance and the average trip distance of transporting woody biomass feedstock to ABFF in the road network are the highest, because this power plant is located near the southwest corner in the research area and the road cells in the northeast part are far from it (Figure 4.1). On the other hand, in comparison with other power plants the maximum trip distance, the median trip distance and the average trip distance of transporting woody biomass feedstock to AGS in the road network are the lowest, because this power plant is located near the middle of the research area and the road cells are evenly distributed around it. The average trip time for DDPP is the lowest in comparison with other power plants, as DDPP is located near the middle of the research area and has comparatively straighter and higher class routes of transportation (Figure 4.1).

4.3.2 Minimum Raster Resolution

The results of analysis of variance for trip time and transportation cost for 50 km (N-S) x 50 km (E-W) raster show that both location ($p < 0.001$) and grid size ($p = 0.003$) have significant effects on trip time of woody biomass for supplying woody biomass for energy production (Table 4.3). However, there is no interaction effect of location and grid size ($p = 0.993$) on trip time. Similarly, the results for trip distance for 50 km (N-S) x 50 km (E-W) raster show that location ($p = 0.015$) has a significant effect on trip distance, whereas grid size ($p = 0.228$) and the interaction of location and grid size ($p = 0.303$) does not have a significant effect on trip distance.

Table 4.3 Average trip distance, time and transport cost (standard deviations in parentheses) of woody biomass for two raster networks and various grid resolutions. Values with same letters are not significantly different at α = 0.05.

Raster network and Grid size	Trip distance (km)	Trip time (h)	Transport cost ($\$\cdot gt^{-1}$)
50 km (N-S) x 50 km (E-W) network			
100 m x 100 m grid	32.35^{a} (2.19)	1.27^{c} (0.16)	7.31^{g} (0.31)
1 km x 1 km grid	29.97^{a} (1.95)	1.12^{d} (0.13)	7.02^{h} (0.26)
2 km x 2 km grid	30.20^{a} (4.56)	1.05^{d} (0.16)	6.90^{h} (0.31)
160 km (N-S) x 240 km (E-W) network			
1 km x 1 km grid	149.08^{b} (51.13)	5.09^{e} (2.16)	14.73^{i} (4.20)
2 km x 2 km grid	151.92^{b} (48.94)	5.37^{e} (2.07)	15.28^{i} (4.02)
4 km x 4 km grid	144.82^{b} (48.19)	4.35^{f} (1.82)	13.29^{j} (3.54)

The results show that there is a significant difference between 100 m x 100 m grid size and 1 km x 1 km grid size for trip time and cost, but there is no significant difference for distance in a 50 km (N-S) x 50 km (E-W) raster. The density of roads is a key factor, which plays a vital role on the woody biomass transportation time, cost and distance. When the density of roads is less, the woody biomass transportation time, cost and distance are higher and vice-versa (Figure 4.3). The lengths and classes, as well as density of roads are different in different locations. So the effects of locations are significant on time, cost and distance of woody biomass transportation for energy production. The grid size (100 m x 100 m, 1 km x 1 km and 2 km x 2 km) effect is significant on woody biomass transportation time and cost, but is not significant on the distance of woody biomass transportation. A number of roads which fall within a 2 km extent of a raster road network had to be removed while using a grid size of 2 km x 2 km, because only one road could be kept in the cell. However, more roads could be retained while using both 1 km x 1 km and 100 m x 100 m grid sizes. In the road selection process, higher-class roads are given preference over lower-class roads. For example, location RN3 has a dense road network as compared to other locations, because it falls in a city area (Figure 4.3). Therefore, many lower-class roads are removed from this location using a higher grid size. Since higher-class roads have higher driving speeds, the biomass transportation time is lower in this location. As the biomass transportation time is less in location RN3, the cost of biomass transportation is also less in this location.

The results of analysis of variance for trip time and transportation cost for 160 km (N-S) x 240 km (E-W) raster are similar to 50 km (N-S) x 50 km (E-W) raster (Table 4.3). These results show that both location ($p < 0.001$) and grid size ($p = 0.002$) have significant effects on trip time. But there is no interaction effect of location and grid size ($p = 0.922$) on the trip time. The results for trip distance for the same raster (160 km (N-S) x 240 km (E-W)) show that location ($p < 0.001$) has a significant effect on trip distance of woody biomass. However, grid size ($p = 0.761$) does not have a significant effect on the trip distance. Similarly, the interaction of location and grid size ($p = 1.00$) does not have a significant effect on trip distance. The results show that there is no significant difference between 1 km x 1 km grid size, 2 km x 2 km grid size and 4 km x 4 km grid size for trip time, cost and distance in 160 km (N-S) x 160 km (E-W) raster. The results for both raster networks (small and larger areas) show that 1 km x 1 km grid sized raster gives consistent results and we do not lose many roads in the analysis (Table 4.3). The running of the network optimization model was also still efficient at a 1 km x 1 km raster; for optimization of all 26,405 road nodes it takes 75 seconds with an i7 processor. Going to a 100 m x 100 m grid and assuming linearity in processing time it would take 7,500 seconds or 2.1 hours which limits the model's usefulness and user friendliness when running multiple sinks. Therefore, we adopted a grid size of 1 km^2 for all our analyses.

4.3.3 Variable Cost Zones

The results of variable cost zone analysis for the research area of 324 km (N-S) x 516 km (E-W) are shown in Figures 4.5 to 4.8 for ABTB, ABFF, AGS and DDPP power plants, respectively. The variable cost zones are different for supplying woody biomass feedstock to different power plants from different locations. The traveling time through the road network from any particular geographic location to different power plants is different. These variable cost zones provide information to be used in a decision support system (DSS) for generating bioenergy in NWO.

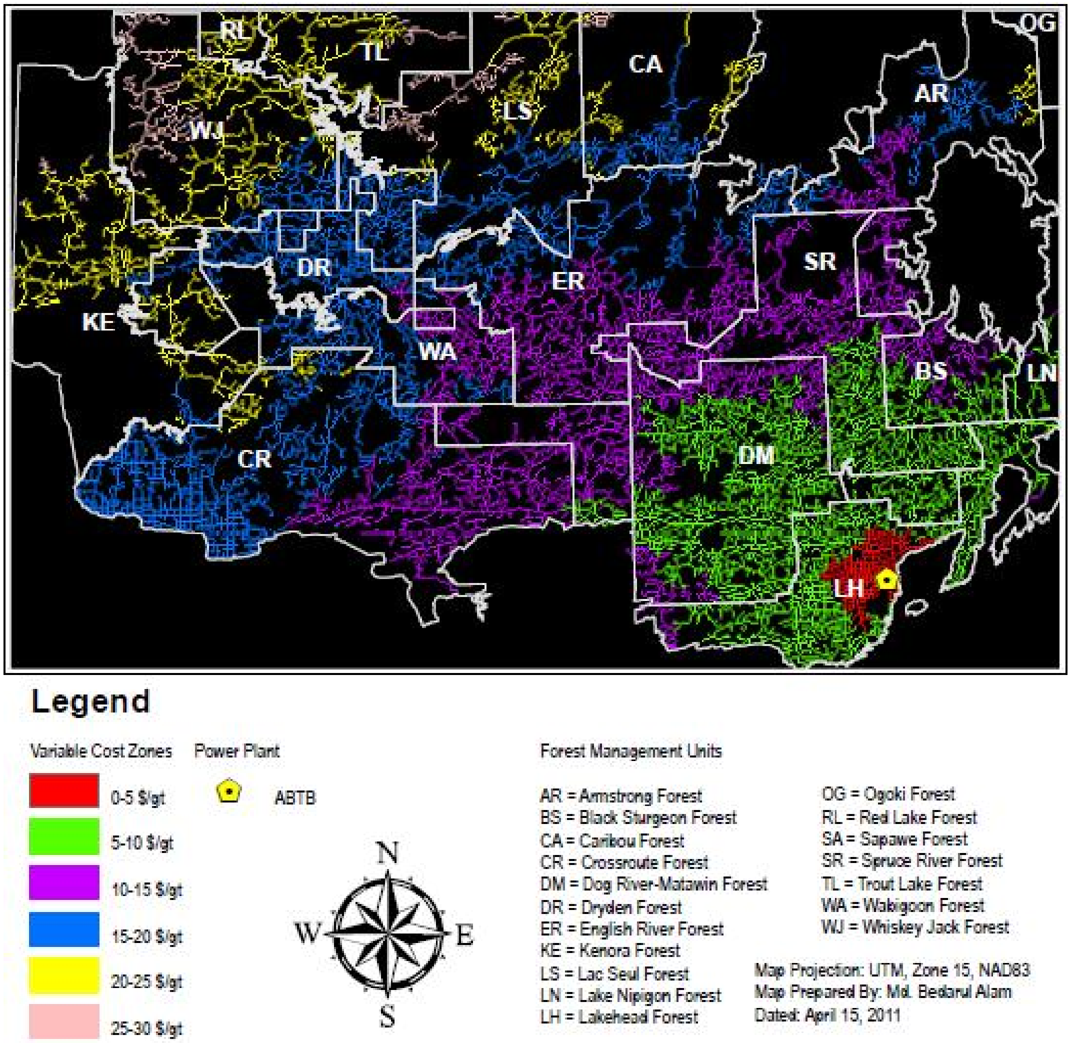

Figure 4.5 Variable cost zones for the ABTB in different forest management units (FMUs).

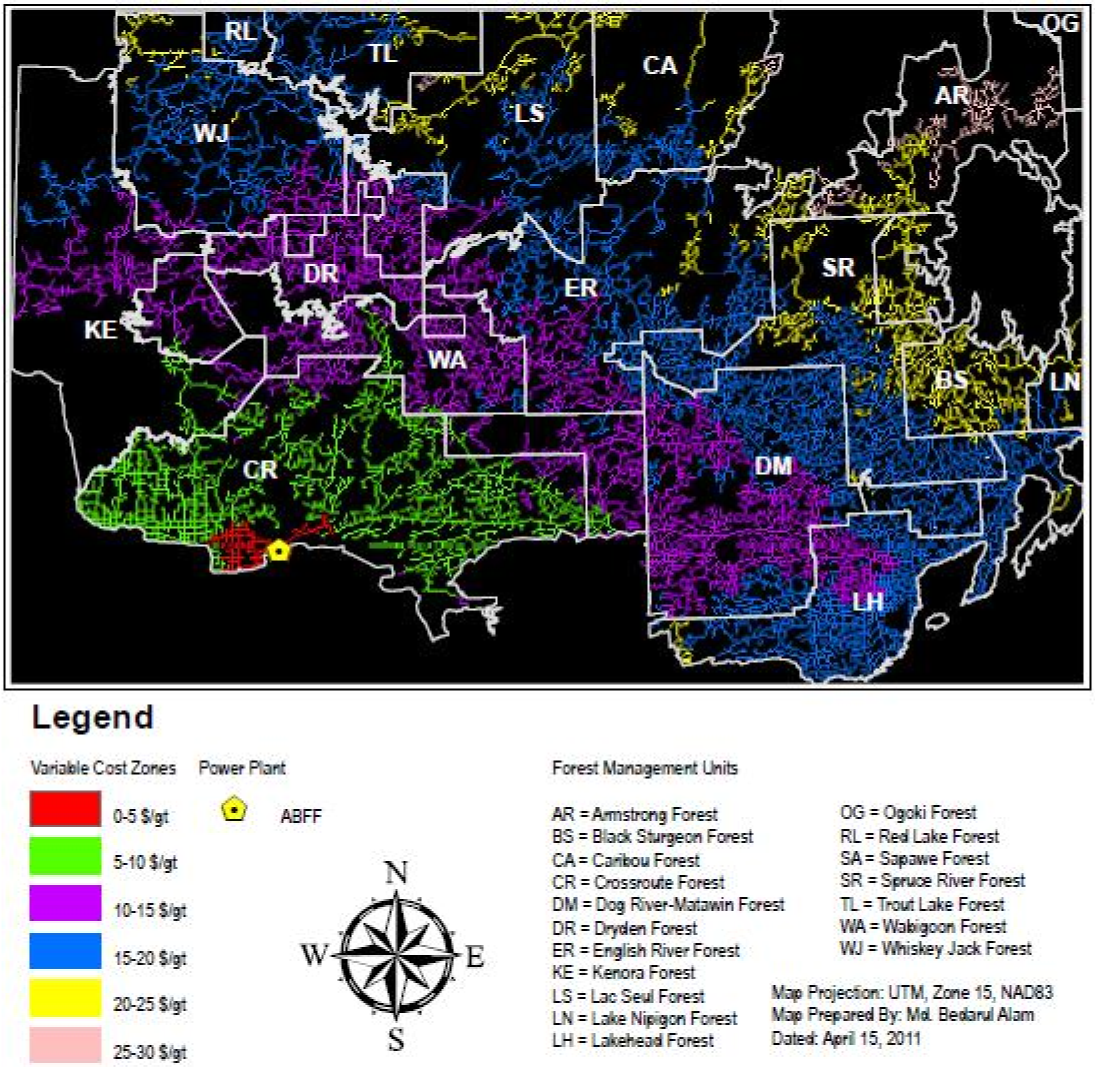

Figure 4.6 Variable cost zones for the ABFF in different FMUs.

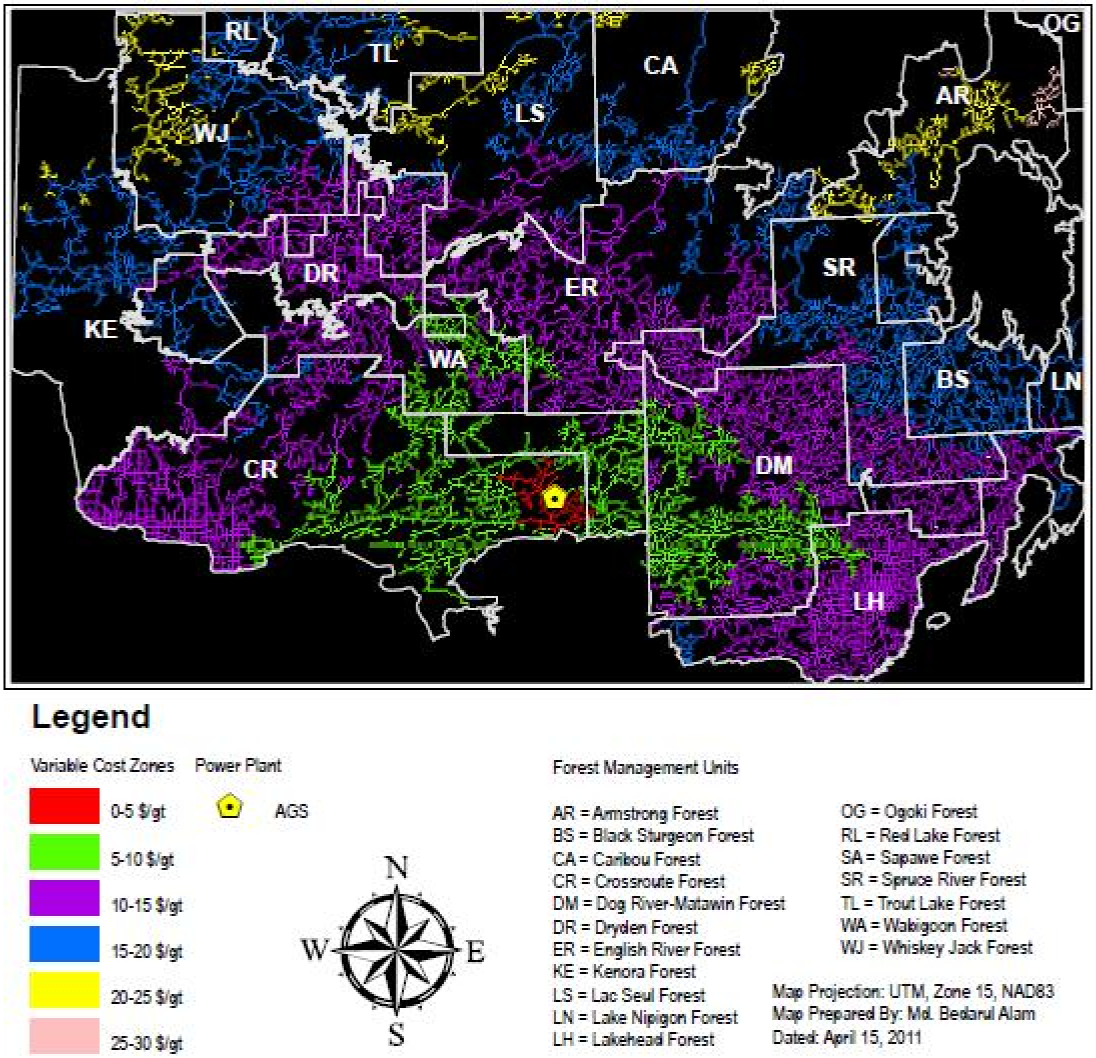

Figure 4.7 Variable cost zones for the AGS in different FMUs.

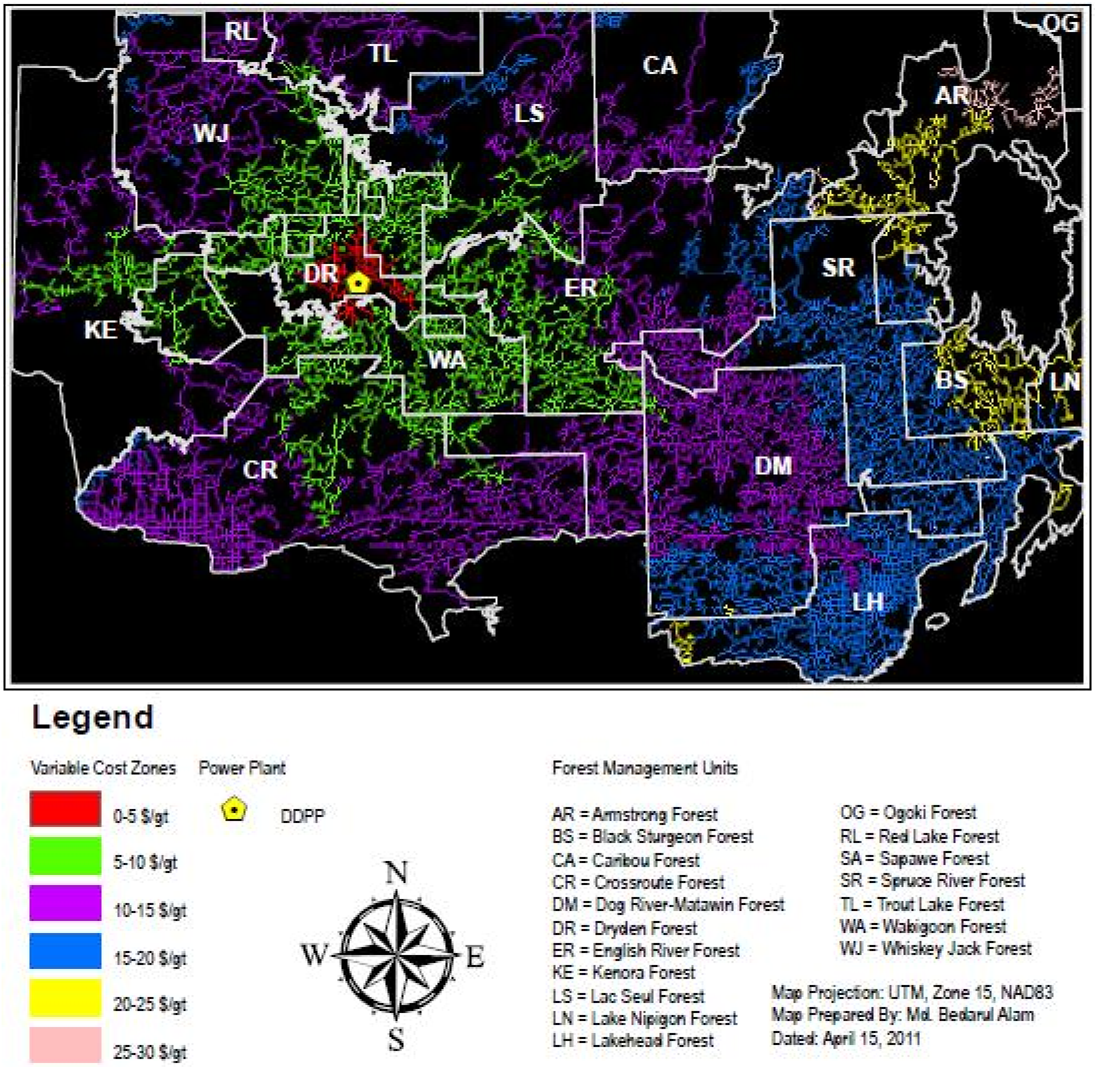

Figure 4.8 Variable cost zones for the DDPP in different FMUs.

4.3.4 Application of Road Network Model to Transport Woody Biomass

Table 4.4 shows the summary of unit transportation costs ($\$\cdot gt^{-1}$) of woody biomass feedstock from productive and depleted forest cells to four power plants in NWO. The unit costs ($\$\cdot gt^{-1}$) of woody biomass transportation from productive and depleted forest cells to ABFF are in general higher in comparison with the other three power plants. ABFF is located near the southwest corner of the research site, and there are not many forest cells closer to this power plant. So the unit cost ($\$\cdot gt^{-1}$) of woody biomass transportation from the forests to this plant is higher as compared to other power plants. The mean unit costs ($\$\cdot gt^{-1}$) and the median unit costs ($\$\cdot gt^{-1}$) of woody biomass transportation from productive and depleted forest cells to DDPP are lower in comparison with the other three power plants. DDPP is located near the middle of the research area, and there are many forest cells closer to this power plant along with a denser network of higher class and straighter roads.

Table 4.4 Summary of transport cost ($\$\cdot gt^{-1}$) of woody biomass feedstock from productive and depleted forest cells.

Power plant	Transport cost of woody biomass from productive forest ($\$\cdot gt^{-1}$)			Transport cost of woody biomass from depleted forest ($\$\cdot gt^{-1}$)		
	Mean	**Median**	**Maximum**	**Mean**	**Median**	**Maximum**
ABTB	21.90	22.03	49.09	20.20	19.64	39.76
ABFF	22.31	22.16	53.67	20.58	20.32	53.19
AGS	20.18	19.69	48.05	18.11	17.41	47.56
DDPP	18.82	17.76	50.98	17.39	16.44	50.49

4.4 Conclusions

This study develops a novel approach of spatial and economic aspects of road network optimization for transporting woody biomass feedstock for energy production in NWO. The minimum time and cost (or shortest distance) road network model provides efficient and effective information to be incorporated into a DSS to supply woody biomass feedstock for energy production. Careful planning of woody biomass supply logistics plays a key role in the success of a woody biomass-based industry. However, location specific data are essential for developing such road network optimization models across Canada, which can help supply woody biomass feedstock to power generating stations in a profitable and sustainable way. The variable cost zones surrounding a bioenergy power plant developed in this model can act as valuable information to be used in DSS tools. A grid size of 1 km^2, for road network rasters for areas ranging from 50 km (N-S) x 50 km (E-W) to over 300 km (N-S) x 500 km (E-W) in size, provides consistent and accurate results for minimum time and cost (or shortest distance) without excessive computer processing time. This road network optimization model is not only applicable for woody biomass feedstock supply it can also be used for optimizing transport of any other product through the road network. One of the limitations of this model is that it does not take into account the available supply at source nodes and demand of biomass at sink nodes. Future research in this area will incorporate these variables in the model.

Chapter 5

Modeling woody biomass procurement for bioenergy production at the Atikokan Generating Station in northwestern Ontario[6]

5.1 Introduction

Biomass has great potential to be converted into renewable bioenergy, which not only has the advantage of reducing greenhouse gas (GHG) emissions, but also ensures a sustainable supply of energy (Ediger and Kentel 1999; Ushiyma 1999; Nagel 2000; Pari 2001; Berndes *et al.* 2003; Gan and Smith 2006). In addition, replacing fossil fuels with bioenergy provides an excellent opportunity to develop energy security and increase rural economic activities (Bradley 2006b). In this context, the Ontario Government has set an ambitious plan for the Atikokan Generating Station (AGS) in northwestern Ontario (NWO) to replace lignite coal with renewable woody biomass as feedstock by 2014. The AGS is located 190 km west of Thunder Bay, presently utilizes lignite coal, and operates at 30% of capacity (Sygration 2011). The AGS has a full capacity of 230 MW of electricity production (Forest BioProducts Inc. 2006; McCarthy 2009). In order to assess the economic feasibility of bioenergy production at the AGS, it is important to understand and improve the efficiency of the woody biomass supply chain from the forest management units (FMUs) surrounding the AGS. There has been little published research on improving the efficiency of woody biomass supply chains due to the lack of

[6]A version of this chapter has been submitted to the Canadian Journal of Forest Research for publication.

precise data for biomass availability and distribution (Chauhan *et al.* 2009). A few studies, that address the biomass supply chain management problem in the forestry sector, have only focused on a single aspect of the problem and not taken a holistic approach (Rönnqvist 2003; Caputo *et al.* 2005). For example, supply chain management studies related to the pulp industry focus specifically on harvesting, transportation of pulp, production scheduling and distribution of products to customers (Bredström *et al*. 2004).

The recent interest in the bioenergy sector has resulted in the development of location and problem specific models for optimization of woody biomass collection (Mitchell 2000; Davide *et al.* 2004; Manfred 2007; Dunnet *et al.* 2008; Sylvain *et al.* 2008; Rentizelas *et al.* 2009). For example, Rentizelas *et al.* (2009) developed a model for a multi-biomass supply chain for a tri-generation facility (production of electricity, heat and forest products) to maximize financial benefits by reducing costs, warehousing requirements and capital costs. Cundiff *et al.* (1997) used linear programming (LP) for designing a supply system (harvesting, storing and transporting) of herbaceous biomass to bioenergy plants. LP models have also been used to optimize (minimize) the overall energy cost for biomass-based combined cooling, heating and power generation (CCHP) systems (Kong *et al.* 2005; Ren *et al.* 2010). The problem with these models is that they have been designed based on the LP modeling approach that simplifies complex problems into simpler forms (linear equations).

Mixed-integer programming (MIP) models are used for optimizing logistics of woody biomass for energy production to account for discrete as well as continuous decision variables (Nagel 2000; Gunnarsson *et al.* 2003; Chauhan *et al.* 2009; Wu *et al.*

2011). The use of MIP models in bioenergy production has been further extended by formulating dynamic mixed integer programming (DMIP) models to optimize the design of supply networks based on financial criteria (Mas *et al.* 2010; Kim *et al.* 2011a). However, the MIP and DMIP models do not account for all real life uncertainties encountered in complex and difficult woody biomass-based energy production systems, due to over simplified linearity assumptions (Kaylen *et al.* 2000). To overcome the limitations of LP, MIP and DMIP models a non-linear dynamic programming (NLDP) approach is more appropriate.

Woody biomass is usually scattered over a large geographic area and its supply chain modeling requires accurate information about its location and availability (Sokhansanj *et al.* 2006). Also, biomass demand can vary considerably between months and by season depending on energy demand. A geographic information system (GIS) is a versatile tool that helps in capturing, managing, analyzing and displaying all forms of geographically referenced information in a systematic way. GIS models have been used to solve biorefinery location problems (Graham *et al.* 2000), planning logistics of bioenergy production using forest and agricultural biomass, as well as industrial and urban wood wastes (Frombo *et al.* 2009), and for transportation network analysis (Tittmann *et al.* 2010). A GIS can be used together with mathematical programming methods to develop an integrated model for supplying woody biomass for energy production (Noon 1996; Graham *et al.* 2000; Voivontas *et al.* 2001; Freppaz *et al.* 2004; Ranta 2005; Geijzendorffer *et al.* 2008; Sylvain *et al.* 2009). Such models can integrate spatial and aspatial data to solve location specific and real time problems in woody biomass supply chain management for energy production.

The purpose of this study is to develop an integrated NLDP model for procuring woody biomass from the FMUs surrounding the AGS in the most economical and sustainable way. The associated objectives are: (i) to determine the type and quantity of woody biomass, from forest cells (each of 1 km^2 size), supplied to the AGS over a one year horizon based on monthly electricity production by the AGS; (ii) to compute the optimized monthly woody biomass procurement costs; and (iii) to perform sensitivity analyses for examining the effect of key parameters (harvesting factor (HF), conversion efficiency (CE), biomass moisture content (MC) and per unit biomass processing costs on woody biomass feedstock supply costs.

5.2 Methodology

The flow chart in Figure 5.1 presents the methodology for the integrated NLDP model developed for procuring woody biomass for the AGS. The study area, 324 km (N-S) × 516 km (E-W) (167,184 km^2), consists of 18 FMUs surrounding the AGS (Figure 5.2). GIS data were collected from Land Information Ontario, Sustainable Forest Licence (SFL) holders, and consultant companies in the formats of Shapefile and Geodatabase (Abitibi-Bowater Inc. 2009; Greenmantle Forest Inc.2009; GreenForest Management Inc. 2009; LIO 2010). The original vector data was first converted to raster and finally to spatial database text files for the entire research area using ArcGIS software. Three main spatial layers (land use, forest depletion and cost layers) were prepared on a raster grid size of 1 km×1 km (1 km^2), where each cell represents a feature (Nichols *et al.* 2006; ESRI 2010). Different data input methods were followed for different types of features. The dominant data input method was used to create a raster layer of forest land use class (ESRI 2010). In this method, a grid code entity (1 = productive forest, 2 = water/lake, and 3 = other land use) is assigned to each feature, which occupies more than 50% of the cell area (Figure 5.2).

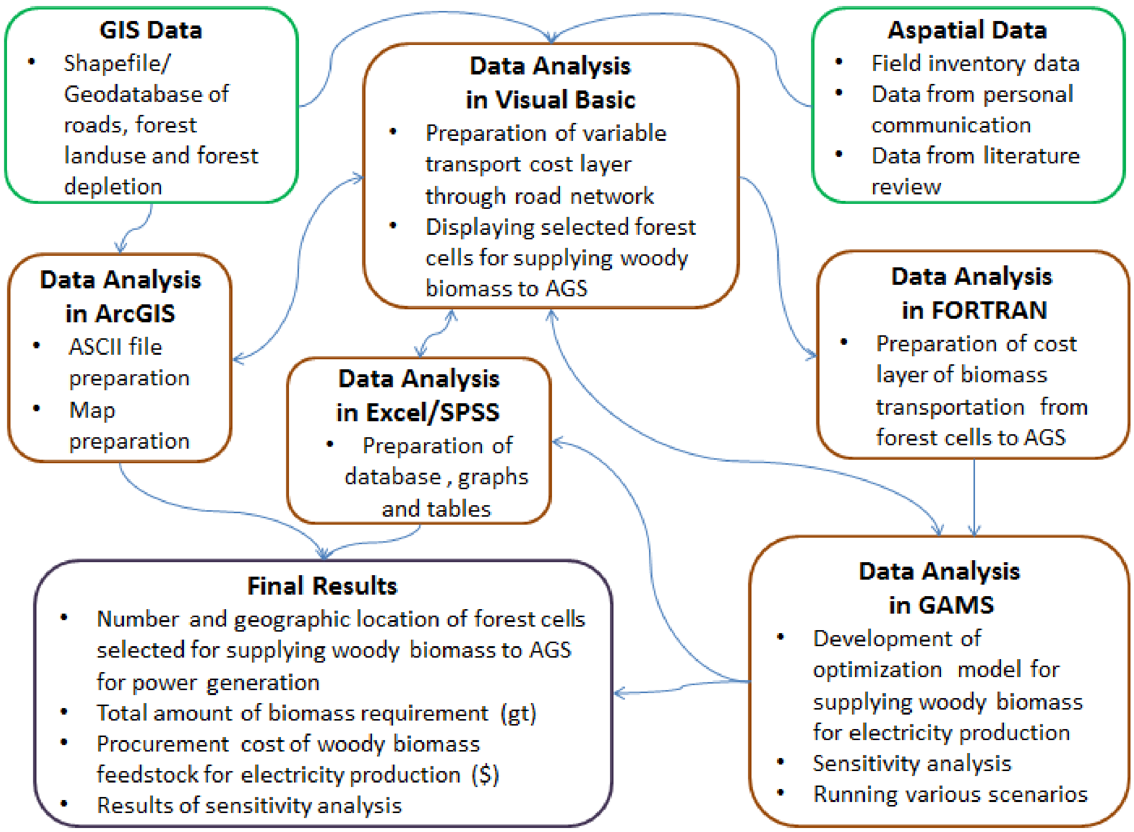

Figure 5.1 Flow chart of integrated non-linear dynamic programming optimization model for supplying woody biomass to the Atikokan Generating Station (AGS) in northwestern Ontario (NWO).

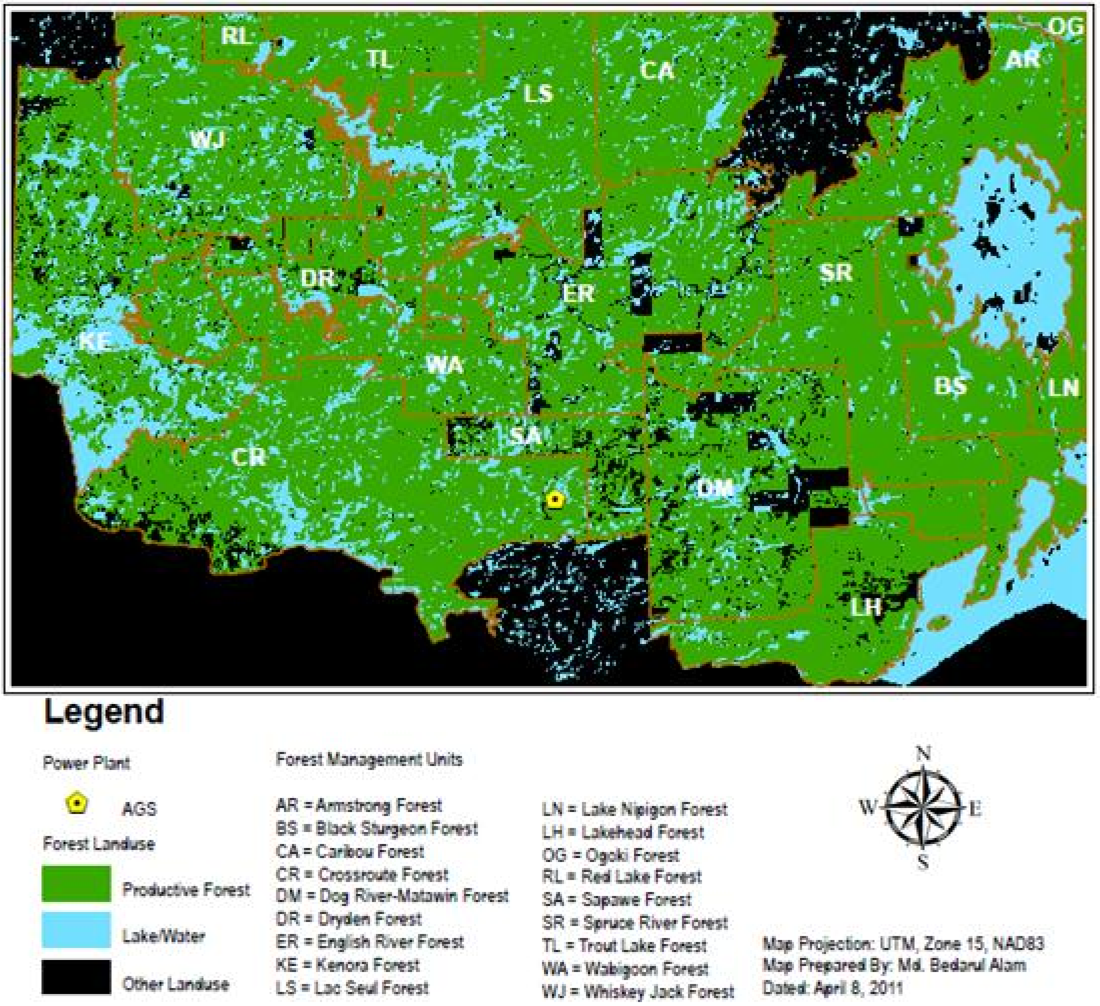

Figure 5.2 Forest land use in FMUs around the AGS in NWO.

The percent occurrence method is used to prepare the depletion layer. In this method, a code number is assigned to the grid cell depending on its depletion percentage (percent of the cell area harvested) (1 is 100%, 2 is from 80% to 100%, 3 is from 60% to 80%, 4 is from 40% to 60%, 5 is from 20% to 40%, 6 is from more than 0% to 20% depletion, and 7 is no depletion) (Figure 5.3).

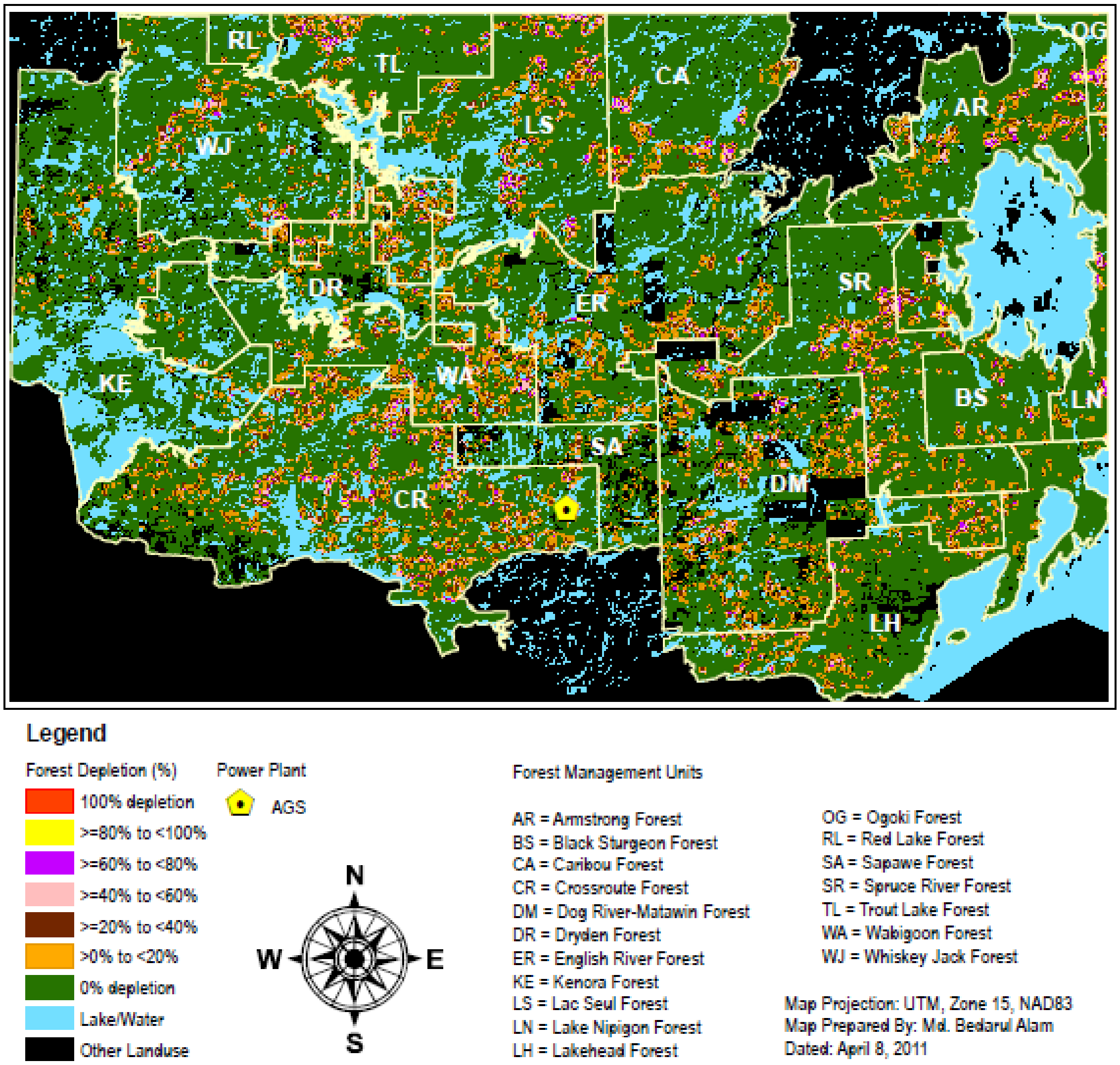

Figure 5.3 Forest depletion in different FMUs around the AGS.

Before developing the marginal transport cost layer for the AGS, a raster layer of the road network for the research area was also developed using the presence/absence method of data input (ESRI 2010) (Figure 5.3). A grid code was assigned depending on the presence of different types of roads (1 = highway-I, 2 = highway-II, and 3 = primary, 4 = secondary and 5 = tertiary/operational forest roads, and 9 = no road) in a cell. The raster layer of the road network was converted to ASCII (.txt) format. Visual Basic software was used to prepare the minimum cost layer for transporting woody biomass through the road network to the AGS (Figure 4.7). The location of the AGS was used as the sink node during the data input and optimization processes. The driving speeds of (90, 80, 60, 40 and 30 km per hour ($km \cdot h^{-1}$)) for an empty vehicle and (90, 70, 50, 30 and 20 $km \cdot h^{-1}$) for a loaded vehicle were used on highway-I, highway-II, and primary, secondary and tertiary/operational forest roads, respectively. The vehicle considered for transporting woody biomass feedstock is a tractor with a 53 foot semi-trailer (with belly). In Ontario the allowable legal payload weight for this type of tractor-trailer is taken as 40.55 tonnes (t) (this will vary depending on tractor and trailer tare weight). The charge-out rate for a biomass truck with operator is assumed to be 85 $\$ \cdot h^{-1}$ (2009 based). A fixed time for loading, unloading and delay of 2.5 hours per trip is assumed. In this cost layer, the cost of transporting woody biomass from each road cell (1 km^2) of the research area to the AGS was established.

The NLDP model was developed using GAMS software. Forest land use layer, depletion layer and cost layer were used as data input layers in data analysis models to establish the cost of transporting woody biomass from each cell of productive forest area to the AGS. Along with cost data other relevant data were used to feed the model in GAMS. The woody biomass feedstock is available in two product forms (forest harvest residues (FHR) and underutilized wood (UW)) from the surrounding 18 FMUs. The FHR constitute leftover tops, branches and other parts of the trees in the forest after harvesting trees from the forest mainly for the lumber, and pulp and paper industries. UW are the tree species and unmerchantable wood, which are not commercially important to harvest for lumber and pulpwood production, and trees damaged by wildfire, windthrow and insects that are currently not salvaged. The theoretical availability of FHR and UW from the productive forests of the study area was estimated at 60 m^3.ha^{-1} each (Alam *et al.* 2012a). A pre-harvest inventory conducted by Alam *et al.* (2012a) in the Crossroute Forest found the UW volume to be 65 $m^3 \cdot ha^{-1}$. However, only 36% of trees, which constitute 38% wood volume, fall under the UW category. Alam *et al.* (2012a), therefore conservatively estimated the average theoretical UW availability as 60 $m^3 \cdot ha^{-1}$. Reynolds *et al.* (2008) found similar results in their study in the Black Sturgeon Forest, where 43% of trees were under the UW category. The theoretical availability of FHR and UW in depleted cells, with different depletion percentages, of productive forest area was assumed on the basis of depletion percentages. For example, in a cell with 100% depletion there is 6,000 m^3 FHR and no UW, in a cell with 90% depletion there is 5,400 m^3 FHR and 600 m^3 UW, and in a cell with no depletion there is no FHR. In addition, no UW is planned for harvesting from the forest cell with 0% depletion.

The number of depleted forest cells over a historically seven-year period (2002-2009) was found to be 19,315 cells. We also assumed that 1 m^3 woody biomass can produce to 0.876 green tonne (gt) woody biomass (OMNR 2007b; Alam *et al.* 2012a). The two-way travel times (hours) and transportation costs ($\$ \cdot gt^{-1}$) of woody biomass from all (19,315) depleted forest cells of 1 km^2 size to the AGS were determined using the road network optimization model (Alam *et al.* 2012b). The model selects the optimal harvest of forest cells in order to meet the feedstock requirements for the given monthly production schedule, and calculates the costs for biomass procurement. The sets, indices, parameters and variables used in this model are as follows:

Sets:

I: Set of woody biomass production and supplying time (12 months)

J: Set of forest cells (19,315 cells)

Indices:

i = Woody biomass production and supplying month (i = 1, 2, 3, …, 12).

j = Forest cells (j = 1, 2, 3, …, 19,315)

Parameters:

CE = Conversion efficiency of AGS

ED = Energy density of woody biomass (gigajoule per oven-dry tonne ($GJ \cdot ODt^{-1}$))

MC = Moisture content in green biomass (% green weight basis)

EG = Equivalency of energy (gigajoule per megawatt hour ($GJ \cdot MWh^{-1}$))

EP_i = Demand of electricity production of AGS in i^{th} month (MWh)

BD_i = Total amount (gt) of biomass required by AGS in i^{th} month, calculated in Equation (1).

$$BD_i = \frac{EP_i \times EG}{(ED - 0.2164 \times MC) \times CE} \quad (1)$$

HF = Harvesting factor

PR = Harvesting and grinding/chipping (processing) cost ($\$ \cdot gt^{-1}$) of FHR at roadside

PU = Harvesting and grinding/chipping (processing) cost ($\$ \cdot gt^{-1}$) of UW at roadside

P = Rate of payment ($\$ \cdot h^{-1}$) for woody biomass truck including operator

L = load size (m^3) of woody biomass truck

F = Conversion factor for biomass from cubic metre to green tonne

T_j = Variable time to transport woody biomass from a forest cell AGS (h)

VC_j = Variable cost ($\$\cdot gt^{-1}$) to transport woody biomass from a forest cell to AGS, calculated in Equation (2).

$$VC_j = \frac{T_j \times P}{L \times F} \tag{2}$$

FT = Fixed time (h) for loading, unloading and delay per trip

FC = Fixed cost (($\$\cdot gt^{-1}$) to transport woody biomass from a forest cell to AGS, calculated in Equation (3).

$$FC = \frac{FT \times P}{L \times F} \tag{3}$$

TC_j = Biomass transportation cost (($\$\cdot gt^{-1}$) from the j^{th} forest cell to AGS, calculated in Equation (4).

$$TC_j = VC_j + FC \tag{4}$$

FR_j = Theoretical FHR availability (gt) in a forest cell over 7 years horizon (2002-2009)

FU_j = Theoretical UW availability (gt) in a forest cell over 7 years horizon (2002-2009)

IR_j = Initial technical FHR availability (gt) in a forest cell in the 12 months horizon, calculated in Equation (5).

$$IR_j = \frac{\mathrm{FR}_j \times HF}{7} \tag{5}$$

IU_j = Initial technical UW availability (gt) in a forest cell in the 12 months horizon, calculated in Equation (6).

$$IU_j = \frac{\mathrm{FU}_j \times HF}{7} \tag{6}$$

Variables:

R_{ij} = Amount FHR harvested (gt) in i^{th} month from j^{th} forest cell

U_{ij} = Amount UW harvested (gt) in i^{th} month from j^{th} forest cell

TB_i = Total amount of biomass harvest in i^{th} month

TPC = Total biomass procurement cost ($)

RT_{ij} = Total amount of FHR available (gt) in i^{th} month from j^{th} forest cell

UT_{ij} = Total monthly UW available (gt) in i^{th} month from j^{th} forest cell

$RT_{(i+1)j}$ = Total amount of FHR available (gt) in $(i+1)^{th}$ month from j^{th} forest cell

$UT_{(i+1)j}$ = Total amount of UW available (gt) in $(i+1)^{th}$ month from j^{th} forest cell

The objective function is to minimize the overall procurement costs for a given monthly demand of the AGS for a one-year time horizon. As this complex problem is formulated as a non-linear dynamic programming problem, the difficulty to solve this type of problem is linked to the combinatorial complexity of the problem, and the solution space increases exponentially with the problem size. The objective function and the constraints of the model are described by the following equations:

$$Minimize\ TPC = \sum_{i=1}^{12} \sum_{j=1}^{19315} (R_{ij}(PR + TC_j)) + \sum_{i=1}^{12} \sum_{j=1}^{19315} (U_{ij}(PU + TC_j)) \tag{7}$$

Subject to:

$$RT_{1j} = IR_j \tag{8}$$

$$UT_{1j} = IU_j \tag{9}$$

$$\sum_{j=1}^{19315} R_{ij} + \sum_{j=1}^{19315} U_{ij} = TB_i \tag{10}$$

$$R_{ij} \leq RT_{ij} \tag{11}$$

$$U_{ij} \leq UT_{ij} \tag{12}$$

$$RT_{(i+1)j} = RT_{ij} - R_{ij} \tag{13}$$

$$UT_{(i+1)j} = UT_{ij} - R_{ij} \tag{14}$$

$$TB_i \geq BD_i \tag{15}$$

$$R_{ij}, U_{ij} \geq 0 \tag{16}$$

Equation (7) is the objective function of the model, which minimizes total cost ($), which is the summation of total harvesting and grinding/chipping costs and transportation costs of FHR and UW, respectively. Equations (8) to (16) are the constraints in the model. Equations (8) and (9) specify the constraints that the total amount (gt) of FHR and UW available in 1^{st} month in j^{th} forest cell is equal to the initial technical FHR and UW availability (gt) in the forest cell, respectively. Equation (10) specifies the constraint that the total amount of biomass procured (gt) in i^{th} month for AGS is the sum of the total amount (gt) of FRH and UW harvested from the forest cells in the i^{th} month. Equations (11) and (12) specify the constraints that the total amount (gt) FHR and UW harvested is less than or equal to the amount (gt) of FHR and UW available in the i^{th} month from the j^{th} forest cell, respectively. Equations (13) and (14) are the availability constraints for FHR and UW, which ensure that the total amount (gt) of FHR and UW available in a forest cell for the next month is equal to the balance of the amount (gt) of FHR and UW in the cell after harvesting FHR and UW, respectively from this cell in the present month. Equation (15) is the biomass procurement constraint, which confirms that the total amount (gt) of biomass procured in i^{th} month is greater than or equal to the total amount (gt) of biomass required in i^{th} month to generate desired amount of power in this month at AGS. Finally, equation (16) ensures that the decision variables (amount of FHR and UW harvested) are positive.

The model becomes non-linear due to the inherent nature of the solution procedure in GAMS, where one endogenous variable (amount of biomass to be harvested in the next period) is determined with the help of another endogenous variable (the amount harvested in the previous periods). The model is dynamic in the sense that it provides a global solution to the entire planning horizon of 12 months operation of the power plant by simultaneously taking the capacity constraints and requirements for each month into account.

The assumptions in base scenario include a harvesting factor of 67%, harvesting and grinding/chipping (processing) cost for FHR and UW of \$26 and \$31, respectively (Gautam *et al.* 2010), conversion efficiency of power plant of 35%, and moisture content of woody biomass of 40%. The heat value of woody biomass is taken as 19.6 $GJ \cdot ODt^{-1}$ (Hosegood 2010), and 3.6 $GJ \cdot MWh^{-1}$ are used to convert the heat value to electricity units. Figure 5.4 shows the monthly power production (MWh) over the planning horizon of one-year (Sygration 2011).

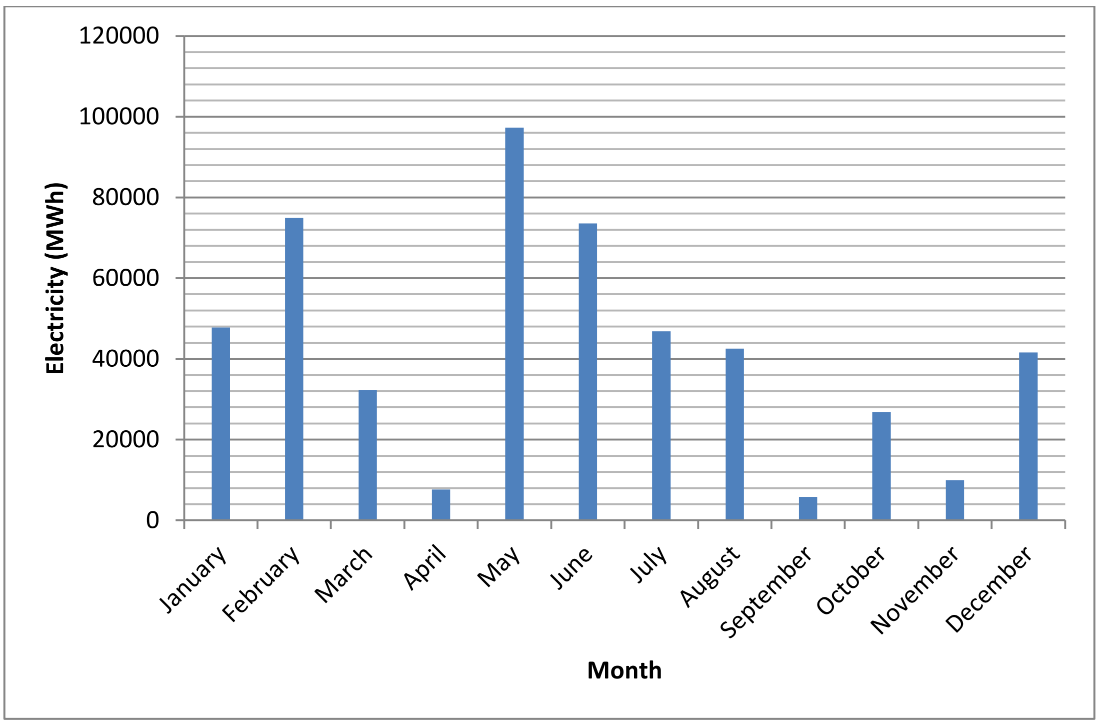

Figure 5.4 Monthly power production schedules at the AGS. The bars represent actual monthly power production in 2010 at the AGS to meet electricity demands (Sygration 2011).

Sixteen alternate scenarios (Table 5.1) were run to test the sensitivity of HF, CE, MC and processing costs (PC) of both FHR (which is PR) and UW (which is PU), in order to analyze different cost scenarios for producing power at the AGS in an economically viable and sustainable way. First, the effect of HF was explored, keeping other parameters the same as in the BASE scenario. For example, in HFIA, the HF was increased to 73.7% (10% increase compared to the BASE), in HFIB the HF was increased to 80.4% (20% increase), in HFDA the HF was decreased to 60.3% (10% decrease), and in HFDB the HF was decreased to 53.6% (20% decrease). Second, the sensitivity of CE was explored, keeping other parameters the same as in the BASE scenario. In CEIA and CEIB, the CE was increased by 10% and 20% respectively, whereas in CEDA and CEDB, the CE was decreased by 10% and 20% respectively. Third, the sensitivity of MC was tested by increasing MC by 10% (MCIA) and 20% (MCIB), and by decreasing MC by 10% (MCDA) and 20% (MCDB). Finally, the effect of PC was tested by increasing PC by 10% (PCIA) and 20% (PCIB), and by decreasing PC by 10% (PCDA) and 20% (PCDB) (Table 5.1). The results are displayed in ODt because MC does not have any effect on it.

Table 5.1 Description of different scenarios of the model. Numbers in brackets indicate % change of parameters from the BASE scenario in sensitivity analyses.

Scenario	Key parameters						
	HF (%)	**PR ($·gt^{-1})**	**PU ($·gt^{-1})**	**CE (%)**	**MC (%)**	**ED (GJ·ODt^{-1})**	**EG (GJ·MWh^{-1})**
BASE	67	26	31	35	40	19.6	3.6
HFIA	73.7 (+10%)	26	31	35	40	19.6	3.6
HFIB	80.4 (+20%)	26	31	35	40	19.6	3.6
HFDA	60.3 (-10%)	26	31	35	40	19.6	3.6
HFDB	53.6 (-20%)	26	31	35	40	19.6	3.6
CEIA	67	26	31	38.5 (+10%)	40	19.6	3.6
CEIB	67	26	31	42 (+20%)	40	19.6	3.6
CEDA	67	26	31	31.5 (-10%)	40	19.6	3.6
CEDB	67	26	31	28 (-20%)	40	19.6	3.6
MCIA	67	26	31	35	44 (+10%)	19.6	3.6
MCIB	67	26	31	35	48 (+20%)	19.6	3.6
MCDA	67	26	31	35	36 (-10%)	19.6	3.6
MCDB	67	26	31	35	32 (-20%)	19.6	3.6
PCIA	67	28.6 (+10%)	33 (+10%)	35	40	19.6	3.6
PCIB	67	31.2 (+20%)	37.2 (+20%)	35	40	19.6	3.6
PCDA	67	23.4 (-10%)	27.9 (-10%)	35	40	19.6	3.6
PCDB	67	20.8 (-20%)	24.8 (-20%)	35	40	19.6	3.6

Note: HF = Harvesting factor; PR = Harvesting and grinding/chipping (processing) cost ($·gt^{-1}) of forest harvest residue (FHR); PU = Processing cost ($·gt^{-1}) of underutilized wood (UW); CE = Conversion efficiency of Atikokan Generating Station (AGS); MC = Moisture content in green biomass (% green weight basis); ED = Energy density of woody biomass (GJ·ODt^{-1}); and EG = Equivalency of energy (GJ·MWh^{-1})

5.3 Results and Discussion

The model provides a global optimal solution over a one-year planning horizon by minimizing the objective function of biomass procurement costs (including harvesting, processing and transportation) based on woody biomass availability in each cell and monthly biomass demand based on electrical power production requirements. In the BASE scenario, out of 19,315 forest cells, the model selects 3,097 cells for harvesting FHR and 377 cells for harvesting UW to fulfill the annual woody biomass demand for the AGS (Figure 5.5). The forest cells selected for collecting FHR are mainly located in the following five FMUs: Crossroute Forest, Sapawe Forest, Dog River-Matawin Forest, Wabigoon Forest and Dryden Forest (Figure 5.5). Only two forest cells from the Lakehead Forest are selected for FHR (Figure 5.5). All forest cells selected for harvesting UW are located in the Crossroute Forest (Figure 5.5). Out of 18 FMUs (Figure 5.2), 12 FMUs are not selected to harvest woody biomass for energy production (Figure 5.5). The selected forest cells are located near the AGS and in lower cost zones (Figures 4.7 and 5.5). Depending on the monthly production schedule at the AGS (Figure 5.4), the optimal amount of woody biomass harvesting required for each month is illustrated in Figure 5.6. The total monthly amount of woody biomass harvesting ranges from 3,283 ODt (September) to 54,857 ODt (May). The average monthly amount of woody biomass harvesting is 23,827 ODt.

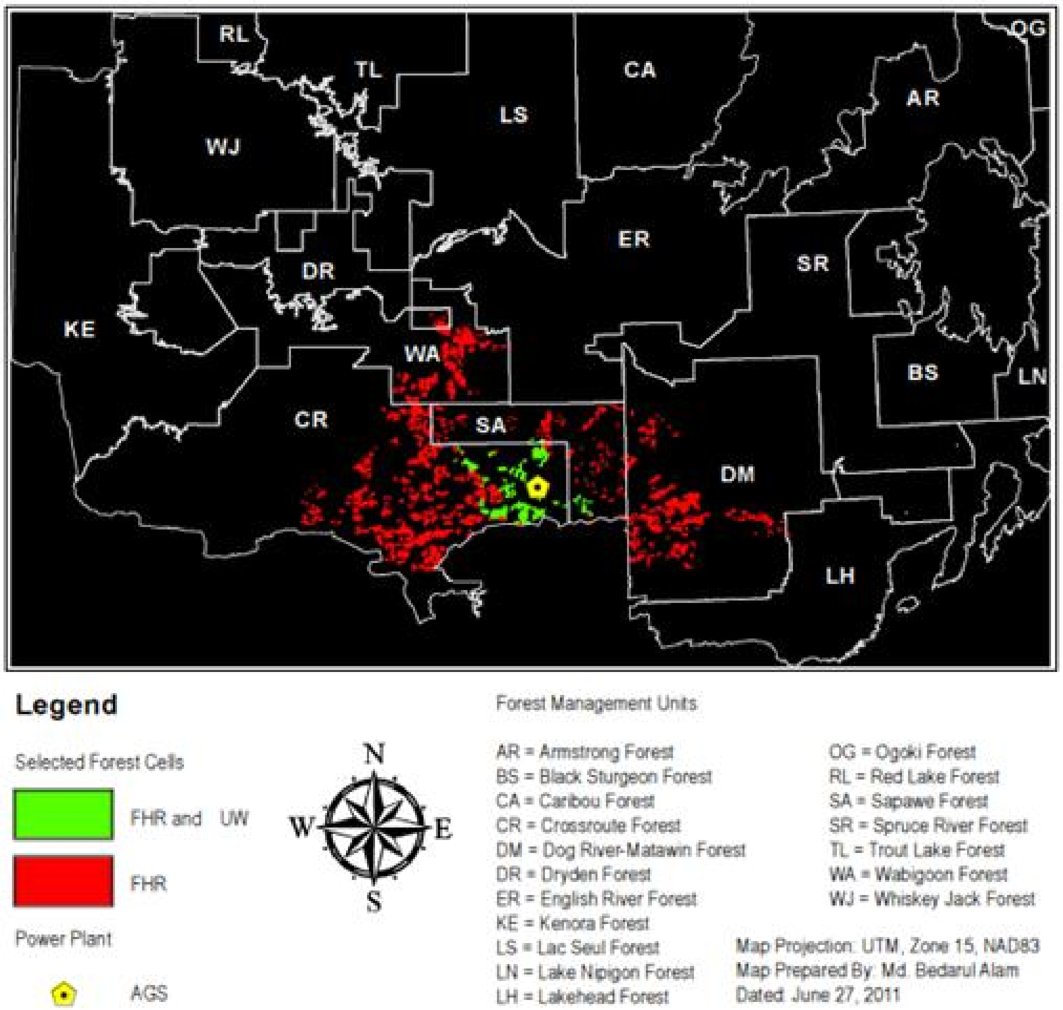

Figure 5.5 Selected forest cells to harvest FHR and UW for the AGS (BASE Scenario).

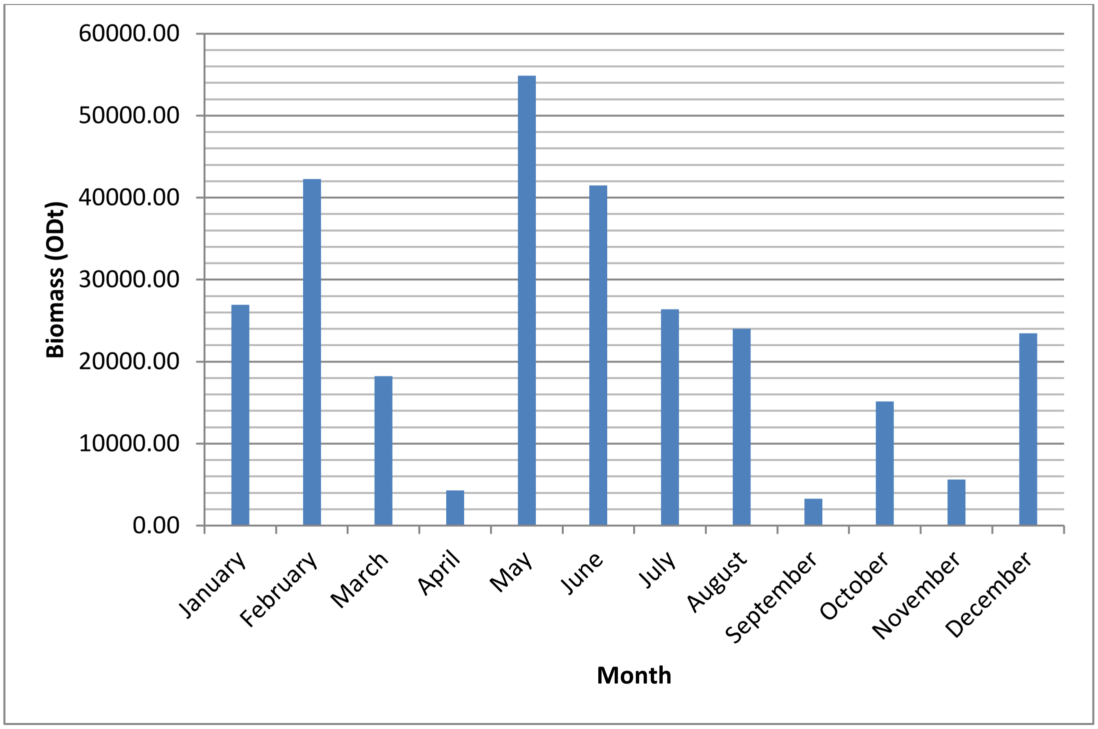

Figure 5.6 Monthly amount of woody biomass consumption at the AGS to meet electricity power production requirements (BASE Scenario).

Figure 5.7 shows the total monthly woody biomass feedstock procurement cost for electricity production at the AGS. The total monthly woody biomass procurement cost ranges from \$204,420 (September) to \$3,406,709 (May). The average monthly woody biomass procurement cost is \$1,470,265. Monthly per unit woody biomass procurement costs for electricity production at AGS are shown in Figure 5.8. The minimum, maximum and average per unit woody biomass feedstock procurement costs are 58.11 $\$\cdot ODt^{-1}$ (January), 64.02 $\$\cdot ODt^{-1}$ (November) and 61.74 $\$\cdot ODt^{-1}$, respectively.

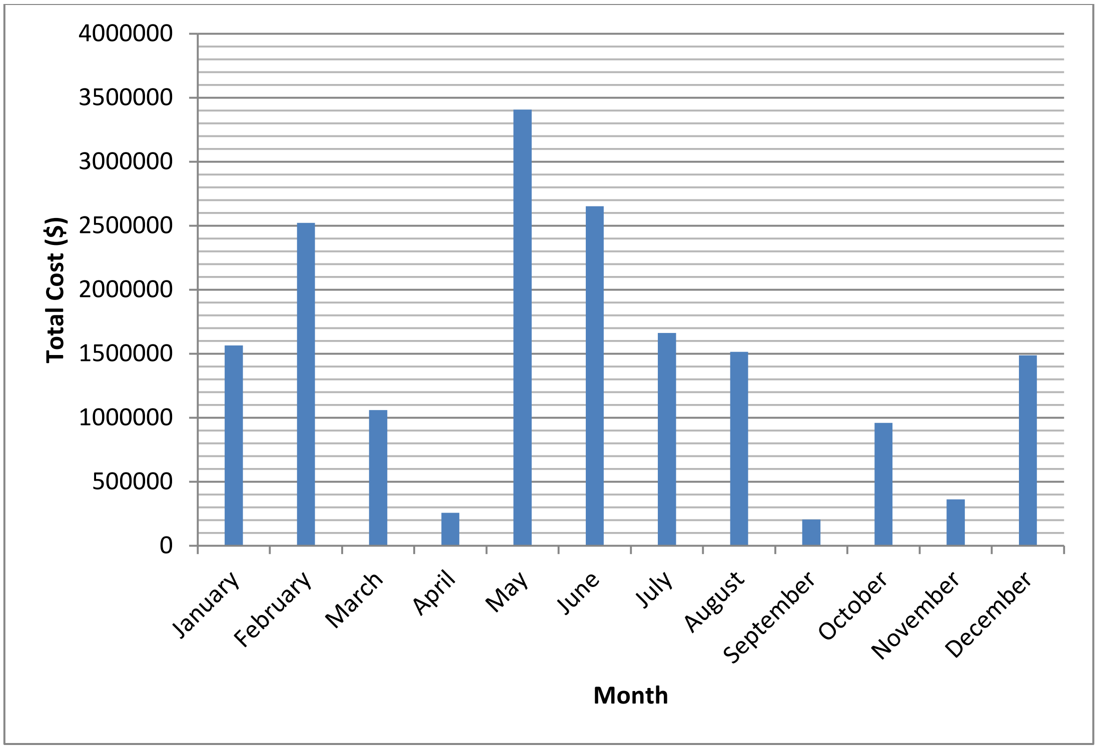

Figure 5.7 Monthly total procurement cost of woody biomass feedstock for electricity production at the AGS (BASE Scenario).

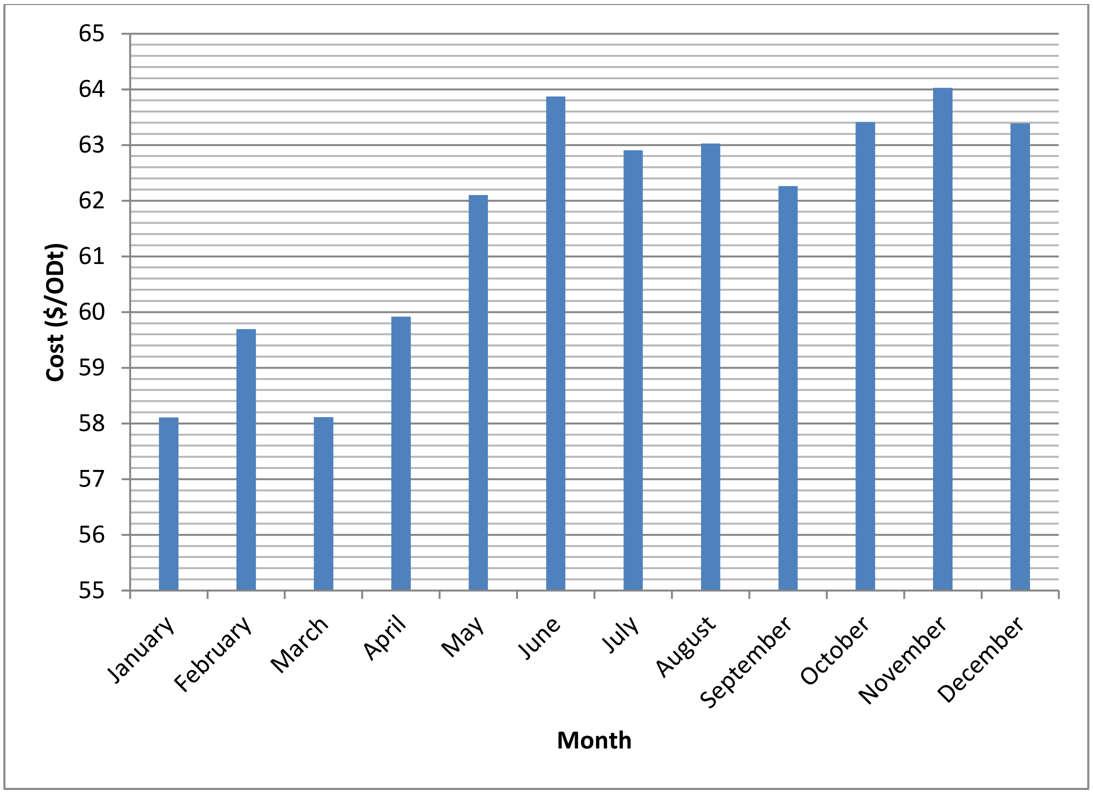

Figure 5.8 Monthly per unit woody biomass procurement cost for electricity production at the AGS (BASE Scenario).

Figure 5.9 shows the monthly woody biomass feedstock costs per unit electricity production at the AGS. The feedstock cost per unit electricity production ranges from 32.77 $\$\cdot MWh^{-1}$ (January) to 36.10 $\$\cdot MWh^{-1}$ (November). The average feedstock cost is 34.81 $\$\cdot MWh^{-1}$, which is the weighted average based on monthly power produced/biomass used and not just a straight average of the 12 months.

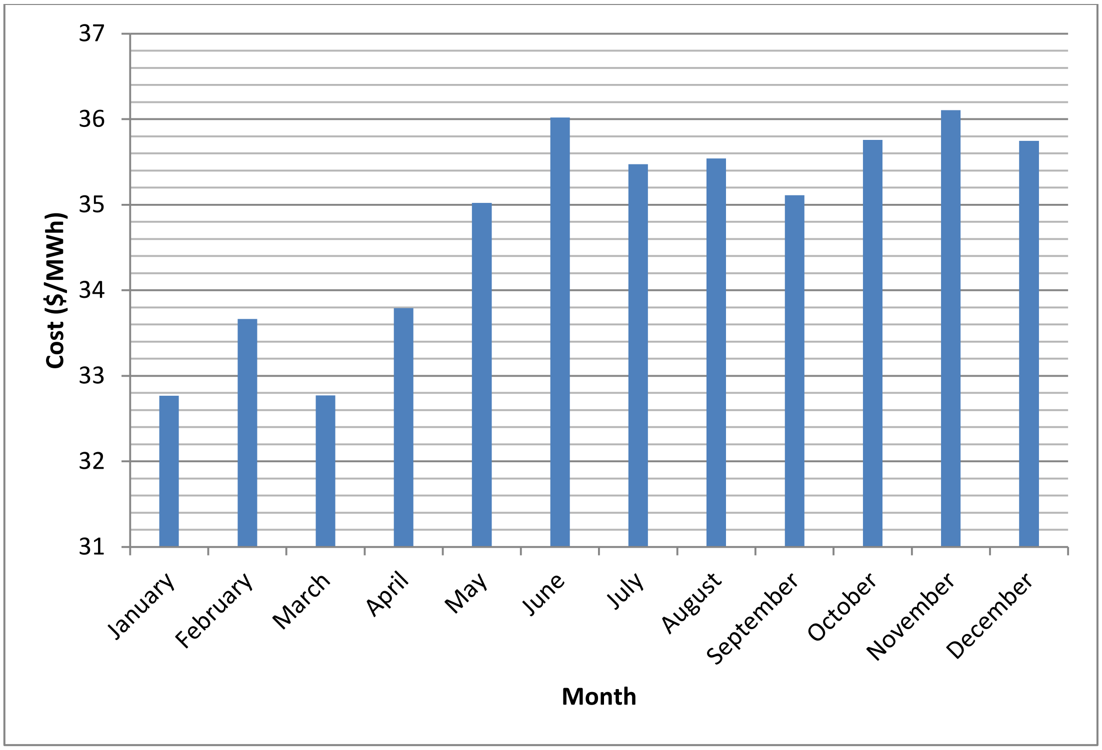

Figure 5.9 Monthly feedstock cost per MWh at the AGS (BASE Scenario).

In order to produce 507,037 MWh of electricity annually at AGS, a total annual 285,923ODt of woody biomass is required, with a total annual cost of \$17,643,182, per unit biomass procurement cost of 61.71 $\$\cdot ODt^{-1}$, and feedstock cost of 34.80 $\$\cdot MWh^{-1}$, respectively (Table 5.2). The lower amounts of monthly total woody biomass requirements and lower monthly costs in some months (such as April, September and November) are due to the fact that the AGS produces lower amounts of electricity in these months (Figures 5.4, 5.6 and 5.7).

Table 5.2 Sensitivity analyses on the total amount of annual biomass harvesting, total biomass procurement cost, unit biomass procurement cost and the unit electricity production cost. Numbers in brackets represent % change from the BASE scenario.

Scenario	**Electricity (MWh·yr^{-1})**	**Biomass (ODt·yr^{-1})**	**Total cost (\$·yr^{-1})**	**Cost (\$·ODt^{-1})**	**Cost (\$·MWh^{-1})**
BASE	507,037	285,923	17,643,182	61.71	34.80
HFIA	507,037	285,923	17,554,193 (-0.5%)	61.39 (-0.5%)	34.62 (-0.5%)
HFIB	507,037	285,923	17,474,000 (-1%)	61.11 (-1%)	34.46 (-1%)
HFDA	507,037	285,923	17,743,139 (+0.6%)	62.06 (+0.6%)	34.99 (+0.6%)
HFDB	507,037	285,923	17,858,161 (+1.2%)	62.46 (+1.2%)	35.22 (+1.2%)
CEIA	507,037	259,930 (-9.1%)	15,958,357 (-9.5%)	61.39 (-0.5%)	31.47 (-9.5%)
CEIB	507,037	238,269 (-16.7%)	14,561,666 (-17.5%)	61.11 (-1%)	28.72 (-17.5%)
CEDA	507,037	317,692 (+11.1%)	19,714,598 (+11.7%)	62.06 (+0.6%)	38.88 (+11.7%)
CEDB	507,037	357,404 (+25%)	22,322,701 (+26.5%)	62.46 (+1.2%)	44.03 (+26.5%)
MCIA	507,037	289,781 (+1.3%)	19,243,078 (+9.1%)	66.41 (+7.6%)	37.95 (+9.1%)
MCIB	507,037	294,365 (+3%)	21,154,264 (+19.9%)	71.86 (+16.5%)	41.72 (+19.9%)
MCDA	507,037	282,630 (-1.2%)	16,284,095 (-7.7%)	57.62 (-6.6%)	32.12 (-7.7%)
MCDB	507,037	279,787 (-2.1%)	15,115,495 (-14.3%)	54.02 (-12.4%)	29.81 (-14.3%)
PCIA	507,037	285,923	18,951,114 (+7.4%)	66.28 (+7.4%)	37.38 (+7.4%)
PCIB	507,037	285,923	20,246,318 (+14.8%)	70.81 (+14.8%)	39.93 (+14.8%)
PCDA	507,037	285,923	16,322,779 (-7.5%)	57.09 (-7.5%)	32.19 (-7.5%)
PCDB	507,037	285,923	14,990,927 (-15%)	52.43 (-15%)	29.57 (-15%)

It is observed that at first the model selects the cells, which are closer to the AGS, and in later months farther cells are selected. The behaviour of the model is consistent with an a priori hypothesis of mode of biomass collection or procurement. The cells which are located at longer distances from the AGS (Lake Nipigon, Ogoki, and Red Lake) are not utilized by the model for woody biomass procurement, as it is not economically feasible to transport biomass over such long distances.

The results of the 16 sensitivity analyses are shown in Table 5.2. The HF and procurement cost were found to be inversely related: i.e., when HF increases the procurement cost decreases and vise-versa. In HFIA and HFIB scenarios the total woody biomass procurement cost, per unit woody biomass procurement cost and per unit electricity production cost all decrease by 0.5% and 1%, respectively in relation to an HF increase by 10% and 20%, respectively. On the other hand in HFDA and HFDB scenarios the total woody biomass procurement cost, the per unit woody biomass procurement cost and the feedstock cost per MWh all increase by 0.6% and 1.2%, respectively in relation to an HF decrease by 10% and 20%, respectively. The electricity production cost decreases with an increase in HF because more woody biomass could be harvested from nearby forest cells that further reduces the transportation cost of woody biomass feedstock for energy production (Alam *et al.* 2009b). However, increases or decreases in HF by up to 20% from the BASE scenario of 67% had a limited impact on procurement and feedstock cost per MWh.

The CE and procurement cost are also inversely related: i.e., when CE increases the procurement cost decreases and vise-versa. In CEIA and CEIB, the amount of woody biomass harvested, the total woody biomass procurement cost, the per unit woody biomass procurement cost and the feedstock cost per MWh decrease by (9.1%, 9.5%, 0.5% and 9.5%) and (16.7%, 17.5%, 1% and 17.5%) in relation to a CE increase by 10% and 20%, respectively. Whereas in CEDA and CEDB, the amount of woody biomass harvested, the total woody biomass procurement cost, the per unit woody biomass procurement cost and the feedstock cost per MWh cost increase by (11.1%, 11.7%, 0.6% and 11.7%) and (25%, 26.5%, 1.2% and 26.5%) in relation to a CE decrease by 10% and 20%, respectively. Therefore, with changes in CE, though the changes in the per unit woody biomass procurement cost is minimal, the changes in the amount of woody biomass harvested, the total woody biomass procurement cost and the feedstock cost per MWh are very high. This is because, with higher CE, the required amount of woody biomass feedstock to produce the same power at the AGS is reduced, and hence the feedstock cost per MWh becomes lower (Berndes 2003; Koppejan 2007; Alam *et al.* 2009b). Therefore, there is high potential for cost savings through efforts to increase CE.

The MC and procurement cost are positively related: i.e., when MC increases the procurement cost increases and vice-versa. In MCIA and MCIB, the amount of woody biomass harvested, the total woody biomass procurement cost, the per unit woody biomass procurement cost and the feedstock cost per MWh increase by (1.3%, 9.1%, 7.6% and 9.1%) and (3%, 19.9%, 16.5% and 19.9%) in relation to a MC increase by 10% and 20%, respectively. Whereas, in MCDA and MCDB, the amount of woody biomass harvesting, the total woody biomass procurement cost, the per unit woody biomass procurement cost and the feedstock cost per MWh decrease by (1.2%, 7.7%, 6.6% and 7.7%) and (2.1%, 14.3%, 12.4% and 14.3%) in relation to a MC decrease by

10% and 20%, respectively. With a change in MC, the changes in the total woody biomass procurement cost, the per unit woody biomass feedstock procurement cost and the feedstock cost per MWh are very high, with increases in MC having a higher impact than decreases in MC. This is because, with higher MC, the net heat value decreases at a higher rate in woody biomass and a higher volume of woody biomass is required for producing the same amount of electricity and eventually the cost of electricity increases (Nurmi 1999; Berndes 2003; Koppejan 2007). Efforts to decrease MC and control it at an acceptable level (e.g., < 30% green weight basis) have high potential for reducing biomass procurement and electricity generating costs (Gautam 2010).

The PC and procurement cost are positively related: i.e., when PC increases the procurement cost increases and when PC decreases the procurement cost also decreases. In PCIA and PCIB, the total woody biomass procurement cost, the per unit woody biomass procurement cost and the feedstock cost per MWh all increase by 7.4% and 14.8% in relation to a PC increase by 10% and 20%, respectively. Whereas, in PCDA and PCDB, the total woody biomass procurement cost, the per unit woody biomass procurement cost and the feedstock cost per MWh all decrease by 7.5% and15% in relation to a PC decrease by 10% and 20%, respectively. With a change in PC, the change in the total woody biomass procurement cost, the per unit woody biomass procurement cost and the feedstock cost per MWh are very high. Previous studies conducted by Berndes (2003), Tatsiopoulos and Tolis (2003) and Sokhansanj *et al.* (2006) show similar results. Research and efforts to reduce biomass processing costs also have high potential for reducing biomass procurement and electricity generating costs.

These 16 scenarios along with the BASE scenario provide interesting information on where to focus further research in the woody biomass procurement chain for bioenergy production to reduce biomass procurement and electricity generating costs: i.e., on managing moisture content (MC), improving the technological processes of biomass to bioenergy conversion (CE) and using efficient processing techniques (PC). Similar suggestions have been made by previous studies in the U.S. (Gan and Smith 2006) and in Canada (Alam *et al.* 2009b). Increasing the biomass-harvesting factor above the 67% used in the BASE scenario shows only marginal benefits in reducing costs, and even a decrease of 20% only had a marginal impact on increasing costs.

5.4 Conclusions

The complexities of procurement and efficient supply of woody biomass feedstock to the bioenergy power generating stations in NWO in a cost effective way are handled by developing a non-linear dynamic programming model. The model provides a global optimal solution for quantity and types of woody biomass selection by minimizing the costs of harvesting, processing and transporting woody biomass from the forest cells to the power generating station. Based on the monthly electricity production schedule of the AGS, the total monthly amount of woody biomass harvesting ranges from 3,283 ODt (September) to 54,857 ODt (May). The woody biomass feedstock cost per unit electricity production ranges from 32.77 $\$\cdot MWh^{-1}$ (January) to 36.10 $\$\cdot MWh^{-1}$ (November). The model also shows the potential to analyze the effects of changes in important parameter and choice variables on biomass feedstock cost, thereby providing important information for decision support to reduce the overall procurement costs over time. The conversion efficiency was found the most sensitive followed by the moisture content, whereas the harvesting factor showed the least sensitivity.

One of the limitations of this study is the assumption of availability of harvestable UW from depleted forest cells due to lack of past UW inventory data. Although, conservative estimates are used for UW availability from depleted forest cells in this study, this limitation can be overcome by enhanced forest inventory data in the future. This model could be further improved by incorporating data related to differences between tree species, forest types, moisture contents, heat values, harvesting systems, and variations in the amount of seasonal and weekly power generation. One thought for future research is the production of pellets in a distributed network could reduce the transportation costs and feedstock requirements, as pellets are a more energy dense biomass feedstock. Future versions of this model will reflect these improvements by incorporating new information and will help in developing an integrated decision support system of bioenergy production in NWO. Based on the results of the sensitivity analysis, research and development in the woody biomass to energy supply chain should be initially focused on the following areas: improving the technological processes of biomass to bioenergy conversion, managing feedstock moisture content, and using cost effective and efficient biomass processing techniques. Work on the impact of transport cost needs to be done too, which is incorporated into the next chapter.

Chapter 6

Economic analysis of biomass supply chains: a case study of four competing bioenergy power plants in northwestern Ontario[7]

6.1 Introduction

Woody biomass has been recognized as an alternative energy source since it is renewable and nearly CO_2 neutral (Rauch and Gronalt 2010). However, renewable energy production from woody biomass faces many challenges due to uncertainty of its continuous supply (Gan and Smith 2006; Wang 2007; Thornley *et al.* 2008; Kim *et al.* 2011b). The ever-increasing demand of biomass for bioenergy production has enormously increased the transportation distances and costs for woody biomass procurement, which is spread over large geographical locations at varying distances from the power plant (Rauch and Gronalt 2010; Tahvanainen and Perttu 2010). Further, the optimal harvest schedules become complicated if more power plants compete for available biomass feedstock over a given space and time. This suggests a need for developing and using optimization models to analyze such problems for improved decision making in bioenergy production.

Canada's dependence on fossil fuels has changed in recent times and woody biomass has become an important part of its energy picture, supplying about 6% of our primary energy demand, the second largest source of renewable energy after hydroelectricity (Centre for Energy 2011). A major application of bioenergy is found in

[7]A version of this chapter has been submitted to the Energy Systems for publication.

the forest products industry of Canada. Beyond the forest industry, several independent power plants generate electricity from woody biomass in Canada. There are three major combined heat and power (CHP) plant developments in northwestern Ontario (NWO) west of Lake Nipigon, namely Thunder Bay CHP plant, Fort Frances CHP plant and Dryden CHP plant. Currently, Thunder Bay CHP plant and Fort Frances CHP plant are using woody biomass feedstock, referred to as biofibre by the Ontario Ministry of Natural Resources, though they are not operating at full capacities. At present the Dryden CHP plant is not using any biofibre feedstock, but it has the potential (Duquette 2011). When these plants operate fully and if they use 100% woody biomass feedstock, the planned annual demands of Thunder Bay CHP plant, Fort Frances CHP plant and Dryden CHP plant for woody biomass feedstock are 730,000 green tonnes (gt), 800,000 gt and 480,000 gt, respectively. The Atikokan power generating station, another power plant, is currently being converted to use woody biomass feedstock instead of coal and would require 200,000 gt annually (Forest BioProducts Inc. 2006; OPG 2010). When all these plants become fully operational, the power plant managers (buyers of biomass) will need to have a sustainable supply of biomass cost effectively, and the contractors (suppliers of biomass) would like to increase their gross margins (profits) from biomass supply operations. Therefore, the optimization of woody biomass feedstock supply needs to be addressed both with cost optimization and profit maximization points of views.

Woody biomass is normally available either as forest harvest residue (FHR), which includes tops and branches, and un-merchantable wood left after stand harvesting, or as underutilized wood (UW), which includes un-harvested tree species that are not commercially important for timber, and trees damaged by wildfire, windthrow and insects that are currently not salvaged. Further, there are numerous options for comminuting woody biomass, and several trucking and loading options having varying costs. Optimizing biomass procurement is, therefore, a complex problem with numerous supply and demand constraints.

A number of computational techniques from heuristics to advanced optimization models have been developed to model location specific biomass procurement problems (Krarup and Pruzan 1983; Macmillan 2001; Mentzer 2001; Gunnarsson *et al.* 2003; Rönnqvist 2003; Bredström *et al.* 2004; Koppejan 2007; Chauhan *et al.* 2009). These studies focus on bioenergy plant location problems for wide-spread woody biomass applications. The supply network normally consists of a single bioenergy production plant with many biomass supply regions (Erikson and Björheden 1989). In this context, woody biomass transportation costs constitute the majority of forest fuel supply chain costs for energy production.

Further studies in biomass procurement, therefore, focused on reducing overall transportation costs (Sokhansanj and Fenton 2006; Mahmoudi *et al.* 2009; Sowlati 2009; Rauch *et al.* 2010). Linear programming (LP) models, which are a common technique in operations research, have been used to optimize transportation distances and costs for woody biomass procurement for energy production at regional levels (Freppaz *et al.* 2004; Frombo *et al.* 2009). Woody biomass feedstock data have also been analyzed using geographic information systems (GIS) techniques (Noon and Daly 1996; Viana *et al.* 2010). LP models have also been developed using GIS-based woody biomass data both for estimating the feedstock availability and for reducing transportation distances and costs (Ranta 2002; Ranta 2005; Panichelli and Edgard 2008; Perpina *et al.* 2009). However, all these studies have been conducted either in Nordic or in central European countries.

We found no such optimization models dealing with biomass supply competition among various power plants in the Canadian context with large contiguous wood supply areas. The purpose of this study is, therefore, to develop and apply optimization models to analyze the impact of inter-power plant competition for the available biomass feedstock on cost structures and gross margins of each power plant in NWO. Specifically, the two models (one based on cost minimization and other on profit maximization) were developed. The cost minimization model is applied from the power plant managers' (buyers) perspective and the profit maximization model was applied from the biomass suppliers' perspective. Several sensitivity analyses were run to study the impact of changes in parameters relevant to woody biomass processing technology, biomass types, and prices of inputs and outputs.

6.2 Methods

The flow chart in Figure 6.1 presents the methodology for developing the LP models for supplying woody biomass feedstock to the four power generating stations. The study area, 324 km (N-S) × 516 km (E-W) (167,184 km^2), consists of 18 FMUs west of Lake Nipigon in NWO. GIS data were collected from Land Information Ontario, Sustainable Forest Licence (SFL) holders, and consultant companies in the formats of Shapefile and Geodatabase (Abitibi-Bowater Inc. 2009; Greenmantle Forest Inc.2009; GreenForest Management Inc. 2009; LIO 2010). The original vector data was first converted to raster and finally to spatial database text files for the entire research area using ArcGIS software. Three main spatial layers (land use, forest depletion and cost layers) were prepared on a raster grid size of 1 km × 1 km (1 km^2), where each cell represents a feature (Nichols *et al.* 2006; ESRI 2010). Different data input methods were followed for different types of features. The dominant data input method was used to create a raster layer of forest land use class (ESRI 2010), where a grid code entity was assigned to each feature (productive forest, water/lake, and other land use), which occupies more than 50% of the cell area[8]. The percent occurrence method was used to prepare the depletion layer, where a code number was assigned to the grid cell depending on its depletion percentage. Before developing the marginal transport cost layer for each power plant, a raster layer of the road network for the research area was also developed using the presence/absence method of data input (ESRI 2010). A grid code was assigned depending on the presence of different types of roads in a cell. The raster layer of the road network was converted to ASCII (.txt) format. A network optimization model was used to prepare the minimum cost layer for transporting woody biomass through the road network to the four power plants. The location of each power plant was used as the sink node during the data input and optimization processes. The vehicle considered for transporting woody biomass feedstock was a tractor with a 53 foot semi-trailer (with belly). In Ontario the allowable legal payload weight for this type of tractor-trailer was taken as 40.55 tonnes (t). The charge-out rate for a biomass truck with operator was assumed to be 85 $\$\cdot h^{-1}$ (2009 based). A fixed time for loading, unloading and delay of 2.5 hours per trip was assumed. In this cost layer, the cost of transporting woody

[8]Detailed methodology of data input methods is provided by Alam *et al.* (2012a and 2012b).

biomass from each road cell (1 km^2) of the research area to the four power plants was established. Minimum cost zones (tessellations) for transporting woody biomass from each of the 100,061 forest cells to each of the four power plants were established in order to create biomass catchment areas for each power plant.

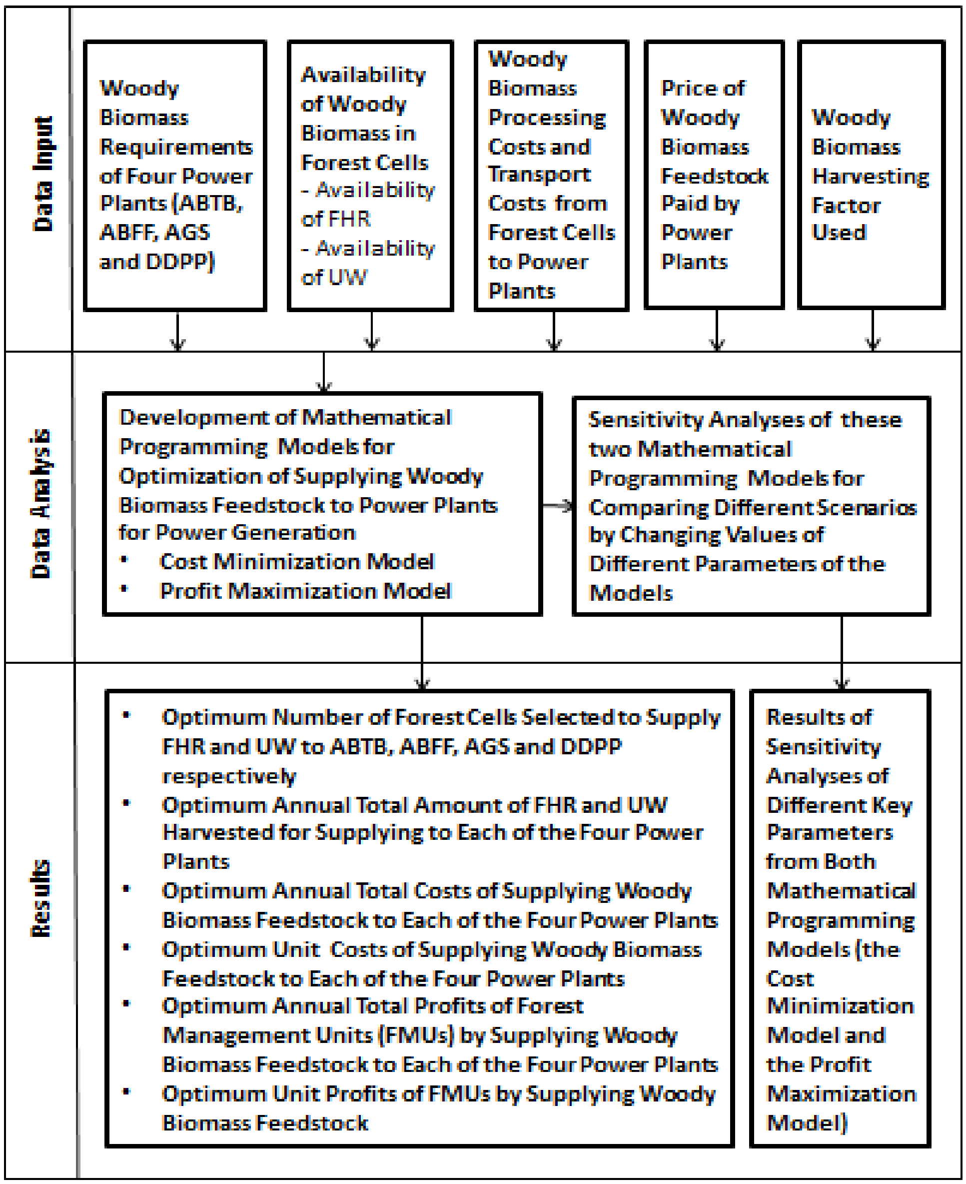

Figure 6.1 Flow chart of optimization models for supplying woody biomass feedstock to four major biomass based power plants in northwestern Ontario (NWO).

Two optimization models are developed for analyzing optimal supply of woody biomass from depletion cells to the four power plants. The objective function in the first model is to minimize the total biomass feedstock procurement costs and in the second model is to maximize total profit (gross margin) of FMUs for supplying woody biomass feedstock from the forest cells to power plants. Even though the two models give the same solutions (one being the dual of other primal problem), the relative impact of changing biomass prices are not captured by the cost minimization model. Changing biomass prices at bigger power plants will change the optimal solutions, which is best handled by the profit maximization model. The results of profit maximization are more relevant to the contractors (biomass suppliers) in order to evaluate the profitability of their operations in the given locations (FMUs). The parameters, indices and variables used for developing the two models using the General Algebraic Modeling System (GAMS) programming language are listed below:

Indices:

i = Power plants (i: 1 = Thunder Bay CHP plant, 2 = Fort Frances CHP plant, 3 = Atikokan generating station and 4 = Dryden CHP plant)

j = Forest cell in the productive forest area (j = 1, 2, 3,…, 19,315)

Parameters:

HF = Harvesting factor

PR = Processing (harvesting and grinding/chipping) cost ($\$\cdot gt^{-1}$) of FHR at roadside

PU = Processing (harvesting and grinding/chipping) cost ($\$\cdot gt^{-1}$) of UW at roadside

DB_i = Annual woody biomass demand (gt) of each power plant

TR_j = Theoretical availability (gt) of FHR in a forest cell over 7 years (2002-2009)

TU_j = Theoretical availability (gt) of UW in a forest cell over 7 years (2002-2009)

AR_j = Annual technical availability (gt) of FHR in a forest cell, calculated using Equation (1)

$$AR_j = \frac{\mathrm{TR_j} \times HF}{7} \quad (1)$$

AU_j = Annual technical availability (gt) of UW in a forest cell, calculated using Equation (2)

$$AU_j = \frac{\mathrm{TU_j} \times HF}{7} \quad (2)$$

TC_{ij} = Biomass transportation cost ($\$\cdot gt^{-1}$) from the j^{th} forest cell to the i^{th} power plant including loading and unloading costs.

P_i = Price ($\$\cdot gt^{-1}$) of woody biomass at the i^{th} power plant

Variables:

R_{ij} = Amount of annual FHR harvested (gt) from the j^{th} forest cell for the i^{th} power plant

U_{ij} = Amount of annual UW harvested (gt) from the j^{th} forest cell for the i^{th} power plant

TB_i = Annual woody biomass (gt) brought in the i^{th} power plant

TCB = Total annual cost ($) of biomass procurement, calculated using Equation (3)

$$TCB = \sum_{i=1}^{4} \sum_{j=1}^{19315} (R_{ij} (PR + TC_{ij})) + \sum_{i=1}^{4} \sum_{j=1}^{19315} (U_{ij} (PU + TC_{ij})) \quad (3)$$

TRB = Total annual revenue ($) from woody biomass supply to power plants, calculated using Equation (4)

$$TRB = \sum_{i=1}^{4} \sum_{j=1}^{19315} (P_i (R_{ij} + U_{ij})) \quad (4)$$

TPB = Total annual profit ($) from woody biomass supply to power plants, calculated using Equation (5)

$$TPB = \sum_{i=1}^{4} \sum_{j=1}^{19315} (P_i (R_{ij} + U_{ij})) - \sum_{i=1}^{4} \sum_{j=1}^{19315} (R_{ij} (PR + TC_{ij})) - \sum_{i=1}^{4} \sum_{j=1}^{19315} (U_{ij} (PU + TC_{ij})) \quad (5)$$

The objective functions of two LP models, which minimize overall procurement costs and maximize total profit, are specified by Equations (6) and (7), respectively. The constraints used in these models are specified by Equations (8) to (12).

$$Minimize\ TCB = \sum_{i=1}^{4} \sum_{j=1}^{19315} (R_{ij} (PR + TC_{ij})) + \sum_{i=1}^{4} \sum_{j=1}^{19315} (U_{ij} (PU + TC_{ij})) \quad (6)$$

$$Maximize\ TPB = \sum_{i=1}^{4} \sum_{j=1}^{19315} (P_i (R_{ij} + U_{ij})) - \sum_{i=1}^{4} \sum_{j=1}^{19315} (R_{ij} (PR + TC_{ij})) - \sum_{i=1}^{4} \sum_{j=1}^{19315} (U_{ij} (PU + TC_{ij})) \quad (7)$$

Subject to:

$$\sum_{j=1}^{19315}(R_{ij} + U_{ij}) = TB_i \tag{8}$$

$$\sum_{i=1}^{4} R_{ij} \leq AR_j \tag{9}$$

$$\sum_{i=1}^{4} U_{ij} \leq AU_j \tag{10}$$

$$TB_i \geq DB_i \tag{11}$$

$$R_{ij},U_{ij} \geq 0 \tag{12}$$

The equation (8) is an intermediate equation summing up the plant-wise total biomass being harvested. Equations (9) and (10) are the FHR and UW harvesting constraints, which specify that the total amount of FHR and UW harvested from j^{th} forest cell is less than or equal to the annual amount of technically available FHR and UW in the j^{th} forest cell, respectively. Equation (11) is the demand constraint, which ensures that the total amount of woody biomass harvested for i^{th} power plant should at least be equal to biomass feedstock demand for the power plant. Finally, equation (12) is non-negativity constraint on decision variables. The estimates of parameters used in the model are presented in Table 6.1.

Table 6.1 Estimates of parameters used in BASE scenario of the model.

Descriptions	**Unit**	**Estimates**	**Remarks**
Harvesting and processing costs of FHR	$\$\cdot gt^{-1}$	26	OME (2006)
Harvesting and processing costs of UW	$\$\cdot gt^{-1}$	31	OME (2006)
Fixed cost due to load/unload overhead	$\$\cdot gt^{-1}$	5.24	Own estimate
Charge rate of biomass truck	$\$\cdot hr^{-1}$	85	Alam *et al.* (2012b)
Biomass demand of ABTB CHP plant	$gt\cdot yr^{-1}$	730,000	Power plant data
Biomass demand of ABFF CHP plant	$gt\cdot yr^{-1}$	800,000	Power plant data
Biomass demand of AGS Power plant	$gt\cdot yr^{-1}$	200,000	Power plant data
Biomass demand of DDPP CHP plant	$gt\cdot yr^{-1}$	480,000	Power plant data
Range of availability of FHR	gt/km^2	525.6-5,256	Alam *et al.* (2012a)
Range of availability of UW	gt/km^2	0-4,730.4	Alam *et al.* (2012a)
Harvesting factor of FHR	% of FHR	61	Own estimate
Harvesting factor of UW	% of UW	61	Own estimate
Price of biomass at power plants	$\$\cdot gt^{-1}$	39	Own estimate
Number of depleted forest cells	No	19,315	Alam *et al.* (2012a)

Note: FHR = forest harvest residue, UW = underutilized wood, gt = green tonne, hr = hour, yr = year

Model Scenarios

Table 6.2 presents the definitions and descriptions of 14 cost minimization model scenarios with their relevancy in relation to the expected changes in technological and economic parameters in the model. Out of 14 scenarios, six scenarios (DEPC, IHRW1, IHRW2, and IHFR) are cost decreasing and seven scenarios (IHOR, DHRW, INPC, DEPC, INDP, DEDP, and INTC) are cost increasing.

Table 6.2 Definition and description of scenarios of cost minimization model.

Scenario	Definition/Description
BASE	The business-as-usual scenario captures the present reality of study area. The parameters used in this scenario are as described in Table 1. This scenario helps compare the model results for the rest of the scenarios.
Economic scenarios	
INTC	BASE, but 20% increase in biomass truck charge rate. This scenario tests the impact of change in transportation costs on the biomass procurement cost structures which might be the case in future as truck charge rate has recently been increased in NWO.
INPC	BASE, but 10% increase in harvesting and processing costs of FHR and UW. This tests the impacts of increased harvesting and processing costs, likely to occur due to changes in economic factors, on procurement cost structures.
DEPC	BASE, but 10% decrease in harvesting and processing costs of FHR and UW. This scenario reflects potential improvements in technology in future, thereby reducing the processing costs.
Technological scenarios	
INBA DEBA	BASE, but 10% increase in availability of both FHR and UW. BASE, but 10% decrease in availability of both FHR and UW. These scenarios test the sensitivity of loosening and tightening of biomass availability constraints. This will help us understand the changes in costs structures over the error margins (± 10%) of present estimates of biomass availability for both types as the present estimates of these variables are based on samples of selected areas in FMUs of NWO, which might have the range of errors tested by these scenarios as the present estimates of biomass availability are based on selected sample forest cells. We feel that these estimates need to be improved in future work.
IHRW1 IHRW2 IHFR	BASE, but 10% increase in harvesting factors of both FHR and UW. BASE, but 20% increase in harvesting factors of both FHR and UW. BASE, but 20% increase in harvesting factor of FHR and no change in harvesting factor of UW. This set of scenarios tests the impacts of loosening the biomass availability constraints due to improved biomass harvesting technology, likely to happen in future.
DHRW DHFR	BASE, but 10% decrease in harvesting factors of both FHR and UW. BASE, but 20% decrease in harvesting factor of FHR and no change in harvesting factor of UW. This set of scenarios tests the impacts of tightening the biomass availability, which might occur due to ecological and environmental concerns in future.
IHOR	BASE, but 20% increase in harvesting factor of FHR, and only FHR is extracted. This scenario explores the situation of increased procurement costs due to present common practice of harvesting only FHR for bioenergy production instead of harvesting both FHR and UW.
INDP	BASE, but 10% increase in woody biomass feedstock demand. This explores the impacts of higher biomass demand, likely to happen due to expansion of power plants in future, on cost structures of biomass procurement.
DEDP	BASE, but 10% decrease in woody biomass feedstock demand of each of the four power plants. This scenario helps understand the costs structures due to loosening of constraints on the biomass feedstock demand of power plants, which might be the case in future. Selection of higher quality biomass and plants not operating in full capacity lead to lesser biomass demands.

Note: The “I” at the beginning of the scenario codes means an increase and “D” a decrease

Table 6.3 shows the definitions and descriptions of eight different model scenarios for the profit maximization model. The results of this model are presented in terms of per unit gross margins for each FMU by scenarios.

Table 6.3 Definition and description of scenarios of profit maximization model.

Scenario	Description
BASE	This is the business-as-usual scenario of the model which reflects the current field situation. The parameters for this scenario are described in Table 1. The results of other model scenarios are compared with that of this scenario.
INTC	BASE, but 20% increase in biomass truck charge rate. This scenario tests the impact of change in transportation costs, which is likely situation in future on gross margin structures for each biomass supplying FMU, as truck charge rate has recently been increased in NWO.
IRTB1	BASE, but 10% increase in price of biomass feedstock by Thunder Bay plant.
IRTB2	BASE, but 20% increase in price of biomass feedstock by Thunder Bay plant.
IRFF1	BASE, but 10% increase in price of biomass feedstock by Fort Frances plant.
IRFF2	BASE, but 20% increase in price of biomass feedstock by Fort Frances plant.
IRTF1	BASE, but 10% increase in price of biomass feedstock by both Thunder Bay and Fort Frances plants.
IRTF2	BASE, but 20% increase in price of biomass feedstock by both Thunder Bay and Fort Frances plants. This set of price increasing scenarios tests the sensitivity of different levels of prices of biomass feedstock to gross margin structures of biomass supplying FMUs. These changes in prices are likely to be offered on the part of bigger power plants as they require huge amounts of biomass to operate their power plants smoothly. Price increases are, therefore, assigned to two bigger power plants, Thunder Bay and Fort Frances, in these scenarios.

Note: The "I" at the beginning of the scenario codes means an increase

While selecting the model scenarios, first we focused on impacts of changing economic parameters (transportation and processing costs, and prices) on cost and gross margin structures. Secondly, the impacts of changing technological parameters (harvesting factors, and biomass demand and availability) were investigated.

6.3 Results and Discussion

6.3.1 Cost Zones

Minimum transportation cost zones (tessellations) for transporting woody biomass from each forest cell of depleted forest area to the four power plants are shown in Figure 6.2. These minimum cost zones show the woody biomass catchment areas for each power plant. The minimum cost zone for the Dryden CHP plant is the largest, while the Thunder Bay CHP plant catchment area is the second largest among the four cost zones. The Dryden CHP plant is located near the middle of the research area, and there are many forest cells closer to this power plant along with a denser network of higher class and straighter roads. There is no competition for the Dryden CHP plant for woody biomass supply from any other power plant in the research area on the northern side. Similarly, Thunder Bay CHP plant is located in the southeastern part of research area. There is no competing power plant on its northern, eastern and southwestern sides in the research area. The other two power plants, Atikokan and Fort Frances, which are located close to each other in the research area, might compete for the same woody biomass from some depletion cells depending upon their requirements. The cost zone map in Figure 6.2 shows the relative cost competitive areas for each power plant based on minimum transportation cost for each power plant from each forest cell. As more attributes (biomass density and economic) are introduced in the forest cells, the dynamics of competition among the four power plants would change.

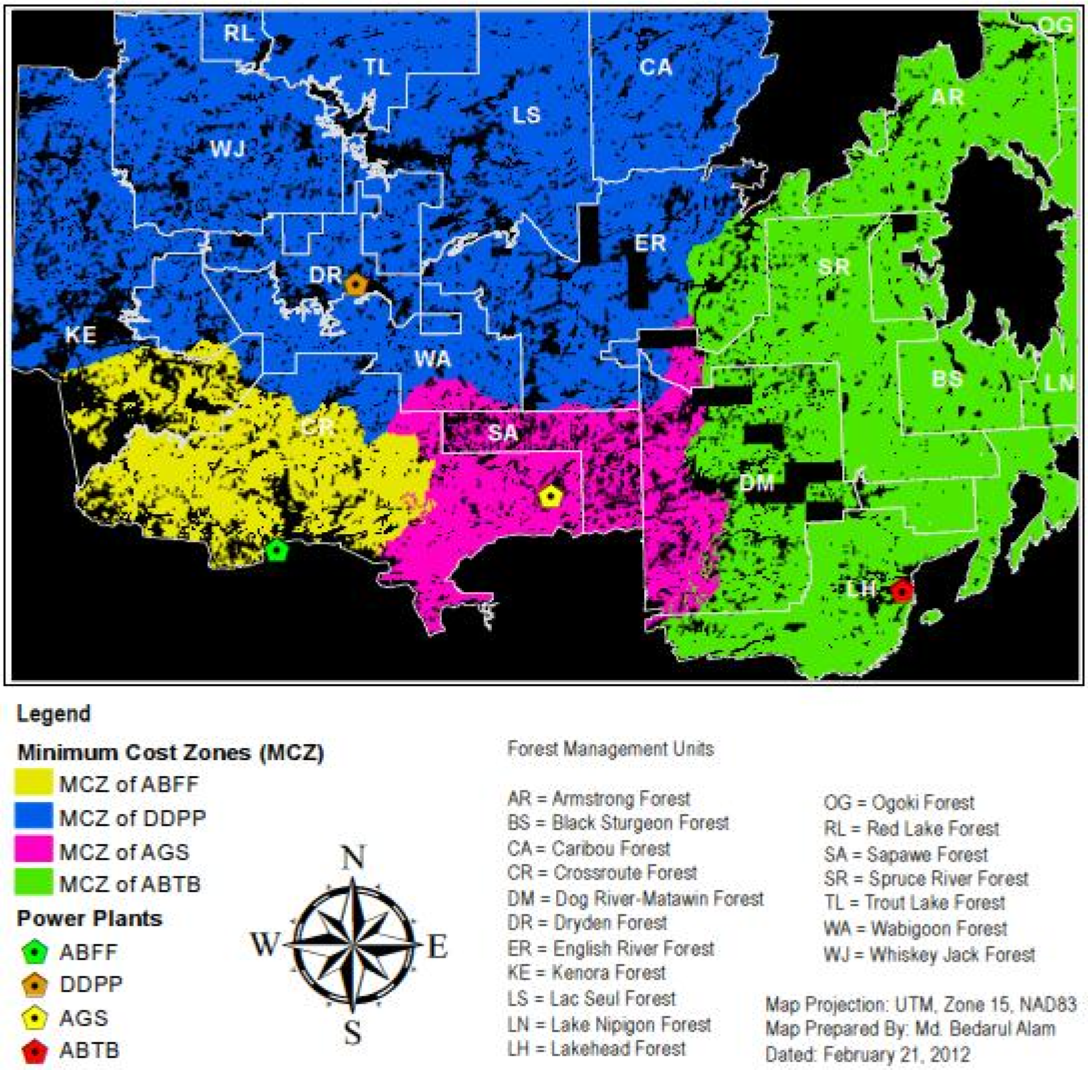

Figure 6.2 Minimum cost zones for four power plants in NWO.

6.3.2 Cost Analysis

The results of the cost minimization model provide an optimal solution for supplying woody biomass feedstock from forest cells to the four power plants on an annual basis by minimizing the total annual procurement (harvesting, processing and transportation) costs of biomass, subject to the availability of woody biomass in each depleted forest cell and demand of each power plant. The model selects 11,790 and 2,991 cells in total for supplying FHR and UW, respectively, for all four plants. More FHR cells are selected because the processing cost for FHR is less as compared to UW woody biomass. Figure 6.3 represents the distribution of optimal depletion forest cells that supply FHR and UW biomass to each power plant in the BASE scenario. Similar distributions of optimal depletion cells for different model scenarios can be produced; these are not reproduced here because of space limitations.

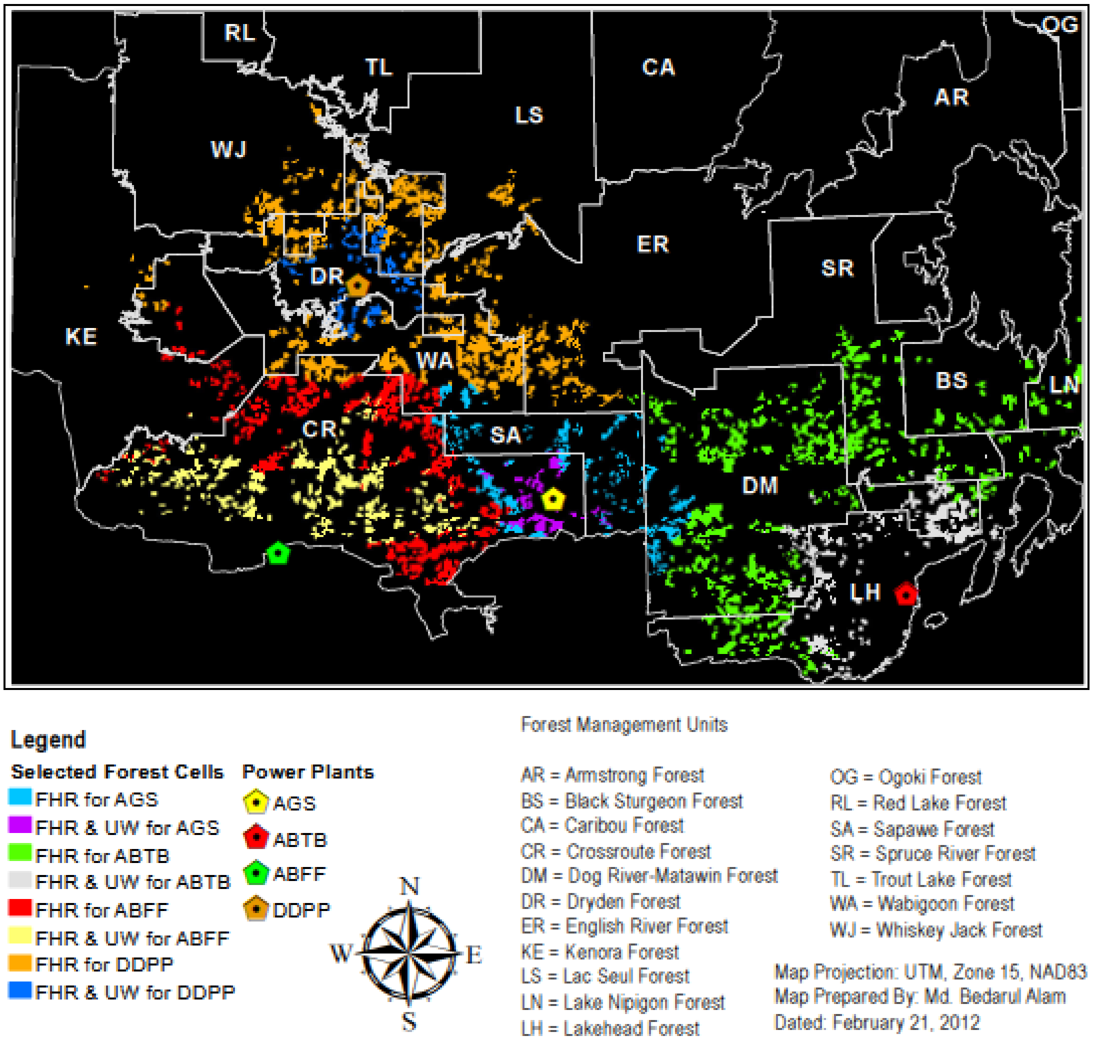

Figure 6.3 Selected forest cells to harvest forest harvest residues (FHR), and underutilized wood (UW) for four power plants (BASE scenario).

First, we discuss the results relating to the impacts of changing economic parameters (transportation and processing costs, and prices) on cost structures. Results of the impacts of changing technological parameters (harvesting factors, and biomass demand and availability) are discussed next. The number of cells selected for supplying FHR and UW woody biomass for each power plant, in each model scenario, is presented in Table 6.4. While observing number of selected cells in Table 6.4, we find more depletion cells for FHR in all scenarios for all plants, but lesser amount of biomass from FHR type is being harvested (Table 6.5) in most of the scenarios. This variation is explained by the fact that, on an average, the availability of FHR is about one fourth of UW biomass type. The source of the information is the input dataset of the model. Table 6.5 describes the distribution of biomass (both FHR and UW) being harvested from the optimal depletion cells for each plant under different model scenarios.

Table 6.4 The number of forest cells selected in different scenarios for supplying woody biomass to four power plants.

Scenario	Cells for ABFF (No.)		Cells for ABTB (No.)		Cells for DDPP (No.)		Cells for AGS (No.)		Total cells for 4 plants (No.)		
	FHR	**UW**	**FHR**	**UW**	**FHR**	**UW**	**FHR**	**UW**	**FHR**	**UW**	**Total**
BASE	3204	1320	3972	1004	3507	404	1107	263	11790	2991	14781
INTC	3127	1338	3612	1093	3213	473	1034	283	10986	3187	14173
INPC	3239	1312	4152	950	3695	355	1142	249	12228	2866	15094
DEPC	3178	1327	3775	1056	3349	442	1055	276	11357	3101	14458
INBA	3138	1139	3816	860	3388	316	1135	197	11477	2512	13989
IHRW1	3138	1139	3816	860	3388	316	1135	197	11477	2512	13989
IHRW2	3090	981	3680	748	3285	242	1143	151	11198	2122	13320
IHFR	3164	1155	3815	853	3334	279	1120	193	11433	2480	13913
DEDP	3133	1120	3808	844	3373	307	1138	190	11452	2461	13913
DEBA	3257	1555	4157	1162	3655	513	1097	328	12166	3558	15724
DHRW	3257	1555	4157	1162	3655	513	1097	328	12166	3558	15724
DHFR	3219	1501	4142	1152	3729	536	1086	325	12176	3514	15690
IHOR	6726	-	6197	-	3728	-	1849	-	18500	-	18500
INDP	3254	1531	4132	1148	3642	502	1098	320	12126	3501	15627

Table 6.5 Annual amount of forest harvest residue and underutilized wood supply to four power plants.

Scenario	Biomass for ABFF ($ODt\cdot yr^{-1}$)		Biomass for ABTB ($ODt\cdot yr^{-1}$)		Biomass for DDPP ($ODt\cdot yr^{-1}$)		Biomass for AGS ($ODt\cdot yr^{-1}$)	
	FHR	**UW**	**FHR**	**UW**	**FHR**	**UW**	**FHR**	**UW**
BASE	194,513	285,487	215,014	222,986	197,421	90,579	62,465	57,535
INTC	190,401	289,599	194,953	243,047	182,339	105,661	57,920	62,081
INPC	196,228	283,772	227,051	210,949	208,057	79,943	64,900	55,100
DEPC	192,864	287,136	203,419	234,581	189,287	98,713	59,541	60,459
INBA	209,309	270,691	227,206	210,795	209,525	78,475	71,251	48,749
IHRW1	209,309	270,691	227,206	210,795	209,525	78,475	71,251	48,749
IHRW2	225,238	254,762	237,835	200,165	222,566	65,434	78,718	41,282
IHFR	230,481	249,519	247,802	190,199	225,040	62,960	76,442	43,558
DEDP	189,924	242,077	206,110	188,090	189,754	69,446	65,021	42,979
DEBA	177,857	302,144	204,864	233,136	185,375	102,625	55,427	64,573
DHRW	177,857	302,144	204,864	233,136	185,375	102,625	55,427	64,573
DHFR	156,204	323,796	181,324	256,676	168,648	119,352	48,631	71,369
IHOR	480,000	-	438,000	-	288,000	-	120,000	-
INDP	197,481	330,519	226,116	255,684	204,956	111,844	61,695	70,305

The variations in number of depletion cells (Table 6.4) and woody biomass amount (Table 6.5) being selected by power plants are explained by the biomass requirement for each plant, availability of FHR and UW in each cell, relative processing costs of each biomass type and the competition among the power plants for the biomass in the given cell. Further, these variations in distribution of optimal depletion cells and amount of biomass for both types explains the per unit biomass procurement cost structures for each power plant under different model scenarios (Table 6.6).

Table 6.6 Per unit procurement cost of woody biomass supply to four power plants.

Scenario	**Unit procurement cost of biomass supply ($\$\cdot ODt^{-1}$)**			
	ABFF	**ABTB**	**DDPP**	**AGS**
BASE	65.64	64.49	61.20	60.76
INTC	76.81 (17.03%)	75.37 (16.87%)	71.31 (16.52%)	70.39 (15.85%)
INPC	70.45 (7.34%)	69.24 (7.37%)	65.79 (7.51%)	65.47 (7.75%)
DEPC	60.81 (-7.34%)	59.72 (-7.40%)	56.57 (-7.56%)	56.03 (-7.79%)
INBA	65.26 (-0.58%)	64.17 (-0.49%)	60.86 (-0.54%)	60.21 (-0.90%)
IHRW1	65.26 (-0.58%)	64.17 (-0.49%)	60.86 (-0.54%)	60.21 (-0.90%)
IHRW2	64.89 (-1.13%)	63.89 (-0.93%)	60.57 (-1.03%)	59.86 (-1.48%)
IHFR	65.08 (-0.85%)	64.01 (-0.74%)	60.61 (-0.95%)	60.02 (-1.22%)
DEDP	65.21 (-0.64%)	64.14 (-0.54%)	60.83 (-0.60%)	60.17 (-0.97%)
DEBA	66.11 (0.72%)	64.86 (0.57%)	61.58 (0.63%)	61.23 (0.77%)
DHRW	66.11 (0.72%)	64.86 (0.57%)	61.58 (0.63%)	61.23 (0.77%)
DHFR	66.26 (0.96%)	65.02 (0.82%)	61.85 (1.07%)	61.46 (1.16%)
IHOR	70.41 (7.27%)	68.07 (5.56%)	67.30 (9.97%)	63.14 (3.93%)
INDP	66.06 (0.65%)	64.82 (0.52%)	61.55 (0.58%)	61.18 (0.70%)

Note: Figures in brackets indicate the % change of per unit biomass procurement costs from the BASE scenario.

The 13 cost minimization model scenarios analyze the impacts of changing relevant economic (three scenarios) and technological (10 scenarios) parameters (as described in Table 6.2) on biomass procurement costs structures of the four power plants as shown in Table 6.6. The results of these scenarios were compared with that of the BASE scenario. The results in Table 6.6 show that per unit costs for Fort Frances, Thunder Bay and Dryden CHP plants, and Atikokan power plant are in descending order for all model scenarios, which indicate that the higher the biomass demand, the higher the per unit procurement cost. The reason for this is that power plants with more biomass demand have to collect biomass from much longer distances. The range of unit procurement cost ($\$\cdot ODt^{-1}$) for Fort Frances, Thunder Bay and Dryden CHP plants, and Atikokan power plant are 60.81-76.81, 59.72-75.37, 56.57-71.31, and 56.03-70.39, respectively. This result shows that the highest per unit procurement cost (for all power plants on average a 16.77% increase from the BASE scenario) occurs with a 20% increase in transportation cost (INTC scenario). The lowest per unit procurement costs occurs with a 10% decrease in processing cost scenario (DEPC scenario). A decrease in processing cost by 10% resulted in a 7.44% decrease in per unit procurement costs for all power plants on average. Since transportation and processing form a major component of biomass supply chain cost, changes in these parameters have major impacts on per unit procurement cost for all power plants. These sensitivity results imply that policy should focus first on controlling transportation costs and then processing costs. The processing cost includes both productive machine time and idle time costs. The productive machine time can be improved by investing in processing technology, and the idle time can be reduced by better scheduling of operations.

Improving road network and vehicle configuration for hauling biomass, and maximizing ODt per load can reduce the transportation costs. Consequently, one can achieve reduced procurement costs in biomass value chains with these improved measures.

After analyzing the sensitivities of changing economic parameters to the model solutions, we investigate further the impacts of changing relevant technological parameters in order to evaluate the resulting cost structures due to potential changing conditions of these parameters in the future. In model scenarios INBA, IHRW1, IHRW2, IHFR and DEDP, the per unit procurement costs decreased from the BASE scenario for all power plants with the highest decrease at the Atikokan power plant (Table 6.6). On the other hand, under the model scenarios DEBA, DHRW, DHFR, IHOR and INDP the per unit procurement costs increased from the BASE scenario for all power plants with the highest increase at the Atikokan power plant. The explanation for these higher changes in per unit procurement costs for the Atikokan power plant is that it has the lowest biomass demand compared to other power plants, it is located near the favourable depletion cells, and biomass availability (Figures 6.2 and 6.3). However, in IHOR (only FHR biomass with 20% more harvesting factor) scenario, the increase in per unit cost for Atikokan power plant is the least compared to others. Although, more FHR biomass is available in the IHOR scenario, there is higher competition for this type of biomass (Figures 6.3, 6.4 and 6.5) because UW is not being collected and hence there is an increase in per unit cost compared to the BASE scenario for all power plants.

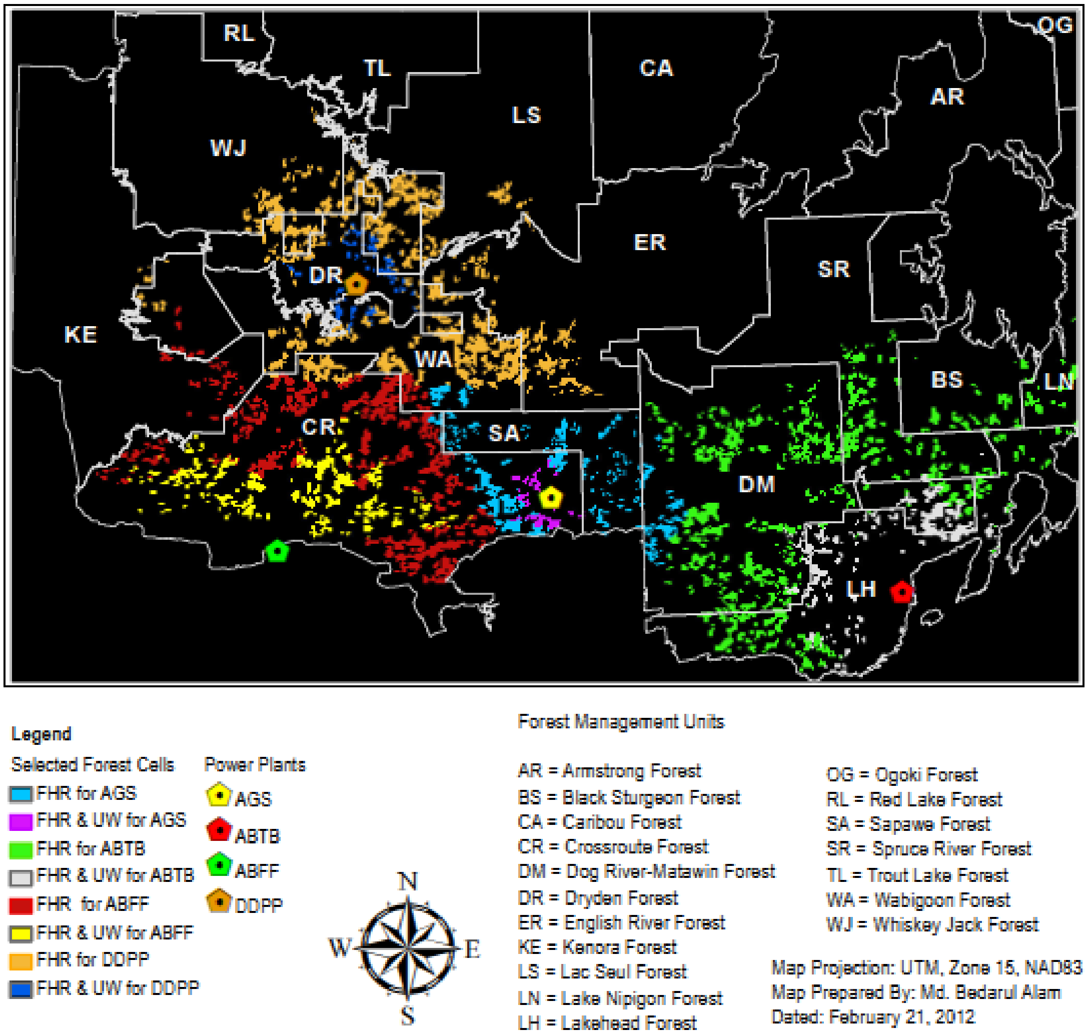

Figure 6.4 Selected forest cells to harvest FHR and UW for four major power plants (20% increase in harvesting factor scenario).

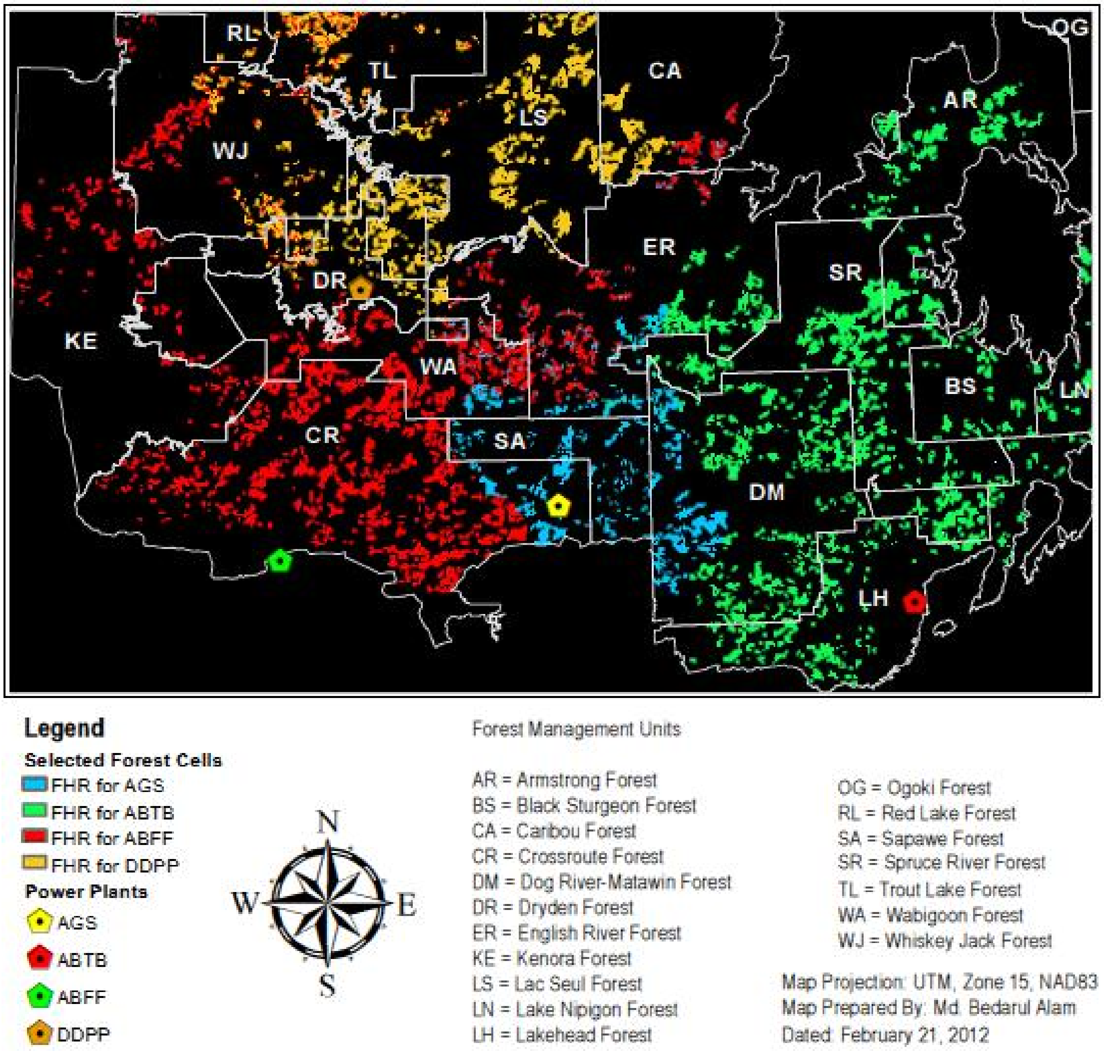

Figure 6.5 Selected forest cells to harvest only FHR for four power plants (20% increase in harvesting factor scenario).

In this scenario, the Atikokan power plant has the least increment in per unit cost due to its lower demand for biomass relative to the other power plants. After the Atikokan plant, Fort Frances, the biggest power plant, shows higher increases and decreases per unit procurement costs for most of the scenarios (Table 6.6), albeit with small variations among the plants by scenarios. The more interesting results are found in the IHOR scenario, where Dryden CHP plant has the highest increase (9.97%) in per unit cost compared to the BASE scenario. Further, the aggregate impacts of the economics and technological model scenarios are reflected in Figure 6.6, where we present the power plant-wise total biomass procurement costs by scenarios. The bars in Figure 6.6 contrast with the results of per unit costs by scenarios. For example, the highest total costs for each power plant is shown in the INDP scenario, whereas the highest per unit cost is found in the INTC scenario.

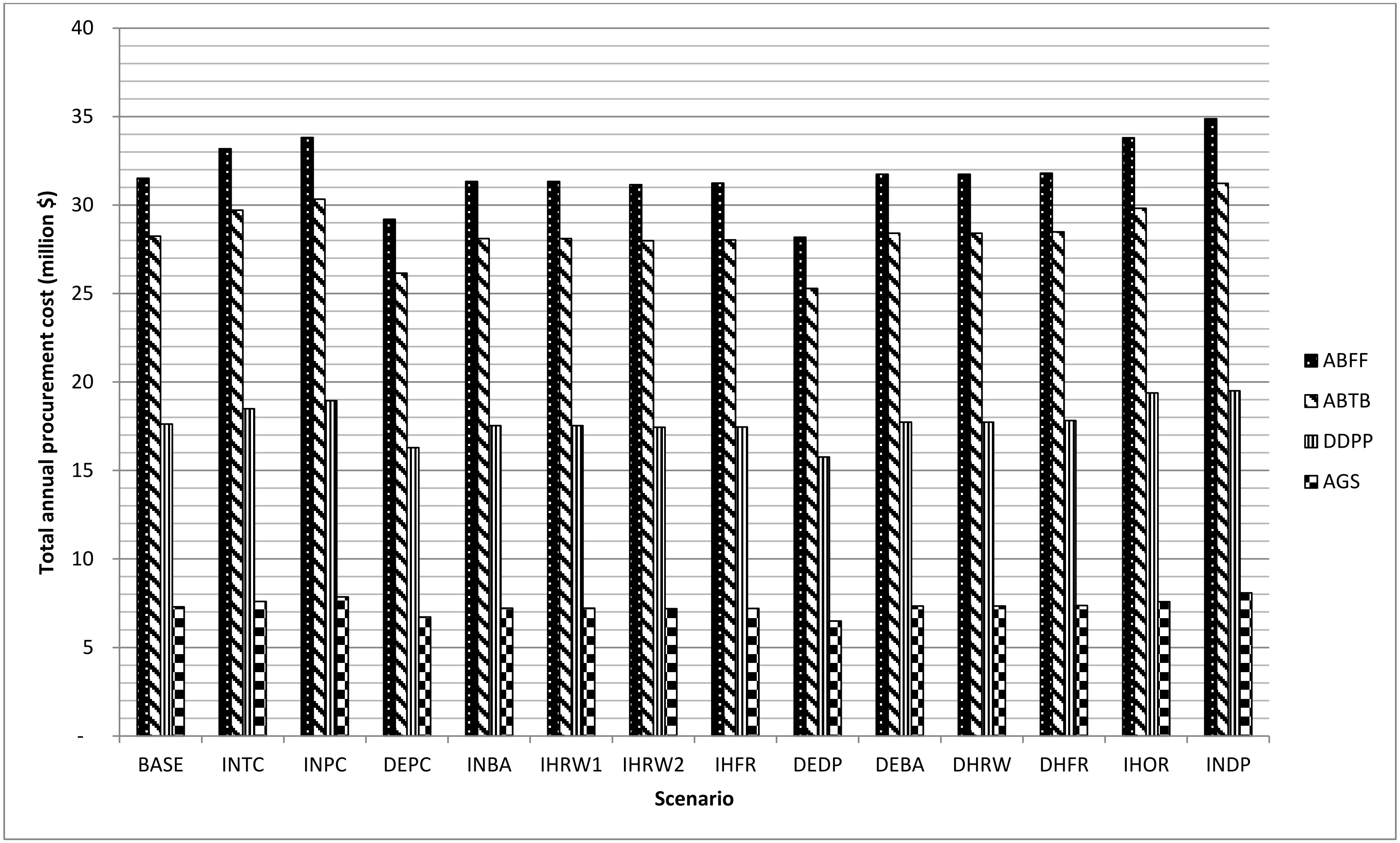

Figure 6.6 Total annual procurement cost of woody biomass supply to four power plants.

Increasing harvesting factors causes more declines in per unit procurement costs suggesting that the present harvesting factor level needs to be increased for reduced per unit procurement cost. This is possible given that the depletion cells being used in this study are only from productive forest areas and excludes ecologically sensitive areas. Further, the IHOR scenario shows the highest per unit procurement cost, which suggests that the current emphasis on collecting only FHR for bioenergy purposes, would lead to higher per unit procurement cost. This, therefore, suggests harvesting standing under-utilized tree species to reduce per unit procurement cost.

6.3.3 Profit Analysis

The results of the profit maximization model provide an optimal solution for supplying woody biomass feedstock from forest cells to the four power plants on an annual basis by maximizing the total gross margin, subject to the availability of woody biomass in each depleted forest cell and meeting the biomass demand of each power plant. These results of gross margin structures are relevant from the biomass supplier's (contractors) perspective as these are based on biomass supplying FMUs (Table 6.7), where the contractors operate their business. The results of per unit profit ($\$\cdot ODt^{-1}$) for each FMU that supplies biomass to the four power plants in the BASE and seven other scenarios are shown in Table 6.7. The profit for any FMU depends on the price of biomass being offered by the power plants. In the BASE scenario, most of the FMUs produce a profit.

Table 6.7 Per unit profit ($\$.ODt^{-1}$) for each FMU from supplying biomass in different scenarios of profit maximization model.

Scenario	Per unit profit ($\$.ODt^{-1}$) for each FMU												
	BS	**CR**	**DM**	**DR**	**ER**	**KE**	**LS**	**LN**	**LH**	**SA**	**SR**	**WA**	**WJ**
BASE	0.73	0.21	0.44	3.67	1.98	-1.01	3.61	-0.40	0.80	4.47	0.10	3.94	3.05
INTC	-0.74	-0.94	0.28	2.66	0.56	-2.00	2.17	-2.71	-0.58	-0.21	-1.85	-0.30	-1.32
IRTB1	7.23	0.21	6.33	3.67	2.03	-1.01	3.61	6.10	7.31	4.47	6.60	3.94	3.05
IRTB2	13.73	0.21	12.22	3.67	2.10	-1.01	3.61	12.60	13.81	4.47	13.10	3.94	3.05
IRFF1	0.73	5.63	0.45	3.67	1.98	4.15	3.61	-0.40	0.80	4.48	0.10	4.19	3.87
IRFF2	0.73	11.05	0.45	3.67	1.98	9.30	3.61	-0.40	0.80	4.50	0.10	4.44	4.68
IRTF1	7.23	5.63	6.33	3.67	2.03	4.15	3.61	6.10	7.30	4.48	6.60	4.19	3.87
IRTF2	13.73	11.05	12.23	3.67	2.09	9.30	3.61	12.60	13.80	4.50	13.10	4.44	4.68

Note: BS = Black Sturgeon Forest; CR = Crossroute Forest:; DM = Dog River-Matawin Forest; DR = Dryden Forest; ER = English River Forest; KE = Kenora Forest; LS = Lac Seul Forest; LN = Lake Nipigon Forest; LH = Lakehead Forest; SA = Sapawe Forest; SR = Spruce River Forest; WA = Wabigoon Forest; and WJ = Whiskey Jack Forest

Although 19,315 depletion cells used in this study are from 18 FMUs, the optimal depletion cells selected by the model fall only in 13 FMUs for all the scenarios. In the BASE scenario, only the Kenora and Lake Nipigon FMUs show negative gross margins (Table 6.7) as the optimal depletion cells falling in these FMUs are relatively far from the power plants (Figures 6.2 and 6.7).

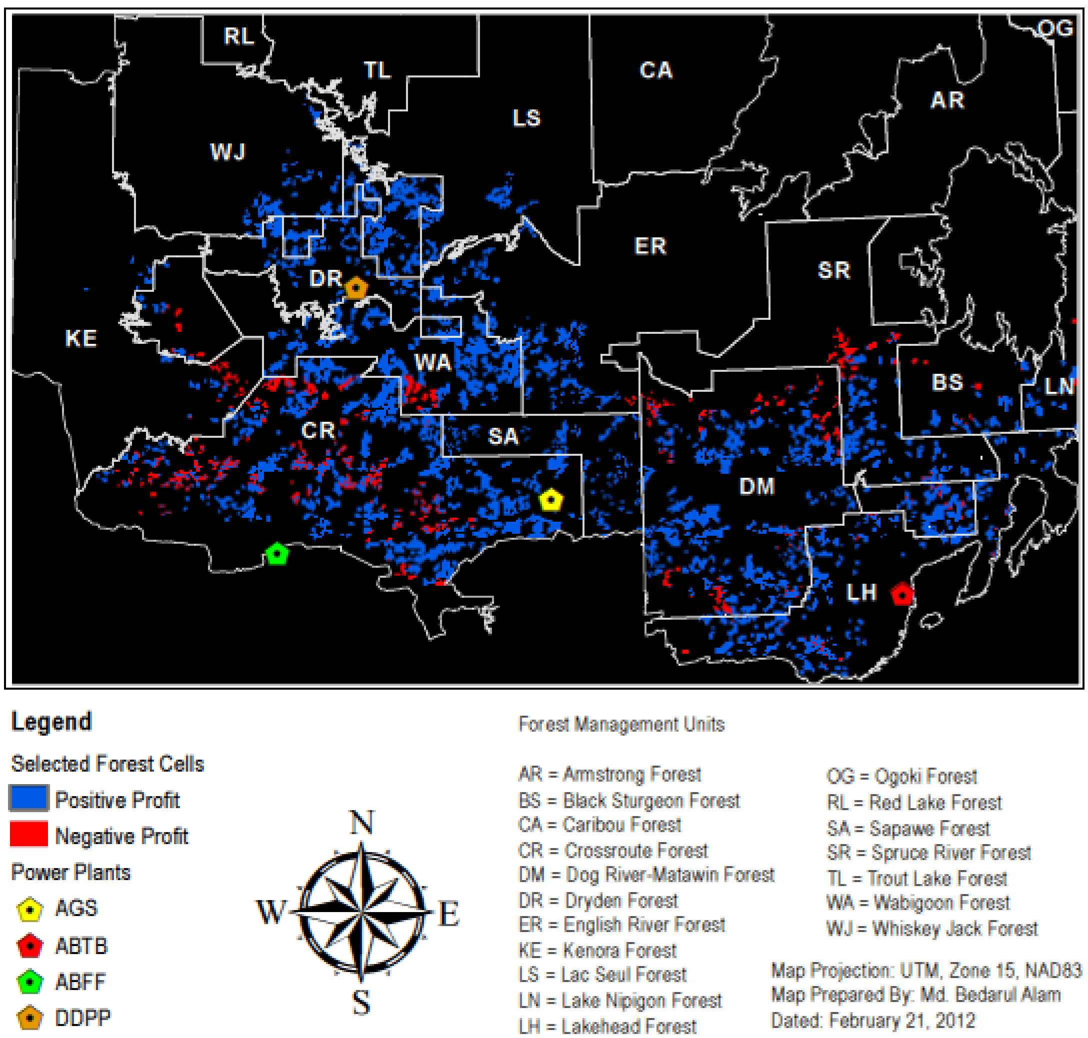

Figure 6.7 Profits (positive and negative) for FMUs in supplying woody biomass feedstock to four power plants.

While testing the sensitivity of increasing truck charge rate by 20% (INTC scenario), only four FMUs (Dog River-Matawin, Dryden, English River and Lac Seul FMUs) make a profit. These results suggest that, in future, contractors operating in most of the FMUs will face negative gross margins, thereby halting the biomass supply and hindering smooth operation of the power plants. We, therefore, tested the sensitivity of increased per unit price on part of the larger power plants to the resultant gross margin structures of biomass supplying FMUs. For this purpose, a combination of price increase scenarios at the two larger power plants (Fort Frances and Thunder Bay) was investigated. For an increase in price by 10% (IRTB1) and 20% (IRTB2) at the Thunder Bay CHP plant, the per-unit profit increased by 148% and 296% on average for all FMUs, respectively. The FMUs, which are located near the Thunder Bay CHP plant (Black-Sturgeon Forest, Dog River-Matawin Forest, English River, Lakehead Forest, Spruce River Forest and Lake Nipigon Forest) make more per unit profit from an increase in price at the Thunder Bay CHP plant (ranging from 3.82 to 7.32 $\$\cdot ODt^{-1}$ in IRTB1 and from 10.32 to 13.82 $\$\cdot ODt^{-1}$ in IRTB2) because the transportation costs from these FMUs to this plant is low. Similarly, for an increase in price by 10% (IRFF1) and 20% (IRFF2) at the Fort Frances CHP plant, the average per unit profit of FMUs increased by 54% and 108% on average for all FMUs, respectively. Finally, if there is an increase in price of woody biomass at both the Thunder Bay and Fort Frances CHP plants by 10% (IRTF1) and 20% (IRTF2), the average per unit profit of FMUs increased by 202% and 404%, respectively. Therefore, an increase in price of woody biomass at a power plant greatly helps to increase the profits of close by FMUs, but only marginally helps to increase the profits of faraway FMUs. It is therefore, advisable to put smaller power plants in a wider range of areas in order to make biomass collection a profitable business for FMUs. This will also help in reducing the distribution cost of power to small communities, and increase rural employment through bioenergy production systems in the region.

6.4 Conclusions

This study investigated an optimal biomass supply chain for four large-scale biomass-based power plants in NWO, which has been a priority research area recently due to greater emphasis put on green energy sources in Canada and around the globe. Two optimization models have been developed and applied to analyze the impacts of biomass competition, likely to be created due to increasing demand for biomass feedstock on part of the four power plants in this region, on cost and gross margin structures for biomass-based power plants. Twenty-two model scenarios (14 for cost minimization and 8 for profit maximization model) were used to study the impacts of changes relevant to economic and technological parameters of biomass procurement for each power plant and FMU. The results show that per unit procurement costs are directly proportional to the size of the power plant in all scenarios. The highest per cent increase in per unit biomass procurement costs from the base scenario is found in the increased truck charge rate by 20% scenario, followed by the scenario where only FHR is used by all power plants.

The results from increased truck charge rate and FHR only scenarios point to some of the important policy implications for biomass supply chain management in NWO. The policy should focus more on controlling transportation costs by investing in transport infrastructure and logistics, maximizing truck payload (ODt), and rethinking the current emphasis on collecting only FHR biomass for bioenergy purpose in order to reduce the biomass procurement costs. Further, harvesting standing under-unutilized tree species reduces per unit procurement costs. Results from other scenarios are also important and interesting to evaluate the impacts of changing economic and technological parameters on cost structures for designing the improved decision making strategies for power plants.

On the other hand, the results from the profit maximization model are more useful to the biomass suppliers (contractors), who are interested in making maximum profits in supplying woody biomass feedstock to power plants from given FMUs. They can maximize their profits from FMUs that are closer to the power plants. However, their profits significantly increase if the power plants offer higher prices. This is possible only if the suppliers meet the quality standards and lead time requirements of the buyers. The variations in costs and gross margin structures under various model scenarios are explained by location of depletion cells relative to power plants, availability of each type of biomass in depletion cells, biomass demands and differential processing costs for two types of biomass. This modeling framework can be applied elsewhere to study similar problems found in biomass supply chain management. The results of such modeling can help decision-makers make improved decisions relating to biomass supply chains for bioenergy production.

Chapter 7

Summary

7.1 Discussion

In order to realize the potential of biomass to be converted into renewable bioenergy, models to aid in decision-making for efficient procurement and optimal utilization of woody biomass are required to form a solid decision support system (DSS) for biomass supply chain management. In view of a lack of such studies on woody biomass supply chain management for bioenergy production in northwestern Ontario (NWO), this dissertation develops and uses various models to analyze woody biomass supply chains. More specifically, exploration of data sources and data input methods, assessment of woody biomass feedstock availability, and development and use of optimization models relating to road network, dynamics of woody biomass logistics for a single power plant and woody biomass competition among four power plants were undertaken in this study.

Exploration of accurate and right types of data, and their preparation in workable formats is the first step in this research work because feeding poor and inaccurate types of data into the model would just result in a 'garbage in garbage out' situation. A detailed background of data sources and input data methods are presented in Chapter 2. In the spatial woody biomass assessment study (Chapter 3), by using pre- and post-harvest inventory in the Crossroute Forest (west part of study area) and combining that with similar data for the Black Sturgeon Forest (east part of study area) (Reynolds *et al.* 2008), and forest depletion spatial data analysis in the 18 forest management units

(FMUs), theoretical availabilities of underutilized wood (UW), and forest harvest residues (FHR) per square kilometre for the whole research area were estimated. However, due to the existence of technical limitations it is not possible to harvest all woody biomass from the forest (Viana *et al.* 2010). Hence, by using a harvesting factor, the technical and economic availability of each type of woody biomass is estimated. The results indicate that after harvesting there is still sufficient material on-site to meet the Ontario Forest Management Guide for Natural Disturbance Pattern Emulation (OMNR 2002). The research findings also determine that there are sufficient FHR and UW available in NWO to run the four major biomass-based power generating plants sustainably.

A detailed study of grid based road network optimization is presented in Chapter 4 as the transportation costs are the major component of the woody biomass supply chain. The findings of this study represent a minimum cost or minimum time for transporting woody biomass to each of the four power plants from each of the 100,061forest cells of the study area. The results show that 1 km x 1 km grid on a regional scale has sufficient resolution and did not lose anything in regard to accuracy or decision-making applicability, but makes the DSS modeling a lot easier. However, there is some truth to the computer quickness and thus usability/user friendliness of only going to the resolution we need and not too fine. With the 1 km x 1 km it took 75 seconds (with an i7 processor) to run the network optimization model (all 26,405 road nodes to a sink). With a 100 m x 100 m grid (assuming linearity in processing time) it would take 7,500 seconds or 2.1 hours which limits the model's usefulness and user friendliness when running multiple sinks. We, therefore, adopt a grid size of 1 km^2 for all our analyses.

The variable cost zones developed for each of the four power plants are different for supplying woody biomass feedstock from different locations because the traveling time through the road network from any particular geographic location to different power plants is different.

The results of the road network optimization model and assessment of woody biomass availability are used as inputs to the woody biomass supply chain optimization models. First, a non-linear dynamic programming (NLDP) model (Chapter 5) was developed to analyze the minimum woody biomass procurement costs based on woody biomass availability in each cell and monthly biomass demand based on monthly electrical power production schedule at the Atikokan Generating Station (AGS). It is observed that at first the model selects the cells, which are closer to the AGS, and in later months far off cells are selected. The behaviour of the model is consistent with an a priori hypothesis of mode of woody biomass collection or procurement. The cells, which are located at longer distance from the AGS, are not utilized by the model for woody biomass procurement as it is not economically feasible to transport woody biomass over long distances.

Scenario analyses of this integrated NLDP model provide interesting information on where to focus further research in the woody biomass procurement chain for bioenergy production to reduce woody biomass procurement and electricity generating costs: i.e., on appropriate harvesting factor (HF), managing moisture content (MC), improving the woody biomass to bioenergy conversion efficiency (CE) and controlling processing costs (PC). Procurement cost and HF were found to be inversely related - when HF increases the procurement cost decreases and vise-versa. The CE and procurement cost were also inversely related: i.e., when CE increases the procurement cost decreases and vise-versa. Therefore, there is high potential for cost savings through efforts to increase CE, and decrease PC and MC. Previous studies conducted by Berndes (2003), Tatsiopoulos and Tolis (2003) and Sokhansanj *et al.* (2006) show similar results.

Finally, economic analysis of biomass supply chains investigated an optimal woody biomass supply chain for four competing biomass-based power plants in NWO in Chapter 6. Two optimization models (cost minimization and profit maximization models) based on mathematical programming models are developed and applied to analyze the impacts of woody biomass competition on cost and gross margin structures for these biomass-based power plants. Various alternative policy scenarios are analyzed to study the impacts of changes in relevant economic and technological parameters of woody biomass procurement for each power plant and FMU. The results of cost minimization model show that per unit procurement costs are directly proportional to the size of the power plants in all scenarios. The highest percent increase in per unit woody biomass procurement costs from the BASE scenario is found in the increased truck charge rate (transport cost) scenario followed by the scenario where only FHR is used by all power plants. Further, harvesting standing under-utilized tree species reduces per unit procurement cost.

By investigating the results of the profit maximization model it was observed that the results of gross margin structures are relevant from the biomass supplier's (contractors) perspective as these are based on biomass supplying FMUs, where the contractors operate their business. It was found that the profit for any FMU depends on the price of biomass being offered by the power plants. Though in the BASE scenario, out of 13 biomass supplying FMUs, two FMUs show negative gross margins due to their relatively longer distance from the power plants. In the increased truck charge rate scenario only four FMUs make a positive profit. These results suggest that, in future, contractors operating in most of the FMUs will face negative gross margins, thereby halting the biomass supply and thus hindering smooth operation of the power plants. Therefore, an increase in price of woody biomass at a power plant greatly helps to increase the profits of closeby FMUs, but only marginally helps to increase the profits of faraway FMUs. It therefore appears more economic to build new power plants at other locations instead of making the power plants larger than present, as the bulky woody biomass transportation cost is high. Thus, it is advisable to put smaller power plants across the landscape area in order to make biomass collection a profitable business for FMUs. This will also help in reducing the distribution cost of power to small communities, and increase rural employment opportunities through bioenergy production systems in the region.

When distance between power plants in relation to the total volume of woody biomass needed is long, and there is no other power plant within the economic woody biomass harvesting zone of an existing power plant, it is appropriate to do an analysis for only a single power plant. When several existing or potential power plants need to compete for the available woody biomass feedstock in the same region, an analysis for competing power plants is required.

7.2 Policy Implications

The development of methodology for assessing woody biomass availability for bioenergy production using forest depletion spatial data in NWO is the first work of this kind in Canada. This methodology could be adapted or applied as a template for other regions/parts of Canada. Variable cost zones established surrounding four NWO power generating stations using woody biomass feedstock show the average woody biomass transportation cost from any particular forest area to a power plant at a first glance. These can be valuable information to be used in DSS for policy makers and planners. By using the road network optimization model developed in this thesis the minimum cost estimates to transport woody biomass feedstock from any geographic location to any other geographic location can be obtained, thereby improving the decision making processes. Although, this network optimization model has been developed to analyze the optimal supply of woody biomass feedstock to the power generating stations, it can be used for analyzing problems relating to transporting any material across the region.

Modeling woody biomass procurement for bioenergy production at the AGS in NWO is a first optimization model, based on the NLDP method, for planning the logistics of woody biomass procurement for conversion to bioenergy in this region. This model is applicable across Canada and abroad for optimizing the feedstock procurement of any biomass-based power plants, which has important policy implications for designing optimal supply chains under dynamic operational frameworks.

Assessment of the impacts of competition on woody biomass feedstock supply to four power plants in NWO using mathematical programming models was developed for the first time in Canada. These models determine the optimal allocation of woody biomass either based on procurement cost minimization or profit maximization, while maintaining a sustainable supply of woody biomass feedstock. This model can be used by woody biomass feedstock suppliers to make decisions based on profit maximization, and by woody biomass feedstock buyers to make decisions based on procurement cost minimization. As an increase in price of woody biomass at a power plant greatly helps to increase the profits of close by FMUs and only marginally helps to increase the profits of faraway FMUs, it is logical to locate smaller power plants across a wider landscape area in order to make biomass collection a profitable business for FMUs. There should also be a focus on controlling transportation costs by investing in transport infrastructure and logistics, and maximizing truck payload size in ODt. Emphasis should not be given on harvesting just FHR to minimize cost, but on harvesting both FHR and UW for overall maximum benefit.

7.3 Future Research Directions

The estimation of the availability of UW in the region is based on the assumption of availability of harvestable UW from depleted forest cells due to lack of past UW inventory data. Although, conservative estimates are used for UW availability from depleted forest cells in this study, this limitation can be overcome through the use of enhanced forest inventory data in the future. To quantify the feedstock supply risk for bioenergy production it is important to determine inter-year variability in woody biomass availability. Alternate feedstock sources for the biomass-based power plants should be identified in future research work to supply woody biomass feedstock during years with lower volumes harvested for traditional wood assortments in the future. The

NLDP model could be further improved by incorporating data related to differences between tree species, forest types, moisture contents, heat values, harvesting systems, combustion efficiencies, and variations in the amount of seasonal and weekly power generation. Production of pellets in a distributed network could further reduce the transportation costs and feedstock requirements, as pellets are a more energy dense biomass feedstock. Future versions of this model could reflect these improvements by incorporating new information and will help in developing an integrated DSS of bioenergy production in NWO and elsewhere. The optimization models do not consider the variation of moisture content and heat value of woody biomass feedstock based on the time of storage and types of tree species. Inclusion of new information in future versions of the models will make the model more robust. More research also needs to be done on optimizing the entire wood procurement chain (e.g., processing, merchandizing yards, transportation and logistics) to ensure maximum value is obtained from the available forest resources.

References

Abitibi-Bowater Inc. 2009. Shape Files of FRI Data (forests, roads and lake layers), Forest Depletion, and Forest Management Planning of Crossroute Forest, Dog River Matawin Forest, Black Sturgeon Forest, English River Forest, and Spruce River Forest Management Units. Personal communication with Martin Kaiser, R.P.F., Manager, Strategic Business Development, Fibre Resources Ontario, Abitibi-Bowater Inc.

Abitibi-Bowater Inc. 2011. Power generating capacities and annual wood biomass feedstock requirements of the Abitibi-Bowater Power Plant Thunder Bay (ABTB) and the Abitibi-Bowater Fort Frances Power Plant (ABFF) respectively. Personal communication with Martin Mr. Kaiser, R.P.F., Manager, Strategic Business Development, Fibre Resources Ontario, Abitibi-Bowater Inc.

Alam M.B., Pulkki, R. and Shahi, C. 2008. Forest biomass availability in northwestern Ontario. In: Council on Forest Engineering: *Addressing Forest Engineering Challenges for the Future*. June 22-25, 2008, South Carolina, USA.

Alam M.B., Shahi, C. and Pulkki, R. 2009a. Wood biomass supply model for bioenergy production in northwestern Ontario. In: Renewable Energy Technology (ICDRET): *1st International Conference on the Developments in Renewable Energy Technology*, December 17-19, 2009, United International University, Dhaka, Bangladesh. Print ISBN: 978-1-4244-6012-0.

Alam, M.B. and Pulkki, R. 2009a. Supply Chain Management Modeling of Wood Biomass Procurement for Energy Production in Northwestern Ontario. 23rd Graduate Student Conference on Forestry and Environmental Sciences 2009 (CONFOR): *Challenge and Change.* January 29 to February 1 2009. YMCA Geneva Park, Orillia, Ontario.

Alam, M.B. and Pulkki, R. 2009b. The Economics and Procurement of Wood Biomass for Energy Production in Northwestern Ontario. Presented in: IUFRO 3.08 Small-Scale Forestry Symposium. Seeing the Forest beyond the Trees: *New Possibilities and Expectations for Products and Services from Small-Scale Forestry*. West Virginia, USA, June 7-11, 2009.

Alam, M.B. and Pulkki, R. 2011. Data Sources for the Research on Wood Biomass Supply Chain for Energy Production in Northwestern Ontario. European Journal of Scientific Research, 49(2): 152-167.

Alam, M.B., Pulkki, R. and Shahi, C. 2012a. Wood biomass availability for bioenergy production using forest depletion spatial data in northwestern Ontario. Canadian Journal of Forest Research, in press.

Alam, M.B., Pulkki, R. and Shahi, C. 2012b. Road network optimization model for supplying wood biomass feedstock for energy production in northwestern Ontario. The Open Forest Science Journal, under review.

Alam, M.B., Pulkki, R., Shahi, C. and Upadhyay, T. 2009b. Wood biomass procurement for bioenergy production in northwestern Ontario: *A decision support system based on mixed integer programming model.* In: International Conference on Logging and Industrial Ecology. November 3-5, 2009, Nanjing, China.

Allen, J., Browne, M., Hunter, A., Boyd, J. and Palmer, H. 1998. Logistics management and costs of biomass fuel supply. International Journal of Physical Distribution & Logistics Management, 28(6): 463-477.

Berndes, G., Hoogwijk, M. and van den Broek, R. 2003. The contribution of biomass in the future global energy supply: a review of 17 studies. Biomass and Bioenergy, 25: 1-28.

Beyer, H.L. 2004. Hawth's Analysis Tools for ArcGIS. http://www.spatialecology.com/htools. Nov. 26, 2009.

Bilyk, A. 2009. Inventorying Forest Biomass: *A Ground-Based Method*. Undergraduate Thesis, Lakehead University, Thunder Bay.

Borjesson, P. 2000. Economic valuation of the environmental impact of logging residue recovery and nutrient compensation. Biomass and Bioenergy, 19(3):137-152.

Bradley, D. 2006a. Canada Biomass- Bioenergy Report. Climate Change Solutions – IEA Bioenergy Task 40-Biotrade; Canada Country Report. http://bioenergytrade.org/t40reportspapers/0000009a190b6270c/0000009b0808ec301.html. Sept. 10, 2010.

Bradley, D. 2006b. Climate Change Solutions. Canada Biomass-Bioenergy Report. http://www.climatechangesolutions.net/pdf/canada_country2006.pdf. March 10, 2010.

Bredström, D., Lundgren, J.T., Rönnqvist, M., Carlsson, D. and Mason, A. 2004. Supply chain optimization in the pulp mill industry IP models, column generation and novel constraint branches. European Journal of Operational Research, 156:2-22.

Buckley, D.J. 1998. The GIS Premier: *An Introduction to Geographic Information Systems*.

http://www.innovativegis.com/basis/primer/The_GIS_Primer_Buckley.pdf. June 23, 2011.

Burrough, P.A. 1986. Principles of Geographic Information Systems for Land Resource Assessment. Monographs on Soil and Resources Survey No. 12, Oxford Science Publications, New York.

Campbell, C.J. and Duncan, R.C. 1997. The Coming Oil Crisis. Multi-Science Pub. Co. & Petroconsultants, Brentwood, Essex, England.

CanmetENERGY. 2011. Bioenergy Systems. http://canmetenergy-canmetenergie.nrcan-rncan.gc.ca/eng/bioenergy.html. August 30, 2011.

Caputo, A., Palumbo M., Pelagagge, P. and Scacchia, F. 2005. Economics of biomass energy utilization in combustion and gasification plants: *effects of logistics variables*. Biomass and Bioenergy, 28: 35-51.

Centre for Energy. 2011. Biomass energy in Canada. Canadian Centre for Energy Information. http://www.centreforenergy.com/AboutEnergy/Biomass/Overview.asp?page=6. August 10, 2011.

Chauhan, S.S., Frayret, J.M. and LeBel, L. 2009. Multi-commodity supply network planning in the forest supply chain. European Journal of Operational Research, 196: 688–696.

Cundiff, J.S., Dias, N. and Sherali, H.D. 1997. A linear programming approach for designing a herbaceous biomass delivery system. Bioresource Technology, 59: 47-55.

Davide, F., Riccardo, M., Michela, R., Mauro, R., Roberto, S. and Angela, T. 2004. Optimizing forest biomass exploitation for energy supply at a regional level. Biomass and Bioenergy, 26: 15-25.

Dunnet, A.J., Adjiman, C.S. and Nilay, S. 2008. A spatially explicit whole system model of the lignocellulosic bioethanol supply chain: *an assessment of decentralized processing potential*. Biotechnol Biofuels, 1: 1-13.

Duquette, B. 2011. Biofibre Evaluation and Reporting. Presentation given to the Forestry 3211 class on November 23, 2011 at Lakehead University, Thunder Bay, Ontario.

Ediger, V.S. and Kentel, E. 1999. Renewable energy potential as an alternative to fossil fuels in Turkey. Energy Conversion and Management, 40(7):743-55.

Edward, M., Smeets, W. and Faaij, A.P.C. 2007. Bioenergy potentials from forestry in 2050: *An assessment of the drivers that determine the potentials*. Climatic Change, 81: 353-390.

Ellis, F. 2001. GIS Self Learning Tool. Department of Geomatics, The University of Melbourne. http://www.sli.unimelb.edu.au/gisweb/. Nov. 10, 2009.

Erikson, L. and Björheden, R. 1989. Optimal storing, transport and processing for a forest-fuel supplier. European Journal of Operations Research, 43(1): 26-33.

ESRI. 2009. ArcGIS 9.3 Desktop Help. Environmental Systems Research Institute (ESRI), Inc. http://webhelp.esri.com/arcgisdesktop/9.3/index.cfm. Nov. 14, 2009.

ESRI. 2010. ArcGIS 9.4 Desktop Help. Environmental Systems Research Institute (ESRI), Inc. http://webhelp.esri.com/arcgisdesktop/9.4/index.cfm. Nov. 15, 2010.

ESRI. 2011. ArcGIS 10. Environmental Systems Research Institute (ESRI), Inc. http://www.esri.com/software/arcgis/arcgis10/index.html. May 12, 2011.

Etcheverry, J., Gipe, P., Kemp, W., Samson, R., Vis, M., Eggertson, B., McMonagle, R., Marchildon, S. and Marshall, D. 2004. Smart Generation: *Powering Ontario with Renewable Energy*. The David Suzuki Foundation, Vancouver, BC, Canada. www.davidsuzuki.org/files/Climate/Ontario/Smart_Generation_full_report.pdf. Sept. 20, 2010.

Forest BioProducts Inc. 2006. An Assessment of the Viability of Exploiting Bio-Energy Resources Accessible to the Atikokan Generating Station in Northwestern Ontario. Ontario Ministry of Energy: *Final Report*. Forest BioProducts Inc., 645 Queen Street East, 2nd Floor, Sault Ste. Marie, Ontario, Canada.

FPInnovations FERIC. 2008. Forest Feedstocks (Biomass) Tutorial. FPInnovations FERIC, 580 boul, Saint-Jean, Pointe-Claire, QC H9R 3J9, Canada.

Freppaz, D., Minciardi, R., Robb, M., Rovatti, M., Sacile, R. and Taramasso, A. 2004. Optimizing forest biomass exploitation for energy supply at a regional level. Biomass and Bioenergy, 26: 15-25.

Frombo, F., Minciardi, R., Robba, M., Rosso, F. and Sacile, R. 2009. Planning woody biomass logistics for energy production: *A strategic decision model*. Biomass and Bioenergy, 33: 372-383.

Gan, J. and Smith, C.T. 2006. Availability of logging residues and potential for electricity production and carbon displacement in the USA. Biomass and Bioenergy, 30: 1011-1020.

Gautam, S. 2010. Assessment of Fuel Quality Changes during Storage of Biofibre and Its Effect on Cost. M.Sc. Thesis, Lakehead University, Thunder Bay, Ontario.

Gautam, S., Pulkki, R., Shahi, C. and Leitch, M. 2010. Economic and energy efficiency of salvaging biomass from wildfire burnt areas for bioenergy production in notherwestern Ontario: a case study. Biomass and Bioenergy 34: 1562-1572.

Geijzendorffer, I.R., Annevelink, E., Elbersen, B., Smidt, R. and de Mol, R.M. 2008. Application of a GIS-BIOLOCO Tool for the Design and Assessment of Biomass Delivery Chains. 16th European Biomass Conference and Exhibition, 2-6 June, 2008, Valencia, Spain.

Gold, S. and Seuring, S. 2011. Supply chain and logistics issues of bio-energy production. Journal of Cleaner Production, 19(1): 32-42.

Graham, R.L., English, B.C. and Noon, C.E. 2000. A geographic information system-based modeling system for evaluating the cost of delivered energy crop feedstock. Biomass and Bioenergy, 18(4): 309-329.

GreenForest Management Inc. 2009. PDF files of block area and timber volumes and shape files of FRI Data (forests, roads and lake layers), forest depletion, and Forest Management Planning of Sapawe Forest Management Unit. Personal communication with Richard Shwedack, R.P.F., GreenForest Management Inc., Thunder Bay, Ontario.

Greenmantle Forest Inc. 2009. Shape files of FRI Data (forests, roads and lake layers), forest depletion, and Forest Management Planning of Lakehead Forest Management Unit. Personal communication with Dave MacIsaac, Area Forester, Greenmantle Forest Inc., Thunder Bay, Ontario.

Gunnarsson, H., Roennqvist, M. and Lundgren, J.T. 2003. Supply Chain Modeling of Forest Fuel: Production, Manufacturing and Logistics. European Journal of Operational Research, 158: 103-123.

Haartveit, E.Y., Kozak, R.A. and Maness, T.C. 2004. Supply chain management mapping for the forest products industry: *Three cases from western Canada*. Journal of Forest Products Business Research, 1(5): 1-30.

Herr, A. and Dunlop, M. 2011. Bioenergy in Australia: *An improved approach for estimating spatial availability of biomass resources in the agricultural production zones*. Biomass and Bioenergy, 35:2298-2305.

Hosegood, S.I. 2010. Fuel characteristics of northwestern Ontario tree species and their components. M.Sc. Thesis, Lakehead University, Thunder Bay, Ontario. 133 pp.

Hosegood, S., Leitch, M., Shahi, C. and Pulkki, R. 2011. Moisture and energy content of fire-burnt trees for bioenergy production: *A case study of four tree species from northwestern Ontario*. The Forestry Chronicle 2011, 87(1): 42-47.

Husdal, J. 1999. Network analysis – network versus vector – A comparison study. Website of husdal.com: *Supply Chain Risk – Business Continuity – Transport Vulnerability.* http://www.husdal.com/1999/10/11/network-analysis-raster-versus-vector-a-comparison-study/. June 22, 2011.

Hutchinson, W. and Warren, M. 2001. Principles of Information Warfare. Journal of Information Warfare, 1: 1-6.

Jensen, J., Saalfeld, A., Broome, F., Cowen, D., Price, K., Ramsey, D., Lapine, L. and Usery, E.R. 2005. Spatial data acquisition and integration. In McMaster RB, Usery E L (Ed.) (2005) A Research Agenda for Geographic Information Science. University Consortium for Geographic Information Science. CRC Press LLC, USA.

Kanzian, C., Holzleitner, F., Stampfer, K. and Ashton, S. 2009. Regional energy wood logistics – optimizing local fuel supply. Silva Fennica, 43(1): 113-128.

Kaylen, M, Van Dyne, D.L., Choi, Y.S. and Blasé, M. 2000. Economic feasibility of producing ethanol from lignocellulosic feedstocks. Bioresource Technology, 72(1): 19-32.

Kerstetter, T.T. and Lyons, J.K. 2001. Logging and Agricultural Residue Supply Curves for the Pacific Northwest. Washington State University Energy Program, and United States Department of Energy.

Kim J., Realff, M.J. and Lee, J.H. 2011a. Optimal design and global sensitivity analysis of biomass supply chain networks for biofuels under uncertainty. Article in press, Computers and Chemical Engineering, 35(9): 1738-1751.

Kim, J., Realff, M.J., Lee, J.H., Whittaker, C. and Furtner, L. 2011b. Design of biomass processing network for biofuel production using an MILP model. Biomass and Bioenergy, 35: 853-871.

Kong, X.Q., Wang, R.Z. and Huang, X.H. 2005. Energy optimization model for a CCHP system with available gas turbines. Applied Thermal Engineering, 25(2, 3): 377-91.

Koppejan, J. 2007. Fuel Storage, handling and preparation and system analysis for biomass combustion technologies. Proceeding of European Biomass Conference, Conference Centre, Berlin, Germany, May 7-11. www.conference-biomass.com. Jan. 15, 2011.

Krarup, J. and Pruzan, P.M. 1983. The simple plant location problem: Survey and synthesis. European Journal of Operational Research, 32(8):672-687.

Kumar, A., Flynn, P.C. and Sokhansanj, S. 2008. Biopower generation from mountain pine beetle infested wood in Canada: *An economical opportunity for greenhouse gas mitigation*. Renewable Energy, 33(6): 1354-1363.

Kurikka, B. 2008. Confederation College Forestry Center – Bowater Biomass Study Inventory and Survey Methods. Confederation College Forestry Center, Thunder Bay, Ontario, Canada.

Land Information Ontario (LIO). 2010. FRI data and Forest Depletion Data. Personal communication with Land Information Ontario, Canada.

Layzell, B.D., Stephen, J. and Wood, S.M. 2006. Exploring the Potential for Biomass Power in Ontario: *A Response to the OPA Supply Mix Advice Report*. BIOCAP Canada Foundation, 156 Barrie Street, Queen's University, Kingston, Ontario K7L 3V2. www.biocap.ca. Sept. 10, 2009.

Lewandowski, I., Weger, J., van Hooijdonk, A., Havlickova, K., van Dama, J. and Faaij, A. 2006. The potential biomass for energy production in the Czech Republic. Biomass and Bioenergy, 30: 405-421.

Luckai, F. 2011. Plonski's Normal Yield Tables, and Local Volume Table 2005. Lakehead University, Thunder Bay, Canada. http://flash.lakeheadu.ca/~fluckai/webpage.html. January 15, 2011.

Macmillan, I. 2001. Biomass Evaluation: *Including a Case Study on Woodchip Utilisation at Ardverikie Estate, Kinlochlaggan*. M.Sc. Thesis, Department of Mechanical Engineering, University of Strathclyde, Glasgow. http://www.esru.strath.ac.uk/Documents/MSc_2001/ian_macmillan.pdf. May 15, 2011.

Mahmoudi, M., Sowlati, T. and Sokhansanj, S. 2009. Logistics of supplying biomass from a mountain pine beetle-infested forest to a power plant in British Columbia. Scandinavian Journal of Forest Research, 24(1): 76-86.

Manfred, G. and Peter, R. 2007. Designing a regional forest fuel supply network. Biomass and Bioenergy, 31: 393-402.

Mas, M.D., Giarola, S., Zamboni, A. and Bezzo, F. 2010. Capacity planning and financial optimization of the bioethanol supply chain under price uncertainty. ESCAPE20.

Mattsson, S.A. 1999. Improving supply chain efficiency and effectiveness. Social Sciences No. 2, Acta Wexionensia, Sweden. 310 pp.

McCarthy, S. 2009. Ottawa takes aim at coal-fired power plants. Toronto Globe and Mail International, April 29, 2009.

McKenney, D.W., Yemshanov, D., Fraleigh, S., Allen, D. and Preto, F. 2011. An economic assessment of the use of short-rotation coppice woody biomass to heat greenhouses in southern Canada. Biomass and Bioenergy, 35: 374-384.

McKinnon, M. 2011. OPG details the move to biomass. Atikokan Progress: *a weekly community newspaper*. www.atikokanprogress.ca. March 23, 2011.

Meehan, P.G. and McDonnell, K.P. 2010. An assessment of biomass feedstock availability for the supply of bioenergy to University College Dublin. Biomass and Bioenergy, 34: 1757-1763.

Mentzer, J.T. 2001. Managing the Supply Chain – Managerial and Research Implications. In: J.T. Mentzer, ed. Supply Chain Management. Sage Publications, Inc, Thousand Oaks, USA. pp. 437-461.

Microsoft. 2010. Microsoft Visual Studio 2010 Express. http://www.microsoft.com/express/Downloads/. December 30, 2010.

Ministry of Northern Development, Mines and Forestry (MNDMF). 2011. Potential biomass estimates for Ontario's tree species. Personal communication with Mr. Joe E. Maure, Forest Bioeconomy Coordinator, Industry Relations Branch, Ministry of Northern Development, Mines and Forestry (MNDMF)**,** Sault Ste. Marie, Ontario.

Mitchell, C. 2000. Development of decision support systems for bioenergy applications. Biomass and Bioenergy, 18: 265-78.

Morgan, J. 2008. Ontario Base Map Series. Maps, University Map Library, University of Waterloo, Waterloo, Ontario. www.lib.uwaterloo.ca. Nov. 24, 2009.

MSDN. 2009. Visual Basic Language Reference: Data Type Summary (Visual Basic). Microsoft Corporation. http://msdn.microsoft.com/en-us/library/47zceaw7(VS.80).aspx. Nov. 2, 2009.

Nagel, J. 2000. Biomass in energy supply, especially in the state of Brandeburg, Germany. Ecological Engineering, 16: 103-110.

Nemec, A. and Davis, G. 2002. Efficiency of six line intersect sampling designs for estimating volume and density of coarse woody debris. Forest Research Technical Report, TR-021. British Columbia Forest Service, Vancouver Forest Region. 14 pp.

Nichols, S.J. 2004. The Effect of South African Provincial Road Condition on the Efficiency of Forest Product Transport. M.Sc. Forest Science Thesis. University of Stellenbosch, South Africa. 129 pp.

Nichols, S.J., Pulkki, R.E. and Ackerman, P.A. 2006. Provincial road condition and roundwood transport in South Africa. Southern African Forestry Journal, 207: 55-61.

Noon, C.E. and Daly, M.J. 1996. GIS-based resource assessment with BRAVO. Biomass and Bioenergy, 10(4-5): 101-9.

Northwestern Ontario Prospectors Association (NWOPA). 2007**.** Forest Management Activities in Northwestern Ontario. http://www.nwopa.net/landuse/fmulist.htm. April 10, 2010.

Nurmi, J. 1999. The storage of logging residue for fuel. Biomass and Bioenergy, 17: 41-47.

Nurmi, J. 2007. Recovery of logging residues for energy from spruce (*Pices abies*) dominated stands. Biomass and Bioenergy, 31(6): 375-380.

Ontario Ministry of Energy (OME). 2007. Ontario Ministry of Energy website. http://www.energy.gov.on.ca. Sept. 16, 2007.

Ontario Ministry of Natural Resources (OMNR). 2002. Forest Management Guide for Natural Disturbance Pattern Emulation. Ontario Ministry of Natural Resources**.** Ontario Government, Ontario, Canada.

Ontario Ministry of Natural Resources (OMNR). 2007a. Forest Information Manual 2007: *Forest Resources Inventory Technical Specifications*. Technical Series, June 1, 2007, Ontario Ministry of Natural Resources.

Ontario Ministry of Natural Resources (OMNR). 2007b. Scaling Manual. Ontario Ministry of Natural Resources, Ontario, Canada. http://www.web2.mnr.gov.on.ca/mnr/forests/forestdoc/reg_manuals/manuals/scaling/file_one.pdf. July 19, 2011.

Ontario Ministry of Natural Resources (OMNR). 2009. Draft Forest Information Manual 2009. Environmental Registry Edition, January 2007, Queen's Printer for Ontario, Toronto, Ontario. 94 pp. www.mnr.gov.on.ca. Nov. 24, 2009.

Ontario Ministry of Natural Resources (OMNR). 2010. Geographic Information System (GIS) data for the Forest Management Units (FMUs) of Northwestern Ontario. Personal Communication with Ontario Ministry of Natural Resources (OMNR).

Ontario Ministry of Natural Resources (OMNR). 2011. Ontario's Forests: *Geographic Profiles*. Ontario Ministry of Natural Resources website. http://www.mnr.gov.on.ca. Sept. 1, 2011.

Ontario Power Generation Inc. (OPG). 2010. Atikokan Generation Station Biomass Repowering Project. Ontario Power Generation Inc. http://www.opg.com/power/thermal/AtikokanFactSheet1009.pdf. May 25, 2011.

Panichelli, L. and Edgard, G. 2008. GIS-based approach for defining bioenergy facilities location: *A case study in Northern Spain based on marginal delivery costs and resources competition between facilities*. Biomass and Bioenergy, 32: 289-300.

Panoutsou, C., Eleftheriadis, J. and Nikolaou, A. 2009. Biomass supply in EU27 from 2010 to 2030. Energy Policy, 37: 5675-5686.

Pari, L. 2001. Energy production from biomass: the case of Italy. Renewable Energy, 22: 21-30.

Perez-Verdin, G., Grebner, D.L., Sun, C., Munn, I.A., Schultz, E.B. and Matney, T.G. 2009. Woody biomass availability for bioethanol conversion in Mississippi. Biomass and Bioenergy, 33: 492-503.

Perpina, C., Alfonso, D., Perez-Navarro, A., Penalvo, E., Vargas, C. and Cardenas, R. 2009. Methodology based on Geographic Information Systems for biomass logistics and transportation optimization. Renewable Energy, 34: 555-565.

Pulkki, R. 1978. Logging waste in the Black Sturgeon Crown Management Area, Northwestern Ontario. B.Sc.F. thesis. Lakehead University, Thunder Bay, Ontario. 56 pp.

Pulkki, R. 1994. Network analysis in studying the impact of reduced water crossings on road and hauling costs. Conference proceedings: COFE/IUFRO Div.3 conference on advanced technology in forest operations: applied ecology in action, Corvallis, Oregon.

Pulkki, R. 1996. Water Crossing Versus Transport Cost: *A Network Analysis Case Study*. Journal of Forest Engineering, 7(2): 59-64.

Pulkki, R. 2001. Role of supply chain management in the wise use of wood resources. Southern African Journal, 191: 89-95.

Ranta, T. 2002. Logging residues from regeneration fellings for biofuel production – a GIS-based availability and supply cost analysis. Doctoral thesis, Acta Universitatis Lappeenrantaensis 128, Lappeenranta University of Technology, 180 pp.

Ranta, T. 2004. Logging residues from regeneration fellings for biofuel production-a GIS-based availability analysis in Finland. Biomass and Bioenergy, 28(3): 171-182.

Ranta, T. 2005. Logging residues from regeneration fellings for biofuel production–a GIS-based availability analysis in Finland. Biomass and Bioenergy, 28(2): 171-182.

Rauch, P. and Gronalt, M. 2010. The Terminal Location Problem in the Forest Fuels Supply Network. International Journal of Forest Engineering, 21(2).

Rauch, P., Gronalt, M. and Hirsch, P. 2010. Cooperative forest fuel procurement strategy and its saving effects on overall transportation costs. Scandinavian Journal of Forest Research, 25(3): 251-261.

Ren, H., Zhou, W., Nakagami, K. and Gao, W. 2010. Integrated design and evaluation of biomass energy system taking into consideration demand side characteristics. Energy, 35: 2210-2222.

Rentizelas, A.A., Tatsiopoulos, I.P. and Tolis, A. 2009. An optimization model for multi-biomass tri-generation energy supply. Biomass and Bioenergy, 33: 223-233.

Reynolds, R., Cormier, D. and Ryans, M. 2008. Feasibility of Forest Feedstock for Bioenergy in Northwestern Ontario. Contract Report CR-0366-3, October 2008, FPInnovations FERIC Division, Pointe-Claire, Quebec.

Ride, K.R. 1998. An investigation of wood fibre recovery and related economics of four harvesting systems common to northwestern Ontario. M.Sc. Thesis, Lakehead University, Thunder Bay, Ontario. 95 pp.

Rönnqvist, M. 2003. Optimization in forestry. Mathematical Programming, Series B 97.

Sapic, T. 2009. GIS, Photogrammetry, and Remote Sensing Labs. Faculty of Forestry and the Forest Environment, Lakehead University, Thunder Bay, Ontario. http://flash.lakeheadu.ca/~forspatial/. Nov. 25, 2009.

Scarlat, N., Blujdea, V. and Dallemand, J. 2011. Assessment of the availability of agricultural and forest residues for bioenergy production in Romania. Biomass and Bioenergy, 35: 1995-2005.

Searcy, E., Flynn, P., Ghafoori, E. and Kumar, A. 2007. The relative cost of biomass energy transport. Applied Biochemistry and Biotechnology, 137-140(1-12): 639-652.

Singh, J., Panesar, B.S. and Sharma, S.K. 2010. A mathematical model for transporting the biomass to biomass-based power plant. Biomass and Bioenergy, 34 (4): 483-488.

Sokhansanj, S. and Fenton, J. 2006. Cost benefit of biomass supply and pre-processing. BIOCAP, Canada. http://www.biocap.ca/rif/report/Sokhansanj_S.pdf. January 12, 2011.

Sokhansanj, S., Kumar, A. and Turhollow, A.F. 2006. Development and implementation of integrated biomass supply analysis and logistics model (IBSAL). Biomass and Bioenergy, 30: 838-47.

Sorenson, L. 2007. Minnesota Logged Area Residue Analysis. Minnesota Department of Natural Resources Division of Forestry, USA.

Sowlati, T. 2009. Forest Products and Forest Biomass Transportation and Logistics. FORAC. www.forac.ulaval.ca. June 28, 2010.

Stasko, T.H., Conrado, R.J., Wankerl, A., Labatut, R., Tasseff, R., Mannion, J.T., Gao, H.O., Sanborn, S.D. and Knott, G. 2011. Mapping woody-biomass supply costs using forest inventory and competing industry data. Biomass and Bioenergy, 35: 263-271.

Stephen, J.D., Sokhansanj, S., Bia, X., Sowlati, T., Kloeck, T., Townley-Smith, L. and Stumborg, M.A. 2010. Analysis of biomass feedstock availability and variability for the Peace River region of Alberta, Canada. Biosystems Engineering 105: 103-111.

Sumac Forest Information Services Ltd (SFISL). 2011. Forest Inventory (Point Survey) Grid. Personal communication with Mr. Tom Shields, Field Services Supervisor, Sumac Forest Information Services Ltd., Thunder Bay, Ontario, Canada.

Sygration. 2011. Ontario Electricity Reports and Tools: *Current Ontario Generator Output*. Sygration. https://www.sygration.com/. January 10, 2011.

Sylvain, L., Dagmar, S., Erik, D., Erwin, S. and Michael, O. 2008. Optimal location of wood gasification plants for methanol production with heat recovery. Int J Energ Res, 32: 1080-91.

Sylvain, L., Erwin, S., Michael, O. and Keywan, R. 2009. Methanol production by gasification using a geographically explicit model. Biomass and Bioenergy, 33: 745-51.

Taha, H.A. 1982. Operations Research: an introduction. Macmillan Publishing Co. Inc., New York. 848 pp.

Tahvanainen, T. and Perttu, A. 2010. Supply chain cost analysis of long-distance transportation of energy wood in Finland. Biomass and Bioenergy, 35(8): 3360-3375.

Tatsiopoulos, I. and Tolis, A. 2003. Economic aspects of the cotton-stalk biomass logistics and comparison of supply chain methods. Biomass and Bioenergy, 24: 199-214.

Thornley, P., Upham, P., Huang, Y., Rezvani, S., Brammer, J. and Rogers, J. 2008. Integrated assessment of bioelectricity technology options. Energy Policy, 37(3): 890-903.

Tittmann, P.W., Parker, N.C., Hart, Q.J. and Jenkins, B.M. 2010. A spatially explicit techno-economic model of bioenergy and biofuels production in California. Journal of Transport Geography, 18: 715-728.

Tyndall, J.C., Schulte, L.A., Hall, R.B. and Grubh, K.R. 2011. Woody biomass in the U.S. Cornbelt? Constraints and opportunities in the supply. Biomass and Bioenergy, 35: 1561-1571.

Ushiyma, I. 1999. Renewable energy in Japan. Renewable Energy, 16(1-4):1174-9.

Velazquez-Marti, B. and Fernandez-Gonzalez, E. 2010. Mathematical algorithms to locate factories to transform biomass in bioenergy focused on logistic network construction. Renewable Energy, 35: 2136-2142.

Viana, H., Cohen, W.B., Lopes, D. and Aranha, J. 2010. Assessment of forest biomass for use as energy. GIS-based analysis of geographical availability and locations of wood-fired power plants in Portugal. Applied Energy, 87(8): 2551-2560.

Voivontas, D., Assimacopoulos, D. and Koukios, E. 2001. Assessment of biomass potential for power production: *a GIS based method*. Biomass and Bioenergy, 20: 101-12.

Wang, J. 2007. Woody Biomass Resources, Utilization, and Opportunities in West Virginia, USA. Proceedings of the 3rd Forest Engineering Conference, Mont-Treblant, Quebec, Canada, October 1-4, 2007.

Wang, W. 1998. Visual Basic 6 for Dummies. IDG Books Worldwide, Inc. New York, USA.

Wood, S.M. and Layzell, D.B. 2003. A Canadian Biomass Inventory: *Feedstocks for a Bio-based Economy.* Final Report. BIOCAP Canada Foundation, Queen’s University, 156 Barrie Street, Kingston, Ont. K7L 3N6.

Wu, J., Wang, J. and McNeel, J. 2011. Economic modeling of woody biomass utilization for bioenergy and its application in central Appalachia, USA. CJFR, 41(1): 165-179.

Yoshioka, T., Aruga, K., Sakai, H., Kobayashi, H. and Nitami, T. 2002. Cost, Energy and Carbon Dioxide (CO_2) Effectiveness of a Harvesting and Transporting System for Residual Forest Biomass. J. For. Res., 7: 157-163.

Yoshioka, T., Hirata, S., Matsumura, Y. and Sakanishi, K. 2005. Woody biomass resources and conversion in Japan: *The current situation and projections to 2010 and 2050*. Biomass and Bioenergy, 29: 336-346.

Zhu, X., Li, X., Yao, Q. and Chen, Y. 2011. Challenges and models in supporting logistics system design for dedicated-biomass-based bioenergy industry. Bioresource Technology, 102: 1344-1351.

Total number of references is 152.